PLANFORM GEOMETRY AND KINEMATICS OF CONFINED MEANDERING RIVERS ON THE CANADIAN PRAIRIES

by

Tami Nicoll
Bachelor of Science with Honours,
University of Alberta, 2003

THESIS SUBMITTED IN PARTIAL FULFILLMENT OF
THE REQUIREMENTS FOR THE DEGREE OF

MASTER OF SCIENCE

In the
Department of Geography

SIMON FRASER UNIVERSITY

Summer 2008

APPROVAL

Name:	**Tami Jo-Allen Nicoll**
Degree:	**Master of Science**
Title of Thesis:	**Planform Geometry and Kinematics of Confined Meandering Rivers on the Canadian Prairies**
Examining Committee:	
Chair:	**Dr. Jeremy Venditti**, Assistant Professor

Dr. E.J. Hickin
Professor
Senior Supervisor

Dr. M.C. Roberts
Professor Emeritus
Committee Member

Dr. Robert Millar, Professor
Department of Civil Engineering
University of British Columbia
External Examiner

Date Approved: May 23, 2008

ABSTRACT

The planform geometry and kinematics of migrating confined-meandering rivers at 24 locations in Alberta and British Columbia are examined. Migration rates range from 0.01 m/yr to 5.8 m/yr, consistent with those published for freely-meandering rivers. Relationships among planform geometry variables are also generally consistent with those described for freely-meandering rivers; exceptions are the increased ratios for channel wavelength/width and bend curvature. Attempts to predict migration rate based on channel flow and morphometry data are modestly successful. Stream power offers the best statistical predictor of migration rate, accounting for up to 52% of variance in migration rate. Bankfull width and mean annual flood account for respectively 32% and 30% of variance in migration rate. Bedload-transport rates are determined using morphologic methods for five of the sites. These estimates are consistent with the general trend of bedload-transport rates published elsewhere but are low when compared to rates for similar-sized drainage areas.

Keywords: fluvial geomorphology; confined meanders; planform geometry; channel migration; bedload transport; Canadian Prairies

ACKNOWLEDGEMENTS

Many people have provided assistance to this study along the way and their contributions have been invaluable to me. I would like to thank Dr. Ted Hickin for his guidance and support, both intellectually and financially, to this research and for making this study possible. Dr. Michael Roberts offered both critical review and ideas for improvement that were much appreciated. Dr. Robert Millar provided an independent review and discerning comments that improved the final work.

Wayne Allen and Greg Bauch were of great assistance in the field, working long hours in what sometimes were not the best of conditions. I would also like to thank the wonderful staff at the Department of Geography who has helped me at so many points throughout my time at SFU. Finally, to my labmates, colleagues and friends who have made my time at SFU very enjoyable and fulfilling – thank-you.

TABLE OF CONTENTS

LIST OF FIGURES

LIST OF TABLES

CHAPTER 1: INTRODUCTION

1.1 Introduction

This research examines the planform and dynamics of a unique category of meandering rivers: confined meanders. A meandering river planform is the most common channel pattern in the landscape. While rivers may be free to migrate over their alluvial plain, frequently they are confined in some way. Most studies described in the literature concentrate on the planform geometry and meander dynamics of freely-meandering rivers (e.g. Hickin and Nanson, 1984; Nanson, 1977); confined-meandering rivers have received much less attention. This neglect is somewhat surprising given their widespread presence in the landscape, particularly in the mid-latitudes of the world. In these locations, large meltwater-channels carved during glacial times are at present frequently occupied by manifestly underfit streams (see Dury, 1964). The distinctive meander pattern of confined meanders and the impedance of normal meander development suggest that the morphology and dynamics of these systems may be fundamentally different from those associated with freely-meandering

channels. This work endeavours to explore this possibility by examining the morphodynamics of a set of confined meanders on the Canadian Prairies.

1.2 Background

1.2.1 River Planform Geometry

Although the scale of river meanders may vary, it has been clear for some time that channel bend geometry does tend to exhibit certain average empirical relations (Leopold et al., 1964). This average channel morphology is the basis of the widely held assumption that a freely-developing river bend will develop an equilibrium planform scaled to the size of the river (Hickin, 1988). There are certain standard bend parameters used to characterize meanders (Figure 1.1), upon which the empirical relations are based.

Figure 1.1: Parameters used to characterize meander geometry

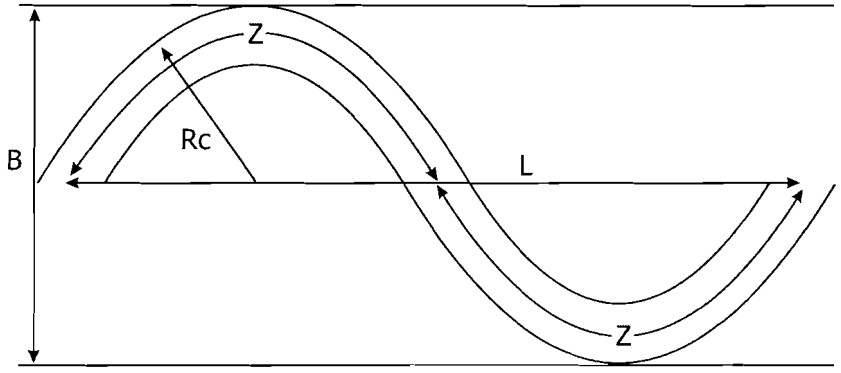

L Wavelength
Rc Radius of curvature
Z Riffle spacing
B Meander belt width
S Sinuosity = (2Z)/L

(Figure adapted from Simon and Castro 2003; Fig. 11.10)

A strong relationship exists between meander wavelength and channel width whereby the wavelength is generally 10 – 14 times the width. Channel

width is also found to be approximately proportional to the square root of discharge; meander wavelength also varies as the square root of discharge, although there is no agreement on which defining discharge to use in the relation (Knighton, 1998). Lastly, most bends have a radius of curvature to width ratio between 2 and 3. Although the above morphometric relationships have been known for some time the underlying causes and controls are still being debated.

Meander-bend curvature (the radius of curvature to channel width ratio, Rc/w) has been a common focus in numerous studies. For 79 natural rivers Williams (1986) found an arithmetic mean for Rc/w of 2.43; the radii of curvature also agreed well with those values predicted by Langbein and Leopold's 1966 sine-generated curve theory. A study of rivers in western Canada (Nanson and Hickin, 1986) describes approximately log-normal distribution of Rc/w values with the peak falling between 2 and 3, a result consistent with that described by Brice (1984). It has been suggested that stable meander geometry requires a curvature in this range (Hooke, 1975). It is argued that a shallow curve would result in a shear-stress distribution that would favour faster migration in the upstream limb, therefore decreasing the radius of curvature. Conversely, a bend of tight curvature would have a shear stress distribution favouring migration of the downstream, and leading to a decrease in radius.

There has been criticism of the traditional approach of describing planform geometry in studies of river meanders. This traditional view is based on the assumption that meanders can be approximated by a simple, symmetrical curve, a supposition that has been called into question by some (Carson and LaPointe,

1983). Other issues arise with the subjectivity involved in delineating meander features and with the variation in definitions of the parameters and the methods used to measure the channel planform. Although there has been some effort to make the measurement of meander geometry more objective (see Andrle, 1996), all approaches involve simplification of the meander form and a certain amount of subjectivity will always be involved in delineating bend features. Nevertheless, the existence of statistically stable relationships, despite the varying degrees of asymmetry found in natural river meanders, demonstrates some kind of underlying regularity in form. River meander planform geometry is complicated but it can be reduced to a limited number of parameters.

1.2.2 River Migration

Lateral migration is a process that is still not completely understood, even for the simplest case of freely migrating, single bends. Numerous factors have been identified as likely controls on lateral migration, including stream power, planform geometry, sediment supply rate, degree of incision or height of the outer bank, and resistance of boundary materials (Hickin, 1988). The degree to which each factor contributes is still under debate and no general model of bend migration exists.

Rohrer (1984) divides the above factors into two opposing groups controlling the rate of bank erosion and therefore migration rate of the channel: the fluid shear stresses acting on the channel boundaries and the resistance to erosion of the boundary sediment. The fluid shear stresses are a function of the planform and cross-sectional geometry of the channel; these combined with

discharge will determine the velocity distribution near the channel boundaries. The idea that planform geometry (specifically bend curvature) controls migration rate was suggested by Bagnold (1960). He reasoned that total resistance to flow around a bend depends on bend-flow hydraulics that in turn are conditioned by Rc/w. From an analysis of previous work, Chen and Shen (1984) found that, indeed, bend curvature is the most important factor in determining the shear-stress distribution in river bends. Work on the Beatton River in British Columbia found a strong relationship between bend curvature and rate of migration (Hickin and Nanson, 1975). Maximum migration rates on this river occurred at a bend curvature of around 3 with rates sharply dropping off at both higher and lower values of Rc/w. Expanding this work to other rivers in western Canada brought more scatter to the relation but revealed the same general connection of maximum migration rates with a Rc/w of 2 to 3 and a decrease in rates on either side of the maximum. Originally the sharp decrease in erosion rate at values less than two was attributed to Bagnold's 1960 theory of flow separation at the inner bank (Hickin, 1974). Bagnold's flume work found that, below Rc/w of 2, flow separation zones became unstable and collapse, increasing turbulence and consequently, resistance to flow through the bend. However, inner-bank flow separation was not observed on the Beatton River, rather the flow separation occurred at the outer bank on bends of tight curvature (Hickin, 1977). The separation zone insulates the outer bank from the full force of flow and is thought to provide an explanation for the sharp decrease in migration rate below Rc/w = 2 on certain rivers (Hickin, 1988). Other authors have found the same general

relation between bend curvature and migration rate (Hooke, 2007; TRB, 2004). Yet it has to be noted that these studies also found very low migration rates at the same Rc/w ratios. Most likely this is because any one single factor may not sufficiently characterize a bend and because migration can be intermittent at a decadal time scale.

The correlation of bend curvature to migration rate indicates that sinuosity may be linked as well. However, studies that have examined this link have been unable to identify a clear relationship; indeed, all are characterized by much scatter in the data (Brice, 1982; Hooke, 2007; Richard et al., 2005). Channel width has been shown to have a strong relationship with migration rate (Brice, 1982; Nanson and Hickin, 1986; Richard et al., 2005). In a study of Rio Grande migration, downstream variation in width alone explained over 50% of the variation in migration rate (Richard et al., 2005). Nanson and Hickin (1986) found width explained 44% of variance in erosion rates in western Canadian rivers. If used as a scaling factor for flow energy or river size, width can be a useful basis for describing migration (Knighton, 1998).

Using drainage area as a proxy for river scale, both Hooke (1980) and Brice (1984) found that migration rate tends to increase with the square root of drainage area. In general, the absolute migration rate tends to increase with the size of the river, although this relationship is lost amongst data scatter for anything less than a few orders of magnitude in drainage area (Hickin, 1988).

Stream power, the rate of potential energy expenditure per unit channel length (expressed as a product of discharge and channel slope), has also been

shown to be strongly correlated to migration rate (Lewin, 1983; Nanson and Hickin, 1986). If all other factors remain constant, migration rate should increase as stream power increases (Hickin, 1988). For the Rio Grande, 52% of the variance in migration rate was explained by stream power (Richard et al., 2005). Lewin (1983) also found a good relationship between stream power and migration rate for three rivers in Wales. Nanson and Hickin (1986) found stream power explained 48% of the variance in migration rate for rivers in western Canada.

Within the same Canadian study it was found that when river scale (in this case expressed through discharge and slope) was used in combination with another variable, sediment size at the base of the outer bank, 70% of the total variance in migration rate was statistically explained. Nanson and Hickin (1986) argued migration rate was essentially limited by the rate of entrainment and transport of bed and basal bank-material. Bed erosion undermines the bank, which then collapses into the channel. In this scenario two other variables that are usually included as controlling factors in migration rate, cohesiveness of upper bank materials and vegetation cover, do not play a significant role. However, vegetation in this study only reached 1 to 2 m root depth which left most of the bank unprotected. Vegetation with a greater root depth may be effective at reinforcing the bank (Thorne, 1982). Similarly, Burckhardt and Todd (1998) found that Missouri stream bends with unforested concave banks had average migration rates three times greater than comparable bends with forested concave banks. Following a large flood event on four streams in interior British

Columbia, Beeson and Doyle (1995) reported that river bends with non-vegetated banks were nearly five times more likely to have experienced significant erosion than those bends having vegetated banks.

Complicating any sort of correlation amongst the above variables and migration rate is the nature of migration itself. Meanders do not migrate continuously through time (Brice, 1973; Nanson and Hickin, 1983). They can remain stable for years then move appreciable distances in a relatively short period of time. Furthermore, bends of similar morphology on the same reach can show differing rates of migration. This intermittent nature of migration will have effects on any attempt at correlating rate of movement to controlling factors. A further confounding factor is the interdependence of meanders within a reach. The migration behaviour of any individual bend can only be properly understood if the interaction with the surrounding meanders is taken into account (Furbish, 1991).

1.2.3 Confined Meanders

While the majority of studies noted above have looked exclusively at river meanders that are freely migrating over their floodplain, in reality many rivers are confined in some way by natural or anthropogenic means. Lewin and Brindle (1977) provide perhaps the best overview of confined meanders, detailing their discussion in the literature as far back as 1902. They go on to recognize three degrees of confinement (Figure 1.2). First-degree confinement occurs in relatively wide-floored valleys, where the channel may only occasionally impinge on the confining medium. In second-degree confinement every outside bend

contacts the confining medium; the amplitude of the meander is greater than the width of its valley and alluvial deposits are discontinuous. However, unlike the situation with entrenched or incised meanders, an alluvial plain exists at the bottom of the valley allowing the confined stream to migrate. The third degree of confinement applies to those channels confined to the extent that a meandering pattern does not have space to develop (Lewin and Brindle, 1977). Many meandering rivers display first-degree confinement at some point along their length. However, surrounding unconfined meanders will have an influence on the morphodynamics displayed by a solitary confined bend. It is with second-degree confinement that those properties intrinsic to confined meanders, such as planform distortion, is the most pronounced.

Figure 1.2: Degrees of confinement found in river channels

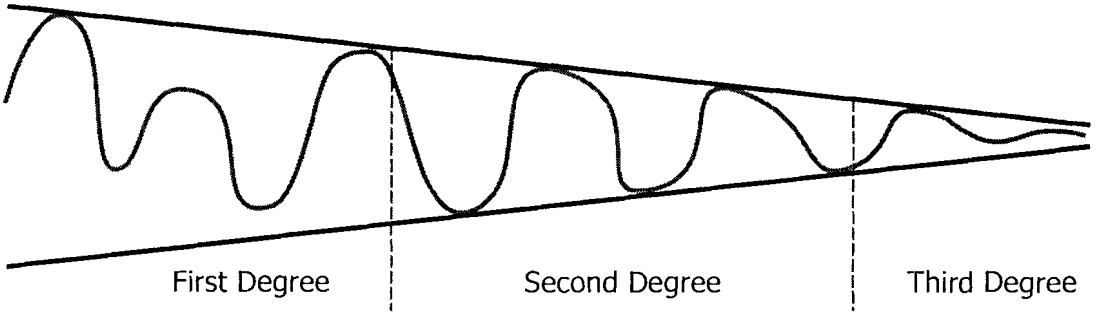

The effect of confinement on meander form has been discussed in the literature for some time. Various studies have noted at least one of the following: a flattening of meanders where the channel impinged on valley walls, acute bends at the point of contact, and a convex-downvalley asymmetry (Hickin, 1988; Hooke and Harvey, 1983; Schattener, 1962; Yarnykh, 1978). Meander dynamics will also obviously be affected by confinement. The three major types of bend

displacement and deformation are translation, extension and rotation (Daniel, 1971), although movement in many bends involves a complex combination of all three. Most river bends will not display pure downvalley translation. By definition, translation implies that all points along the channel are migrating downstream at the same rate, regardless of any change in bend curvature or any other planform property along the reach. This contrasts with the demonstrated relationship between migration rate and bend curvature in freely-meandering reaches of channel (Hickin and Nanson, 1975; Hooke, 2007). Downvalley translation without significant deformation has only been observed within confined meanders whose amplitude is restricted, as well as certain bends of low curvature (Brice, 1982; Ferguson, 1984; Hooke, 1977). Within rivers of second-degree confinement, downvalley translation without deformation of the meander train may be common (Lewin and Brindle, 1977).

Although little research exists on migration dynamics of confined meanders, they have been the focus of research on the development of concave-bank benches, a deposit associated with the sharp meander bends found on second-degree confined rivers (Burge and Smith, 1999; Hickin, 1986; Page and Nanson, 1982). Indirectly, this research has shown that second-degree confinement develops where the ratio of floodplain-width to channel-width ranges from 3:1 to 10:1 (Burge and Smith, 1999; Hickin, 1986). Lower ratios will result in first-degree confinement; higher ratios allow for some form of unconfined meandering.

1.2.4 Bedload Transport and Channel Migration

Bedload transport is notoriously difficult to measure accurately. Nevertheless, estimation of sediment transport provides the basis for much river engineering. The significant spatial and temporal variability of the transport process means direct sampling methods can result in large errors (Carson and Griffiths, 1989). The use of transport formulae has not been very successful; formulae are empirically-derived for specific locations and are not generally transferable (Ashmore and Church, 1998). A third approach, the morphological method, uses the strong link between bedload transport and channel form to provide an estimate. It has been suggested that bank erosion and channel migration is largely controlled by bed-material transport (Nanson and Hickin, 1986). Therefore, the rate of meander migration will be intimately related to the rate of bedload transport in the channel. A distinction must be made here between bedload, which moves primarily in traction along the channel bed, and washload, which moves in suspension through the reach and has little impact on the channel morphology. Morphological methods of estimating sediment transport will thus only provide a transport estimate for the bedload portion of the total sediment load.

Although the first attempt at using channel morphology as a means to estimate sediment transport is generally attributed to Popov (1962), it was Neill's work in 1971 and 1987 that expanded earlier ideas and provided a formal methodology. In the case of strongly-developed meanders, Neill assumed that the material removed from the receding bank of one meander would be

deposited downstream on the next accreting bank. The length of travel for the sediment would consequently be equal to the distance between successive inflection points. The validity of this assumption was first confirmed by Freidkin's 1945 experiments, which showed that, under sustained flow, most particles eroded from a bend were deposited on the next downstream point bar. More recently, Pyrce and Ashmore (2003) reaffirmed that this path length is applicable in meandering rivers under channel-forming discharge, although a small percentage of their tracer particles were recovered farther downstream.

Neill (1987) also noted that as the floodplain was eroded on one side of the channel, it was generally replaced to the same level on the other side. Furthermore, floodplain surfaces are generally composed of a layer of coarse bed-sediment deposits capped by finer-grained overbank deposits. The height of the mobilized bed-material layer, as measured from the channel bottom, can thus be estimated and is assumed to be relatively uniform for the entire floodplain within a reach (Gaeuman and Schmidt, 2003). Knowing the area eroded at a bend over a time period of observation together with the height of the mobilized bed-material layer allows for calculation of the volume of bed material removed from this section of the river and provides an average rate of bedload transport for the reach.

The main limitation of morphological sediment transport rate estimates is their inability to account for throughput (Ashmore and Church, 1998). This can occur as bed material that is carried through the reach without affecting channel morphology (Fuller et al., 2003), or as compensating scour and fill that occurs in

the time interval between successive data collection (Lindsay and Ashmore, 2002). If the assumption of zero throughput is invalid, only a lower-bound sediment transport estimate is obtained. Furthermore, Neill's 1987 method described above deals only with measurement of areas of erosion; all deposition is assumed to take place on next downstream point bar. This method requires that areas of erosion and deposition remain spatially distinct throughout the time interval; amounts of erosion must also exceed the magnitudes of measurement error for sediment transport estimates to be considered meaningful (Ashmore and Church, 1998). In spite of its limitations, bedload estimates based on morphologic approaches do offer distinct advantages. The methods are cost-effective and make use of available historical data (DeBoer et al., 2005), they can be applied at larger spatial scales than other methods (Ham and Church, 2000), they provide valuable information on the direct link between hydraulic processes and form, and possibly best represent the 10 – 100 year timescale that is of principal interest to engineers (Ashmore and Church, 1998).

1.3 Research Objectives and Rationale

Much effort has gone into quantifying the geometry of freely-meandering channels and deriving relationships among the various parameters of meander geometry and meander migration rates (Hey, 1976; Nanson and Hickin, 1986; Williams, 1986). To date, however, the special case of confined meanders has received little attention with respect to these relationships. Whether they hold for highly confined reaches remains to be tested. These are a group of rivers whose meander pattern is a marked change from the norm so their morphometry and

dynamics may also be distinctly different from their freely-meandering counterparts. Although exploring this knowledge gap has value for the field of fluvial geomorphology, the fact that these channels are common in mid-latitudes signifies that this is a matter of practical import as well.

Furthermore, human encroachment on river floodplains is increasing and the need to fully understand the natural state of these river channels is important. Rivers that were once freely meandering can become artificially constrained by the growth of infrastructure located on the floodplain. The derivation of relationships that could aid in prediction of migration rates and sediment transport for these confined streams would be of great interest to those involved in river management, particularly if such relations apply across a range of channel scales.

The overall objective of this research is to describe second-degree confined-meandering fluvial systems. There are two main components in the project to achieve this. The first involves examination of the planform geometry of confined channels. The second is the estimation of confined meander-migration and bedload transport rates. It is anticipated that these variables can be incorporated into a statistical description of confined meanders that may be used in the future for predictive modelling.

Specific questions to be addressed are:

1) What is the statistical nature of confined-meander planform geometry? Are there orderly relationships amongst the variables of planform geometry?

2) What is the rate of migration of confined meanders? How do the migration rates compare to those previously reported for freely meandering rivers?

3) How does migration rate vary with planform geometry as well as other factors, such as discharge? Are the relationships observed for freely meandering rivers applicable to confined meanders?

4) What is the average rate of bedload moving through the study reaches?

CHAPTER 2: METHODOLOGY

2.1 Research Locations and Selection Criteria

2.1.1 Study Site Selection

This study examines a set of second-degree confined meandering rivers located on the Canadian prairies. Only those reaches where meander bends impinged on both valley walls are considered. In these cases, meander geometry displays the convex-downvalley asymmetry typical of confined-meandering rivers (Figure 2.2). The strength of a statistical description of confined meander geometry and kinematics depends on its ability to be independent of river scale. To this end, effort was made to select rivers that varied over a range of channel width. A further consideration is that reaches are not impacted by structures and other disturbances that may have altered natural meander characteristics. A subset of the rivers was selected that had road access for evaluating field conditions relevant to estimating bedload transport.

Initial survey of the region for suitable reaches was based on Google Earth software. The resolution of this imagery varies depending on location so

the identification of suitable confined-meandering rivers at the smaller range of scale was somewhat limited. Once potential study locations were identified through the satellite imagery, topographic maps were consulted to verify that the reach was confined. Lastly, searches at both the Alberta and British Columbia government air photo libraries were undertaken to confirm the air photo record for the potential site spanned a sufficient time interval to detect meander migration and is of appropriate scale for measurement of channel features. This process resulted in the identification of the 24 study locations used in the research.

2.1.2 Research Locations

The twenty-four study sites are scattered throughout Alberta and into British Columbia (Figure 2.1). With the exception of the Kootenay River site, all rivers are located east of the Rocky Mountains on the Canadian prairies. The length of channel examined for each location varied depending on the number of sequential confined-meander bends on the river. At a minimum, three meander bends were examined although typically a selection included 9 bends and ranged up to 25 bends in the case of the Beaver River in Alberta. Figure 2.2 displays a portion of the reach of channel investigated for each river as seen in the most recent aerial photography used for this study. The reaches span a range of channel scale, with mean annual flood discharge varying over two orders of magnitude from 36 to 3870 m^3/s.

Figure 2.1: Locations of study sites within Alberta and British Columbia

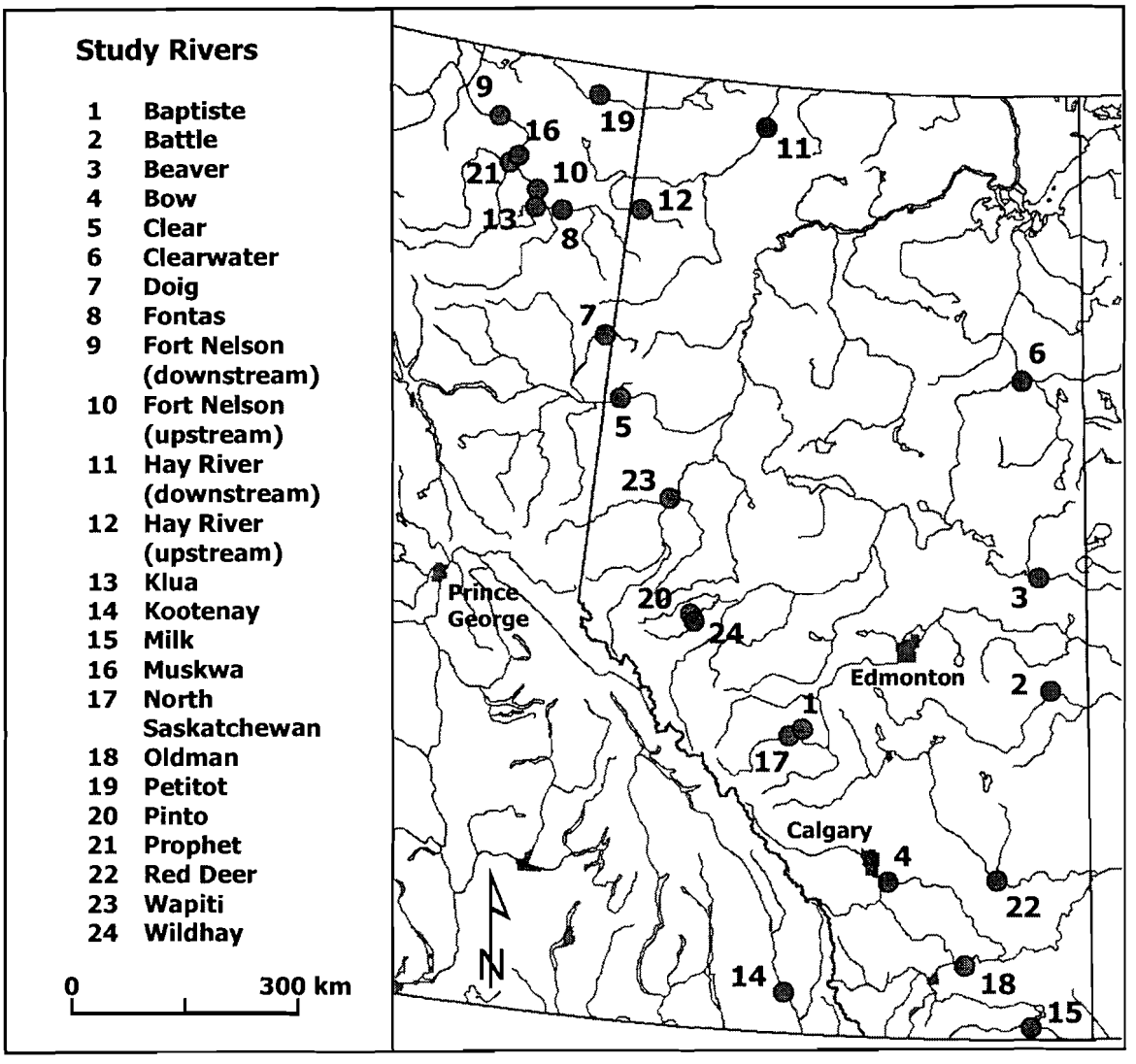

Figure 2.2: A section of each study reach as shown by recent aerial photography

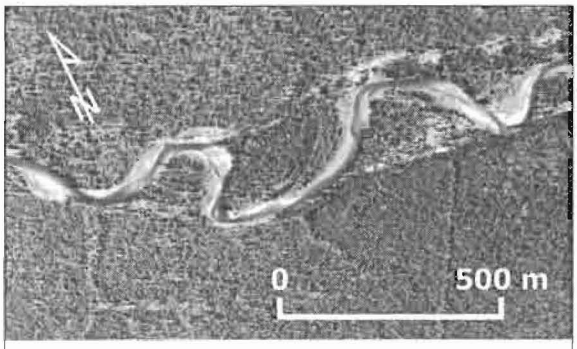

Baptiste River

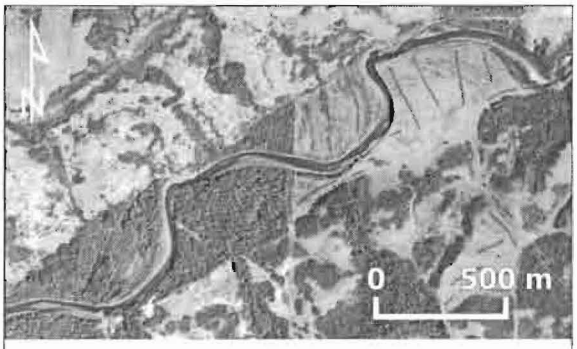

Battle River

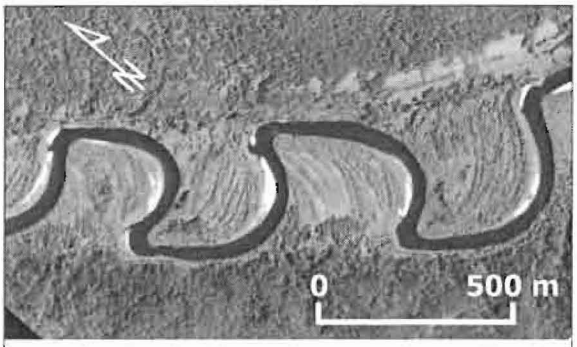

Beaver River

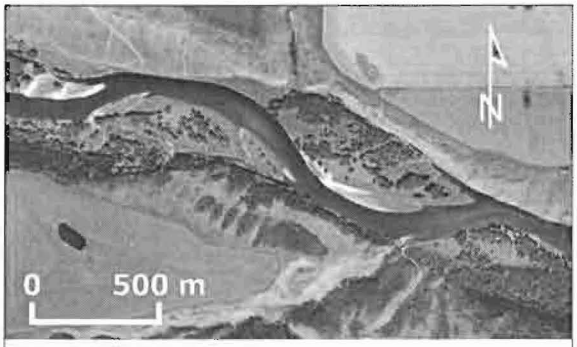

Bow River

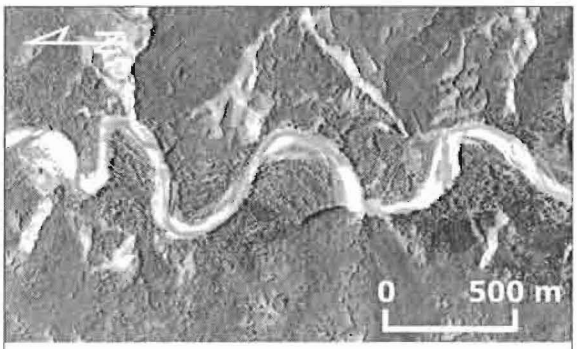

Clear River

Clearwater River

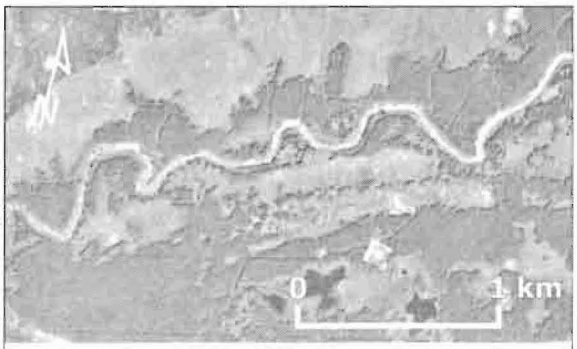

Doig River

Fontas River

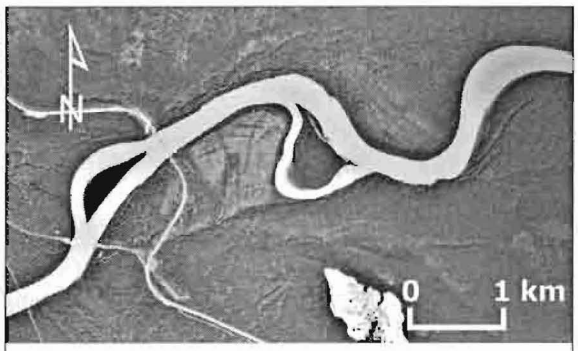

Fort Nelson River (downstream)

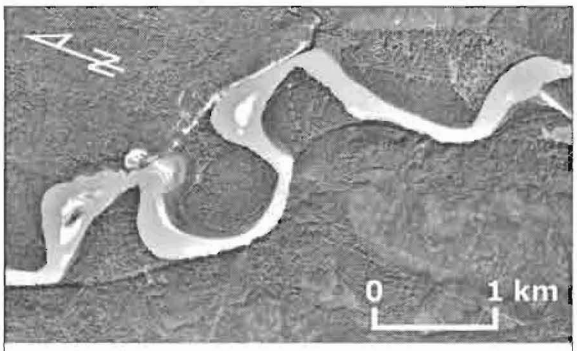

Fort Nelson River (upstream)

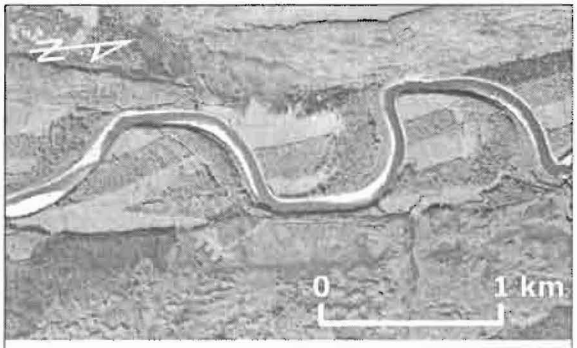

Hay River (downstream)

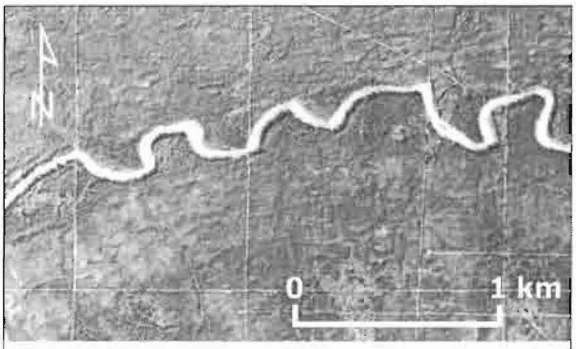

Hay River (upstream)

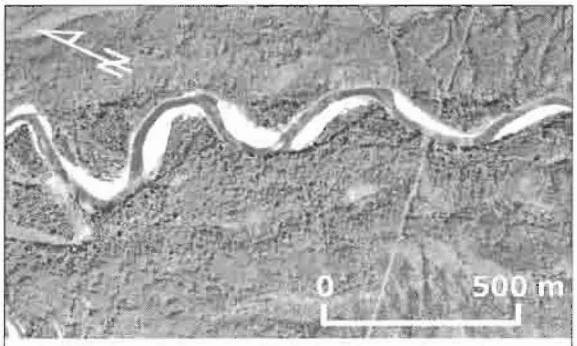

Klua River

Kootenay River

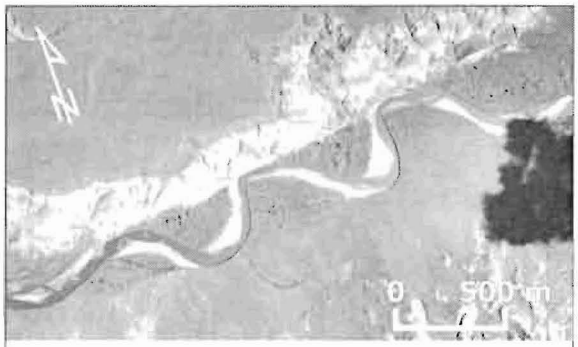

Milk River

Muskwa River

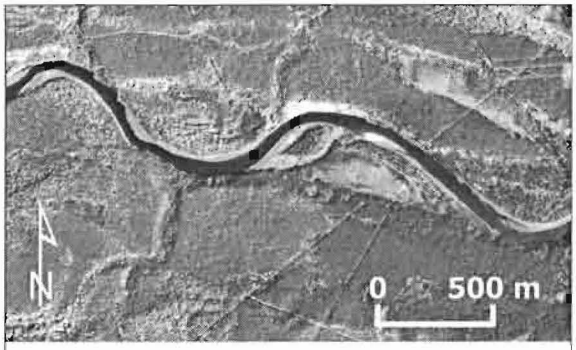

North Saskatchewan River

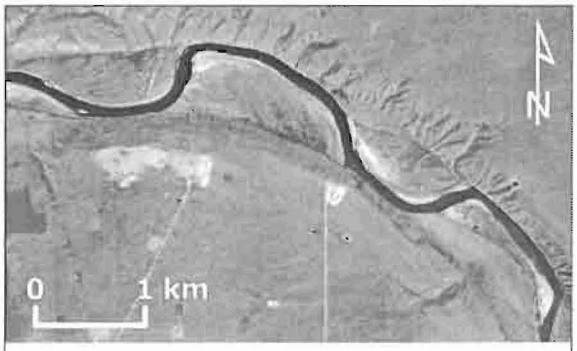

Oldman River

Petitot River

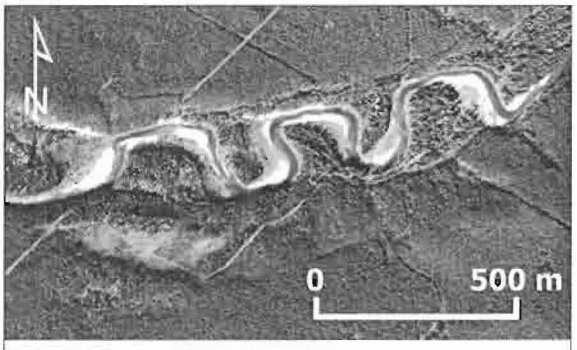

Pinto River

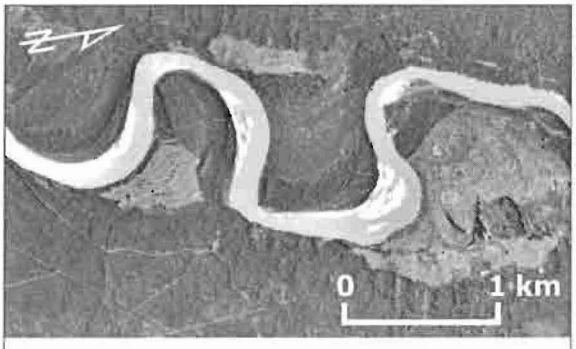

Prophet River

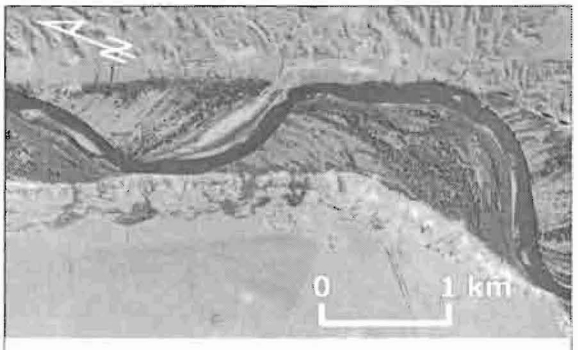

Red Deer River

Wapiti River

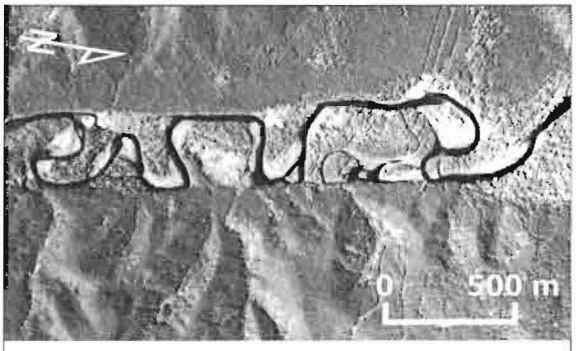

Wildhay River

The hydrologic regime is similar among the sites, generally characterised by peak flows due to snowmelt occurring sometime between late-April and mid-June, followed by a gradual decline in discharge to a minimum during the winter months. Although it is not the aim of this study to determine the origin of the confining valleys, most, if not all, are former glacial-meltwater channels (Kellerhals et al., 1972; Mathews, 1980). Sediment-size data for the study locations are limited. Previously published data combined with field observations reveal basal sediment-size variation from fine sand to large cobbles (Burge and Smith, 1999; Kellerhals et al., 1972; Nanson and Hickin, 1986), although information is lacking for some of the sites.

2.2 Aerial Photography

2.2.1 Considerations for Air Photo Use

Measurement of planform geometry and migration rate for this study was completed through analysis of historical aerial photography. The use of aerial photography to determine river-planform change is commonly reported in the literature (Gurnell, 1997; Petts, 1989; Wellmeyer et al., 2005). At present, the widespread availability of GIS and image rectification software have facilitated the process of scanning and co-registration of aerial photography. The resulting georeferenced data sets can easily be overlain to detect channel change. However, there remain concerns with the quality of the resultant data that need to be recognized.

Results obtained using aerial photography are only reliable if the measured amount of change exceeds the magnitude of errors involved in that measurement. These errors can be significant; the methodology for estimating error proposed by Mount and Louis (2005) for channel migration indicates that 20 to 34% of measured lateral movement could be due to error. There are two main sources of error in using aerial photography for planform analysis. The first relates to spatial distortions remaining within the processed imagery, the second is the error involved in delineating the features of interest (Mount et al., 2003). This second source of error is most likely random in nature (Mount et al., 2003) and can be minimized through use of one operator (Winterbottom and Gilvear, 2000) and by digitizing features at the same photo scale and resolution (Gurnell, 1997). In their investigation of operator error in delineating features, Mount et al. (2003) used bankfull width to suggest a feature could be identified to a precision of +/- 2 pixels in georeferenced imagery. In the present study, this would equate to a precision of around +/- 2 m, although this may decrease in areas of shadow or overhanging vegetation.

The other source of error, residual spatial distortion, varies according to the processing the aerial photography receives. To produce digital overlays for use in channel-migration estimates, photography has to be co-registered. Polynomial rectification is commonly used and is comprised of three steps: matching ground control points (GCPs) on scanned photos to a base layer, transformation of the scanned image to a geographical projection and coordinate system, and pixel resampling. Each step will have some bearing on the

magnitude of error in the final data set. The number, type, and placement of GCPs will impact the quality of the transformation. Hughes et al. (2006) found that the root mean square (RMS) error remained the same when 8 or more GCPs are used in co-registration. However, absolute error in test point displacement still decreases substantially until 12 GCPs are used in the registration process, though this is not reflected in the RMS error (Hughes et al., 2006). The use of hard GCPs (road intersections, building corners) is preferred but introducing a few soft GCPs (solitary trees) does not significantly decrease the overall accuracy of the transformation (Hughes et al., 2006). Gurnell (1997) found further improvement in accuracy when a standard set of GCPs are used for registration of all photos of an area. Accuracy is also improved if GCPs are concentrated within the area of interest rather than spread over the image (Hughes et al., 2006). Additionally, it was found that second-order polynomial transformation provides the highest accuracy; third-order results in excessive warping of the imagery while first-order transformations will only be satisfactory if all GCPs (and the area of interest) are located on a flat floodplain (Hughes et al., 2006). Finally, the resampling method used in the rectification process will have an impact on the ability to discern and demarcate the features of interest through its effect on boundary smoothing. Hughes et al. (2006) found cubic convolution to work best for their study, although it is noted that this may not always be the case.

2.2.2 Processing of Air Photos

Black and white contact prints providing stereo coverage of all research locations were obtained from the government air photo libraries of Alberta and British Columbia. The number of time periods examined for each river reach varies according to the availability of suitable air photos. Those sites with a lengthy photo record have up to four sets of air photos analysed while lack of photo record for certain sites resulted in examination of just two separate years of photography (Table 2.1). Ideally, to optimize consistency and therefore minimize sources of error, photography of similar scale should be used for all time periods examined (Gurnell, 1997). In reality, acting on this recommendation is limited by what historical photography is available. Earlier photography, in particular, tends to be relatively small scale (1:40 000) although the scale of later photography is between approximately 1:15 000 to 1: 40 000 (Appendix A).

Table 2.1: Research locations and years of aerial photography used in analysis

River	Years of Photography
Baptiste River	1951, 1975, 1997
Battle River	1949, 1975, 2002
Beaver River	1952, 1969, 1988, 2000
Bow River	1950, 1982, 1998
Clear River	1952, 1978, 1997
Clearwater River	1951, 1972, 1985, 1997
Doig River	1956, 1975, 1997
Fontas River	1967, 1979, 1997
Fort Nelson River (downstream)	1967, 1997
Fort Nelson River (upstream)	1966, 1979, 1997
Hay River (downstream)	1953, 1976, 1994
Hay River (upstream)	1954, 1979, 1993
Klua Creek	1967, 1991
Kootenay River	1952, 1975, 1991, 2004
Milk River	1951, 1962, 1983, 1995
Muskwa River	1953, 1966, 1975, 1997
North Saskatchewan River	1951, 1976, 1995
Oldman River	1951, 1961, 1975, 1998
Petitot River	1966, 1997
Pinto Creek	1951, 1980, 2001
Prophet River	1966, 1979, 1997
Red Deer River	1950, 1962, 1985, 2001
Wapiti River	1950, 1972, 1989, 2001
Wildhay River	1952, 1963, 1980, 2001

Air photo prints were scanned at 1200 dpi, resulting in a pixel size in ground units of less than 1 m for all scales of photography used. This digital imagery was then brought into ArcGIS 9.1 for georectification using at least 12 GCPs per photograph where possible. When feasible, GCPs are located close to the rivers, with preference given to locating hard targets for GCPs. Given the

remote nature of many of these river reaches, however, choice of GCP targets is limited. The GCPs used for rectification were either collected through GPS survey in the field or, failing that, topographic maps have been used to provide control. The most recent photography for each study site was georeferenced using the GCPs, all other years of photography for the site were then registered to this base layer. An attempt was made to use the same set of GCP locations for rectifying all photo-sets for a site; however, due to temporal changes this is not possible for all time intervals. A second-order polynomial is used for the transformation. Cubic convolution was found to be the best suited method of resampling and all pixels are resampled to a 1 m cell size to coincide with the lowest resolution data, the 1:40 000 scanned photography.

The RMS errors for georectification at all study sites range from 1.1 to 10.9 m with an average of 4.9 m. A complete table of RMS errors for the rectified photos is shown in Appendix A. The RMS errors here are comparable with those reported in similar studies elsewhere (Gilvear et al., 2000; Gurnell et al. 1994; Winterbottom and Gilvear, 2000). Gurnell et al. (1994) concluded that change in channel-boundary positions greater than 5 m is likely due to genuine geomorphological change, an assumption also used by Winterbottom (2000) and Gilvear et al. (2000). With similar photo scales, scanning resolution, and geoprocessing methodology used here, it is likely that this assumed magnitude of error applies to this study as well.

2.3 Measurement of Channel Features in GIS

2.3.1 Channel Boundaries

Channel outlines (and subsequently described channel features) were digitized at 1:1000 scale using ArcGIS 9.1 software. Although several studies use the edge of vegetation or change in vegetation type to denote channel boundaries (Richard et al., 2005; Winterbottom, 2000), initial overview of the research locations illustrated potential concerns with using this approach. First, field sites are distributed over a large geographical area and therefore span markedly different ecological zones. For example, vegetation in one study reach may be dominated by grasses while another has thickly wooded floodplains, causing difficulty in applying the same boundary criteria to all sites. Photo quality and therefore the ability to delineate exposed bars accurately also varies between photos. Finally, the presence of sand splays in certain reaches results in an erroneous outline if edge of vegetation is used. It was decided that using the water boundary to denote the edge of the channel is a more objective approach due to its clarity in the aerial photography. Of course, there remains a concern about the effect of varying water-stage between photography dates. To decrease this particular error air photos were chosen for each site that have been taken within the same time of year. Furthermore, the two digitized channel boundary lines are used in ArcGIS to generate a channel centreline (the line connecting the locus of points equidistant from the channel boundaries). This centreline, rather than either channel boundary, is used for subsequent analysis. This has an

averaging effect that likely decreases the error associated with change in water stage.

2.3.2 Bankfull Width

Bankfull width is measured at meander inflection points and taken to be the distance across the channel, as defined by vegetation boundaries. The first occurrence of visible vegetation is used as the boundary indicator in cases where bars displayed sporadic vegetation cover. Widths are not measured in inflection areas with mid-channel bars. The arithmetic average of measured bankfull width is used in subsequent analysis.

2.3.3 Meander Wavelength

The valley axis is used to obtain the distance downvalley required for calculation of meander wavelength. Each side of the valley bottom is digitized at 1:5000 scale in ArcGIS. These two boundary lines are then used to generate the valley axis (valley centreline). The channel centreline is used to split the valley axis at each meander crossing. The length for each new segment of the valley axis is calculated and multiplied by 2; the average of these calculations is taken to be the meander wavelength for that study reach.

2.3.4 Sinuosity

Much the same as for the calculation of wavelength, the channel centreline is split at each meander crossing using the valley axis. The length of each segment of the channel centreline is calculated and multiplied by 2. This number is then divided by the average wavelength previously calculated for that

river. The arithmetic average of all calculated sinuosity values is used for analysis.

2.3.5 Meander-Belt Width

The meander-belt width is equal to the valley width in the case of confined meanders. This distance is measured perpendicular to the valley bottom at a spacing of ½ wavelength. The average of these lengths is taken to be representative for the reach.

2.3.6 Radius of Curvature

Radius of curvature (Rc) is measured by two different methods. First, a series of circles are drawn in ArcGIS, subjectively determined to be those that best fit the meander bends as represented by the channel centreline. The radius of that circle is then calculated and taken to represent the radius of curvature for that bend. Due to the convex-downvalley asymmetry of the meanders there may be more judgement involved in determining the best-fit circle for a confined meander than in previous studies that have used this technique on more symmetrical bends (Leopold and Wolman, 1960; Williams, 1986). To try to quantify the subjectivity involved in this method several operators independently determined Rc values for one of the river reaches. Where meander bends were regular the Rc values determined varied by 7%. If the Rc values for the more irregular bends (squared bends or those having very long convex-downvalley arcs) are added to the sample, the average difference in measured Rc values

rises to 13%. These values are comparable to those obtained by Williams (1986) in a similar consistency check.

The second method of measuring radius of curvature results in a more objective set of Rc values, created through use of a point-sampling protocol and analysis by formulae. A series of points spaced two channel widths apart are generated along the channel centreline. The UTM coordinates of these points are then exported to a spreadsheet. A running calculation is used to measure the radius of the circle that circumscribes the triangle defined by each consecutive three points. Figure 2.3 depicts the method as well as the formulae used. This yields a distribution of Rc values for the entire study reach.

Figure 2.3: Point-sampling method for calculating Rc values

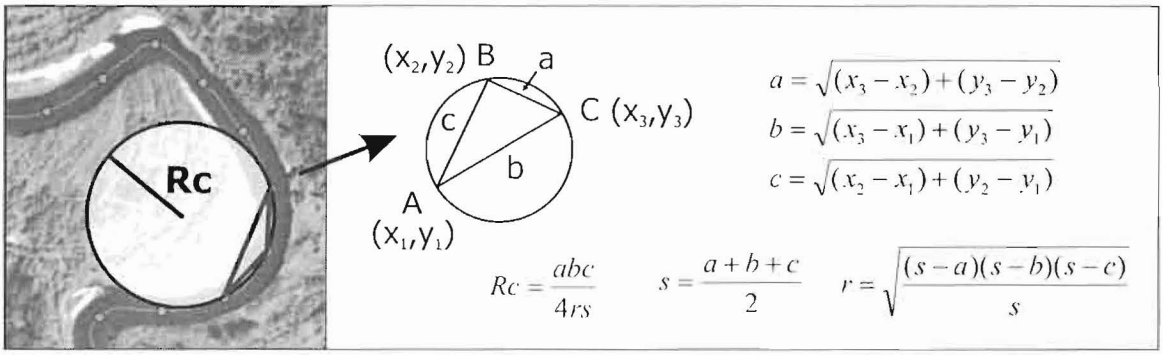

2.3.7 Downvalley Translation

The movement downstream is measured between successive channel centrelines along the valley axis. A further measurement is taken between the centrelines of the earliest and most recent photography to obtain the total downstream movement over the period of photo record. The measured movement is averaged for all bends in a study reach for each time interval. This

average is then divided by the number of years between the sets of photographs to obtain a migration rate.

2.3.8 Channel and Valley Slopes

Where possible, channel slope values are taken from previously published material. To be used, published values have to be calculated for a section of river that includes the study reach; slopes obtained using field-measured water-surface elevations are preferred over those obtained through use of topographic maps. The remaining slopes are calculated using NTS 1:50 000 topographic maps underlain by Canadian Digital Elevation Data (CDED) in OziExplorer 3.95.4e software. The CDED data is extracted from the hypsographic and hydrographic elements of the National Topographic Data Base (NTDB) and therefore have the same level of resolution. The channel centrelines for the study reaches were imported into OziExplorer and underlain with the topographic map and elevation data. The difference in elevations of the channel centreline endpoints is divided by the length of the centreline to obtain a slope value. Valley slopes were obtained in OziExplorer in much the same way; the valley axis is used in place of the channel centreline for the location of endpoints and length of reach.

2.3.9 Drainage Area

Drainage areas are calculated using a combination of available watershed boundaries and 1:50 000 NTS topographic maps. The Prairie Farm Rehabilitation Administration (PFRA) is the authoritative source for the gross and effective

drainage areas in the Canadian prairies; most study reaches are found within their jurisdiction. Furthermore, there is available watershed boundary coverage for those study sites in British Columbia found outside this jurisdiction through the B.C. Watershed Atlas. In certain cases, either the PFRA or B.C. Watershed Atlas drainage areas exactly coincided with the drainage area for the study reach. For most research locations, however, this is not the case. In these situations, as much of the applicable watershed boundary available through the PRFA or B.C. Watershed Atlas is used and the missing portion was digitized using the drainage divides visible on underlain topographic maps in ArcGIS. The area of the resultant polygon is then calculated and used as the drainage area for that research location.

2.3.10 Mean Annual Flood

Water Survey of Canada (WSC) peak flow data for the closest gauge stations to the study sites were imported into a spreadsheet. The arithmetic average of the instantaneous maximum discharge data is calculated and taken to represent the mean annual flood for that gauge site. For years with no instantaneous maximum discharge recorded, the maximum discharge is used after this discharge was adjusted upwards by the average difference between instantaneous and maximum discharge for the years having both fields of data. Where applicable, the relationship between drainage area and mean annual flood is assumed to be linear. Although studies have indicated this may not be the most appropriate representation of this relationship (see Eaton et al., 2002),

given the accuracy of the calculated drainage area as well as the gauging data used within this study the simpler linear relation is justified.

There are four possible relationships between the study sites and the nearest WSC gauge, resulting in differing solutions for calculation of mean annual flood (MAF).

1. WSC gauge is within study reach or less than 15 km away.
    - The average of the instantaneous maximum discharge data for the gauge is used as the MAF for the study site.
2. WSC gauge is more than 15 km upstream or downstream of study reach.
    - The MAF is calculated as described above using the gauge data. This average is divided by the drainage area of the WSC gauge site to find discharge per unit area; this number is then multiplied by the actual drainage area of the study site.
3. WSC gauges exist on either side of the study site but both are more than 15 km away.
    - The MAF is calculated for both gauges as described above and a plot of drainage area versus MAF created using these two points. The equation describing the line connecting the two points is used to calculate the MAF corresponding to the drainage area at the study site.
4. No WSC gauge exists on the river.

- The MAF is calculated as described above for the nearest stream of comparable drainage area that did have a WSC gauge. This MAF is then divided by the drainage area of the gauge site to find discharge per unit area; this average is then multiplied by the actual drainage area of the study site.

2.4 Bedload Transport Estimate

Field work was undertaken on five of the 24 study sites to obtain estimates of bedload transport through the reaches. An average bedload-transport rate was calculated using the following equation:

$$Q_s = \frac{Ah}{t} \qquad (2.1)$$

where Q_s is the bedload-transport rate, A is the area eroded over the time period of observation, h is the thickness of the mobilized bed material layer, and t is the time period of observation in years.

The area eroded at each bend is measured using ArcGIS by overlaying the digitized outlines of the channel for the earliest and most recent aerial photography. This allows for calculation of the eroded area between the two successive concave-bank lines. The time period of observation is equal to the time lapse between the two dates of aerial photography. Field work for estimation of bedload transport was thus concentrated on determining the height of the mobilized bed-material layer above the thalweg.

In the rivers chosen for this work, banks displayed a sharp delineation between the coarser bed materials and finer-grained overbank deposits. To determine the thickness of the coarser layer the difference between the depth of the thalweg and the height of the layer as seen in the channel bank is required (Figure 2.4).

Figure 2.4: Methodology for measuring thickness of the mobilized bed-material layer

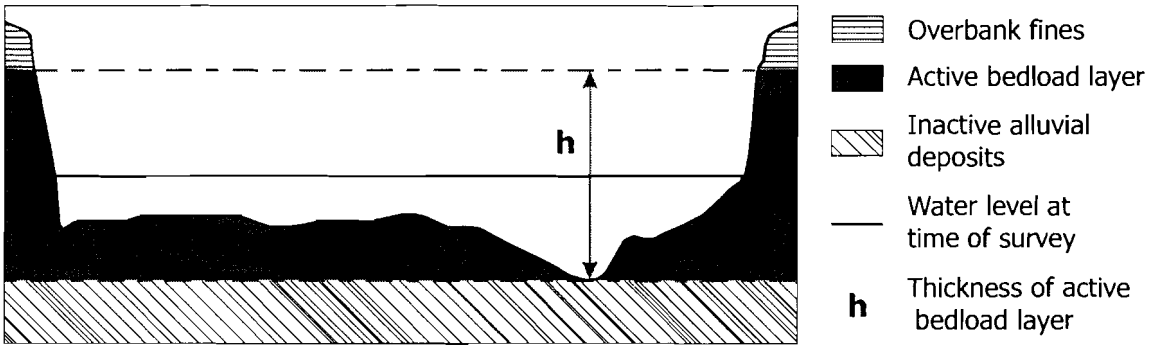

Channel cross-sections were constructed using standard surveying techniques. Three to four channel cross-sections were surveyed per bend, with two bends per river examined for four of the sites and one bend surveyed on the fifth. Cross-sections were chosen on bends with no tributaries and were evenly spaced along the downstream limb of the meander. Channels were surveyed to the top of the bank on either side, with care taken to include the elevation of the water edge and the height of the coarse layer visible in the bank. Endpoints for the cross-section were marked with GPS. Water depths were acquired through a combination of an electronic depth finder and stadia rod. The depth of shallow sections was measured directly using a stadia rod at 1 m intervals. When flow depth made this method unsuitable, an electronic depth finder mounted on a

small Zodiac boat was used to continue the section. Highly visible markings were placed on either bank of the cross section and depths were read off the depth finder every 2 seconds while boating across the channel at a slow, steady speed. Several runs at each cross-section were completed to ensure that there is consistency in the recorded depths. Channel width was measured using an electronic range finder. Finally, numerous photos were taken at the cross-section to record the section characteristics. The channel depths and survey measurements were combined to construct the cross-sections. Each bend yielded several estimates of the height of the mobilized bed layer; the average height was used for inclusion in the transport equation.

2.4.1 Pebble Count

The size of bed material being transported was determined by a 'step-toe' pebble count (Harrelson et al., 1994) for each of the five rivers visited in the field. Two to five bars on each river were examined, depending on the number of bends investigated for the bedload transport estimate. The intermediate axes of 100 clasts were measured on each bar; clasts were blindly selected to avoid bias. Descriptive statistics were used to express the characteristics of the pebble counts.

CHAPTER 3: PLANFORM GEOMETRY AND KINEMATICS OF CONFINED MEANDERS

3.1 Introduction

This chapter is divided into two parts; the first relates to the planform geometry of the confined meanders while the second explores downstream channel migration at the study sites. Each part is organised in much the same way: the data for all study locations are presented, followed by analysis of the data and discussion of identified relationships.

3.2 Planform Geometry

Bankfull width, wavelength, sinuosity, meander belt width and radius of curvature (Rc) were measured for each of the 24 study sites. A summary of these data is shown in Table 3.1; the numbers presented are arithmetic averages except where indicated.

Table 3.1: Summary of planform geometry measurements

River	Channel Bankfull Width (m)	Channel Wavelength (m)	Channel Sinuosity	Meander Belt Width (m)	Median Radius of Curvature (m)
Baptiste River	21	456	1.4	167	135
Battle River	32	991	1.4	412	213
Beaver River	44	757	1.5	337	213
Bow River	117	2098	1.1	403	785
Clear River	57	642	1.5	279	191
Clearwater River	126	1958	1.7	1380	467
Doig River	28	750	1.3	236	165
Fontas River	68	1208	1.6	582	320
Fort Nelson River (downstream)	288	4578	1.4	1491	863
Fort Nelson River (upstream)	163	2036	1.6	802	622
Hay River (downstream)	86	1673	1.4	770	434
Hay River (upstream)	44	627	1.6	312	120
Klua Creek	43	663	1.2	223	217
Kootenay River	123	1825	1.4	991	479
Milk River	74	1219	1.2	318	231
Muskwa River	205	2441	1.3	1032	471
North Saskatchewan River	60	1612	1.2	500	450
Oldman River	140	2214	1.2	598	435
Petitot River	99	662	1.2	255	158
Pinto Creek	33	591	1.8	192	77
Prophet River	142	2109	1.7	990	428
Red Deer River	140	3063	1.2	816	823
Wapiti River	139	2032	1.2	469	464
Wildhay River	39	571	1.8	345	93

Figure 3.1 displays the distributions of bankfull width, wavelength, sinuosity and meander-belt width of the study channels. Bankfull width ranges from 21 m to 288 m. The Fort Nelson River (downstream site) represents the largest of the rivers examined and at 288 m in width is nearly 84 m wider than the next largest river (Muskwa River). Channel wavelength ranges from 456 m to 4578 m and meander-belt width, equivalent to the valley width in the case of

confined meanders, ranges from 167 m to 1491 m. In both cases the Fort Nelson River downstream site yields the largest measurement. The smallest values for bankfull width, wavelength, and meander belt width were measured on the Baptiste River, respectively 21 m, 456 m and 167 m.

Figure 3.1: Histograms for channel width, wavelength, sinuosity and meander-belt width

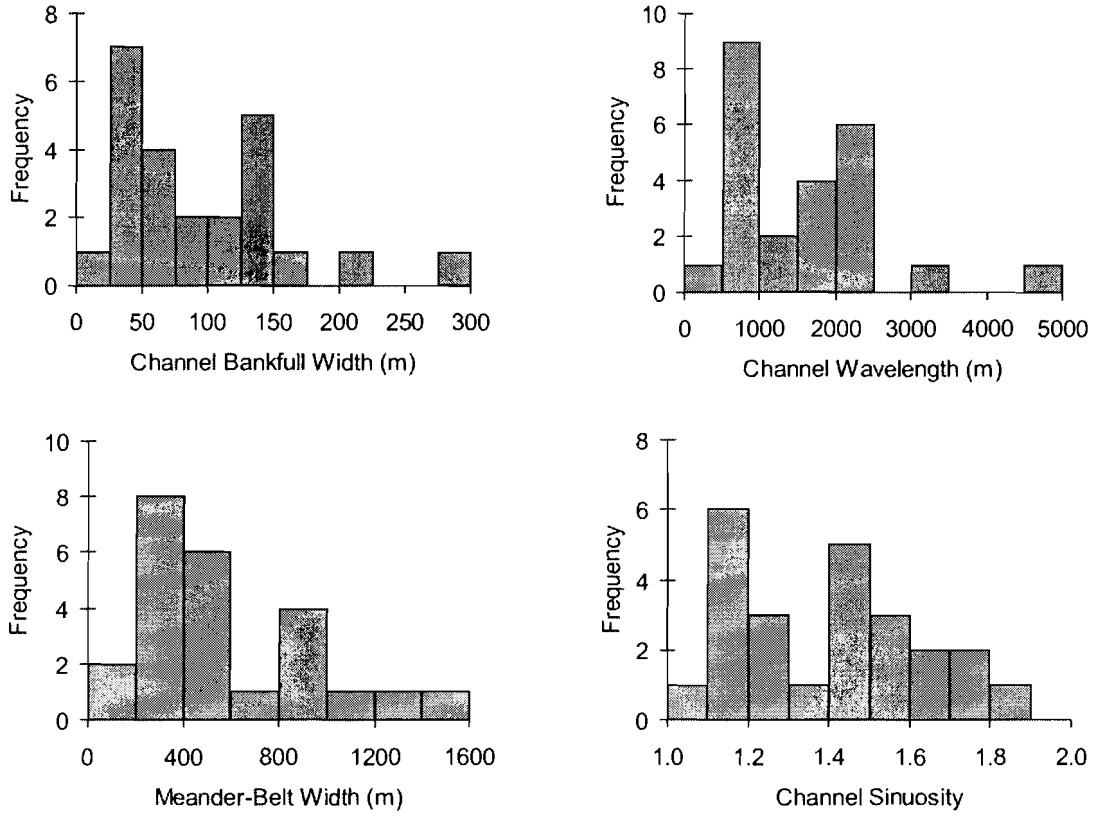

Sinuosity values are similar, ranging from 1.1 to 1.8, across the full range of river scale. The degree of confinement of these rivers limits the sinuosity that

can be achieved, leading to sinuosity values that are low relative to those generally found for meandering rivers (~2.0).

The two different methods of Rc measurement, the 'best-fit' circle method and the point-sampling method, resulted in two distinct sets of Rc values (Table 3.2). With the exception of the Klua Creek site, where the Rc values of the two methods are approximately equal, the point-sampling method consistently generates larger radius of curvature values. On average, the median Rc for each river generated through the point-sampling method is 55% larger than that obtained for the same rivers using the 'best-fit' circle method.

Table 3.2: Median radius of curvature (Rc) for the study reaches

River	'Best-fit' Circle Method		Point-Sampling Method	
	Median Rc (m)	Median Rc/w	Median Rc (m)	Median Rc/w
Baptiste River	135	6.4	200	9.5
Battle River	213	6.6	307	9.5
Beaver River	213	4.9	231	5.3
Bow River	785	6.7	1028	8.8
Clear River	191	3.3	230	4.0
Clearwater River	467	3.7	598	4.8
Doig River	165	5.8	301	10.6
Fontas River	320	4.7	433	6.4
Fort Nelson River (downstream)	863	3.0	1333	4.6
Fort Nelson River (upstream)	622	3.8	639	3.9
Hay River (downstream)	434	5.0	523	6.1
Hay River (upstream)	120	2.8	196	4.5
Klua Creek	217	5.1	212	4.9
Kootenay River	479	3.9	706	5.7
Milk River	231	3.1	449	6.1
Muskwa River	471	2.3	1010	4.9
North Saskatchewan River	450	7.5	582	9.6
Oldman River	435	3.1	793	5.7
Petitot River	158	1.6	353	3.6
Pinto Creek	77	2.4	170	5.2
Prophet River	428	3.0	617	4.3
Red Deer River	823	5.9	1005	7.2
Wapiti River	464	3.3	900	6.5
Wildhay River	93	2.4	197	5.0
Average for all reaches		4.2		6.1

Figure 3.2 shows the distribution of Rc/w values for all meander bends examined in the study; a secondary y-axis is used to facilitate comparison between the two methods. The overall shape of the Rc/w distributions for both methods are very similar. Both methods result in positively-skewed Rc/w distributions but it is more pronounced for those obtained by the point-sampling method. While Figure 3.2 presents data up to an Rc/w value of 25, in actuality,

the point-sampling method produced values up to the extreme of 3762. The majority of values however, were concentrated about the overall median Rc/w of 5.9. The 'best-fit' circle method produced a more limited range of values from 1.1 up to a maximum Rc/w of 13. The overall median of Rc/w values established through this method is 4.1.

Figure 3.2: Rc/w distributions for both measurement methods

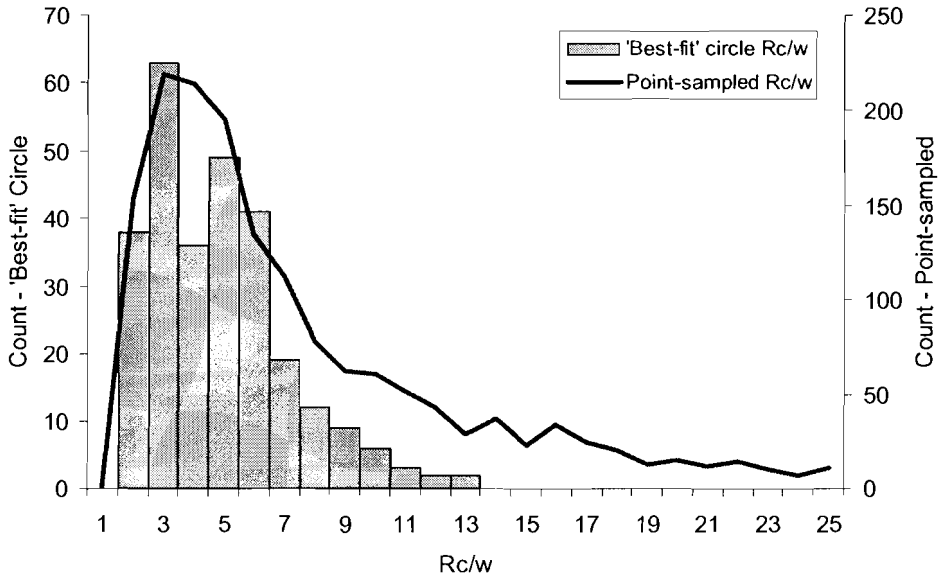

Both measurement methods produce a higher median Rc/w than those of other studies reported in the literature. For example, Williams (1986) found a median Rc/w of 2.43 for 79 rivers in the USA while the distributions of Rc/w values presented in Hooke (2007) from British streams, using both her data and those from the USA Transportation Boards (TRB, 2004), display medians that appear to be between 2.5 and 3. In their study of western Canadian rivers, Nanson and Hickin (1986) found that 78% of measured Rc/w values fall between

2 and 4. In this study, 36% of Rc/w values measured using the 'best-fit' circle method are between 2 and 4. With point-sampling, this percentage drops to 25%.

There appears to be several reasons why the Rc/w is higher for rivers in this study. First, examination of the pattern of meander migration over the photo period reveals that the river meanders generally tend to translate downstream as a package and cut-offs are relatively uncommon compared to the case of freely meandering rivers. Bend over-tightening commonly precedes the generation of a cut-off in meandering rivers, leading to a decrease in the channel curvature. As this process appears to be relatively rare on these confined rivers, the corresponding reduction in Rc/w does not occur. Secondly, freely-meandering rivers may migrate outwards (towards the bend apex) rather than downstream, a process that would also lead to a decrease in total curvature. That is, the meander inflection points remain stationary while the bend moves outward, tightening the bend curvature. This outward movement is not possible for confined meanders. As the bends migrate downstream the inflection points are moving with the bend and the bend curvature remains relatively constant. Furthermore, although these confined meanders have very sharp bends at the point of impingement on the valley wall, most of each meander is comparatively open. Particularly in the case of the 'best-fit' circle method of measurement, it is the curvature of the larger, convex-downvalley arc that has the greatest influence on the value of Rc. There does seem to be some evidence for a bimodal Rc distribution in the 'best-fit' circle Rc/w distribution, which may be a reflection of

these two distinct curvature types (open arc and overtightened impingement segments) found in confined meanders.

That the highest curvature values are found with the point-sampling method is not surprising, and is inherent in the methodology. Points were spaced every two channel widths along the channel centreline and each consecutive three points were used to generate an Rc value. Thus, many of these curvature values will represent the long, straight section of bend that runs along the valley wall, just downstream of the point of channel impingement. Although this method is decidedly the more objective approach, inclusion of these very high curvature values increases the median curvature for the reach. Although somewhat more subjective, the curvature values generated by the 'best-fit' circle method of measurement are those that best represent the curvature of interest for this study and it is these values that will be used in subsequent analysis. The similarity of the two distributions of Rc/w validates the assumption that subjectivity has not compromised the usefulness of the values obtained through the 'best-fit' circle method and that they are representative of the meander curvature. Due to the positively-skewed distributions, in subsequent analysis the median Rc and Rc/w value rather than the mean has been chosen as the representative value for the river.

3.2.1 Relationships in Planform Geometry

The planform-geometry variables of the confined meanders were plotted against each other to determine the nature of any relationships. One strong relationship common in rivers is that between wavelength and channel width.

Channel wavelength generally is 8 – 12 times the width; this relationship is evident in the confined meanders as well (Figure 3.3). However, a line fit using simple linear regression indicates a slightly higher coefficient whereby the wavelength is 15 times the bankfull width. While not significantly different from the free-meandering counterpart, this higher coefficient may reflect the fact that these bends generally migrate downstream as a package and do not develop the shortened wavelengths associated with meanders 'catching up' to neighbouring downstream bends, a feature that can be common in freely-meandering convoluted rivers.

Figure 3.3: Bankfull width versus wavelength

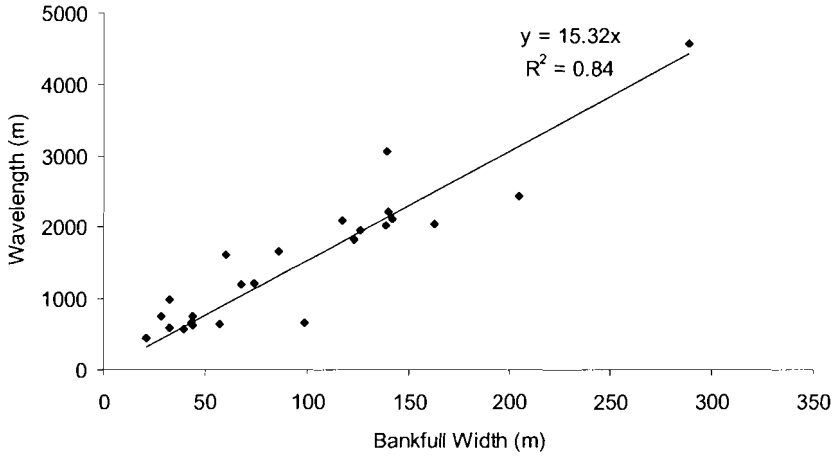

There is also a strong relationship between bankfull width and discharge. Figure 3.4 is a plot of mean annual flood versus bankfull width. A best-fit line generated using a power function fits the data quite well, with a R^2 value of 0.86. The exponent of 0.49 in the equation indicates that bankfull width is

approximately proportional to the square root of discharge, a relation that is well-documented in the literature.

Figure 3.4: Mean annual flood versus bankfull width

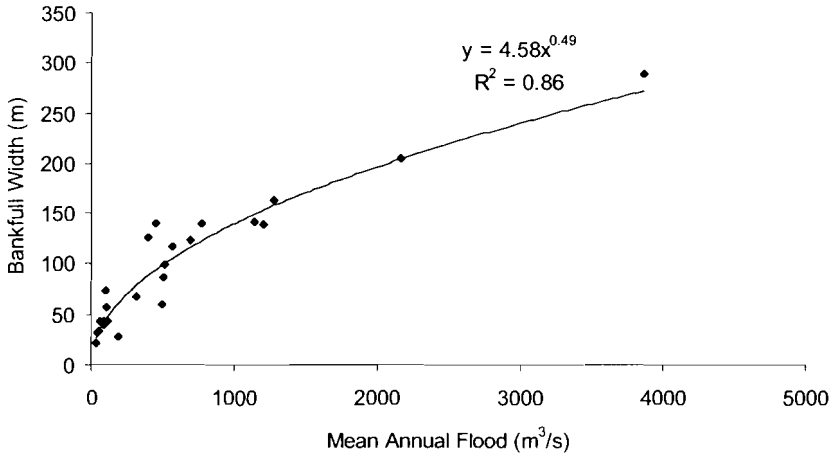

It follows that, if bankfull width is proportional to the square root of discharge, then the same relation should be evident using wavelength in place of channel width (since w α Q). As shown in Figure 3.5, the same general relationship does exist in the data, although there is more scatter. It is interesting to note that, although the Red Deer River and Petitot River sites have bankfull widths which appear to be adjusted to discharge, their wavelengths plot well outside the general trend in Figure 3.5. If these two sites are removed from the analysis the R^2 value increases to 0.86 yet the exponent in the equation changes only slightly, to 0.423.

Figure 3.5: Mean annual flood versus wavelength

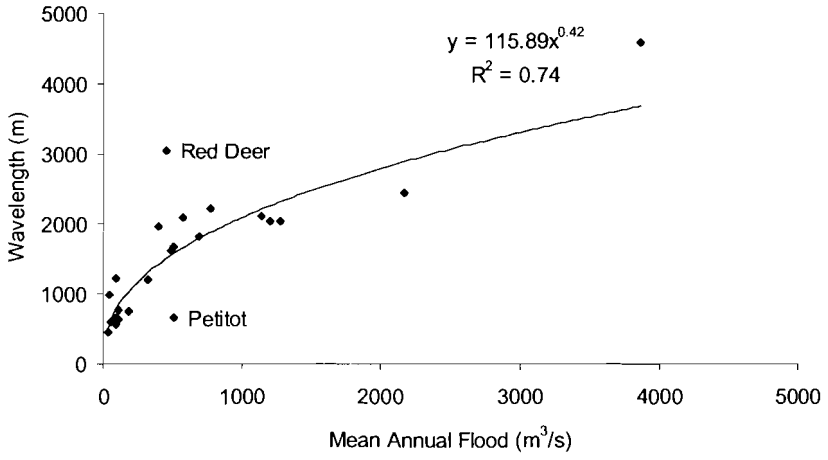

The confined rivers in this study are located in lowland regions and correspondingly, have low channel slopes with values ranging from 0.0001 on the Fontas River to 0.003 at the Clear River site. When slope is plotted with bankfull width and wavelength there is a weak negative correlation with significant scatter (Figure 3.6). The five study sites with the largest slopes are those located closest to the Rocky Mountains, with the exception of the Clear River. This river is a relatively short, steep tributary of the Peace River. Located between mountain ranges, the Kootenay River is also an exception. However, it flows through the rather level plain of the Rocky Mountain Trench; consequently its slope is only 0.00014.

Figure 3.6: Channel slope versus bankfull width and wavelength

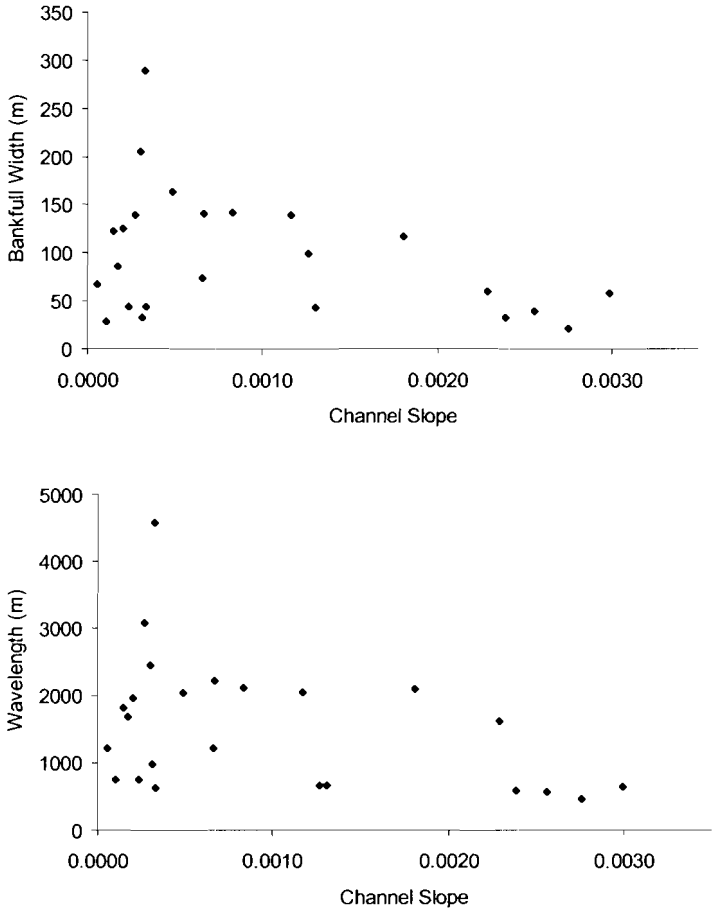

Previous work suggests that the type of confined meanders examined in this study develop where the ratio of floodplain-width to channel-width ranges from 3:1 to 10:1 (Burge and Smith, 1999; Hickin, 1986). A plot of valley width to channel width confirms this is the case for the majority of these rivers (Figure 3.7). The minor exceptions are the Petitot River (2.6:1), the Clearwater River (11:1) and the Battle River (13:1).

Figure 3.7: Confinement ratio of study sites

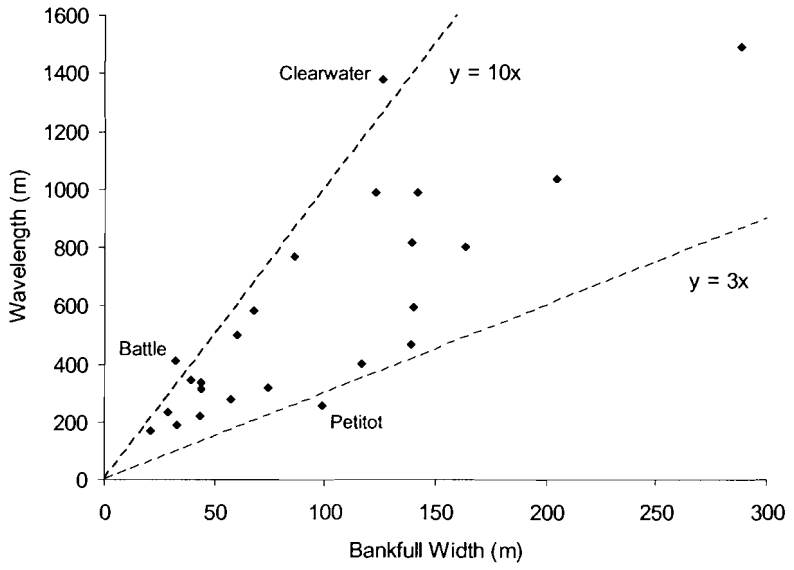

3.3 Downstream Migration

Although the following section presents and analyzes the migration data for the study locations, it must be noted that certain bends remain stable throughout the time span of the aerial photography. Seventeen out of 24 study sites had at least one bend that remained stable throughout the air-photo period. Of these 17 reaches, the proportion of bends displaying no discernable movement on each study reach varied from 3 to 83% (Figure 3.8). The Clearwater River and Petitot River study reaches remained very stable throughout the air-photo period, with 83% and 81% of the total bends examined having no detectable movement. The Hay River (upstream), North Saskatchewan River, and Fontas River sites also had a significant proportion of stable bends. However, when meanders from all study reaches are taken into account downstream movement was detected on the majority of bends. For the

data set as a whole, 22.5% of bends had no discernable movement, a comparable proportion to that obtained by Hooke (1984) who found 24% of bends on the River Dane remained stable through the time period of examination. Although the stable bends in this study may not be migrating there are several reasons to be cautious about assuming a zero migration rate. First, their movement may be too small to be resolved using the methods of this study. Secondly, the time span of aerial photography may not be sufficiently long to capture bend movement in these cases.

Figure 3.8: Proportion of stable (non-migrating) bends in each study reach

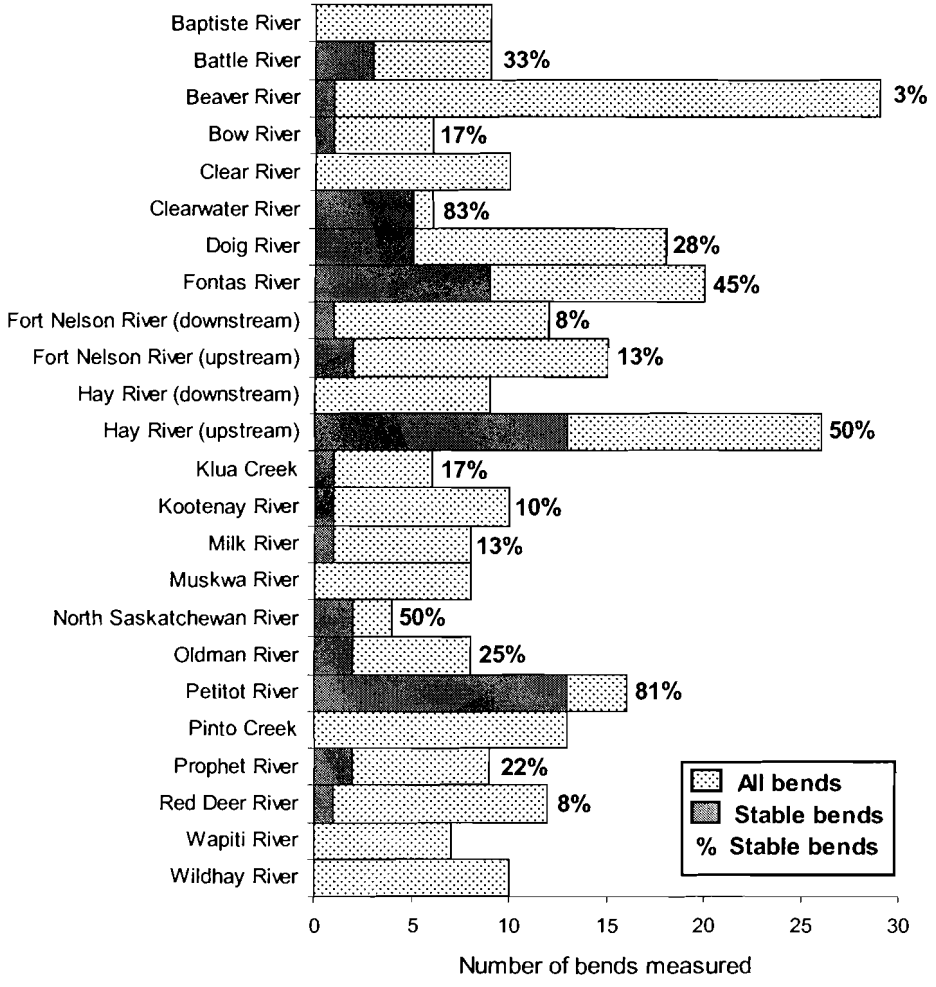

Table 3.3 presents the average migration rates for all study reaches. Due to the confinement of these rivers, the migration rates presented here are in effect, translation rates. These averages are calculated based on the movement observed between the earliest and the most recent photography for each study location. No movement was measured on certain bends in this study. Columns 2 and 4 in Table 3.3 are reach averages that incorporate the cases of zero displacement of bends. Columns 1 and 3 are reach averages based wholly on bends with registered movement. The maximum migration rate is that observed

on one bend within any of the time periods examined for that reach. Although the average migration rate, including those bends displaying zero migration for the time period, may represent the simplest reach average, this is not the migration rate used in subsequent analysis. A major aim of this study is to provide some explanation for the observed rate of migration through analysis of relationships between rate of movement and other measured variables. To achieve this objective, it is more relevant to examine the subset of bends that displayed measurable movement over the time period of study. Therefore, the average rate of migration based on moving bends is used in the subsequent analysis. This approach does not result in artificially high migration rates for those rivers with a significant proportion of stable bends. The average migration rates for such rivers (Clearwater, Petitot, Hay (upstream), North Saskatchewan and Fontas study sites) remain among the lowest observed regardless of which reach average is used.

Table 3.3: Summary of the migration rates over the photo period

River	Average Migration (m/year)	Average Migration incl. stable bends (m/year)	Migration per unit channel width	Migration per unit channel width incl. stable bends	Maximum Migration (m/year)	Air photo time span (years)
Baptiste River	0.6	0.6	0.030	0.030	2.2	46
Battle River	0.6	0.4	0.019	0.012	1.4	53
Beaver River	1.2	1.2	0.028	0.027	3.5	48
Bow River	1.5	1.3	0.013	0.011	3.1	48
Clear River	3.0	3.0	0.053	0.053	9.5	45
Clearwater River	0.01	0.001	0.0001	0.0000	1.3	46
Doig River	0.2	0.1	0.007	0.005	1.1	41
Fontas River	0.6	0.3	0.009	0.005	3.9	30
Fort Nelson River (downstream)	2.5	2.3	0.009	0.008	7.0	30
Fort Nelson River (upstream)	4.1	3.6	0.025	0.022	10.4	31
Hay River (downstream)	0.8	0.8	0.009	0.009	2.2	41
Hay River (upstream)	0.3	0.1	0.006	0.003	1.5	39
Klua River	1.8	1.5	0.042	0.035	2.3	24
Kootenay River	0.6	0.6	0.005	0.005	3.9	52
Milk River	1.6	1.4	0.022	0.019	4.0	44
Muskwa River	5.5	5.5	0.027	0.027	17.5	44
North Saskatchewan River	0.2	0.1	0.004	0.002	0.6	44
Oldman River	1.6	1.2	0.011	0.008	12.4	47
Petitot River	0.2	0.04	0.002	0.000	0.4	31
Pinto River	0.8	0.8	0.024	0.024	2.8	50
Prophet River	3.3	2.6	0.023	0.018	11.1	31
Red Deer River	1.6	1.5	0.012	0.011	11.0	51
Wapiti River	5.8	5.8	0.042	0.042	17.6	51
Wildhay River	0.9	0.9	0.023	0.023	7.6	49
Average for all reaches			0.02	0.02		

Figure 3.9 presents the distribution of migration rates, normalized by bankfull width. On average the rivers in this study were moving downstream at a rate of 0.018 channel widths per year, or 1.8 channel widths per century. This average rate is comparable to that obtained by Hickin and Nanson (1986), whose subset of Canadian rivers had a median migration rate of 2 channel widths per century. The highest rate per channel width of the reaches in this study is the Clear River, which on average moves at about 5 channel widths per century.

Figure 3.9: Migration per unit width

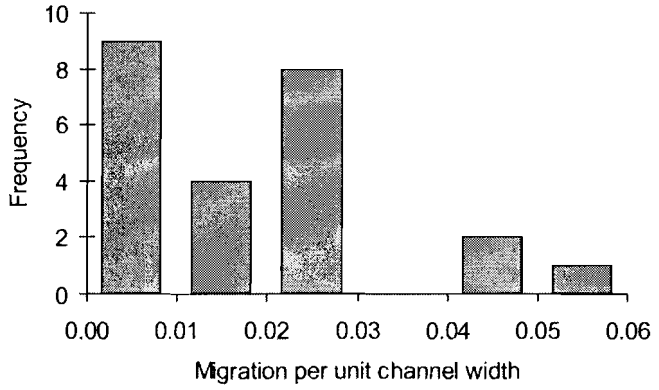

3.3.1 Comparison with Published Migration Rates

To place the migration rates observed in this study in a larger context, compilations of published meander migration rates provided in Van De Wiel (2003) and Hickin (1988) were used for comparison. Overall, the confined meander migration rates obtained through this study fall within the general distribution defined by the previously published rates of erosion (Figure 3.10). This is the case whether drainage area, bankfull width or discharge is used to

scale the data. Many of the average migration rates for the confined meanders here appear to be lower compared to rates for similar-sized rivers elsewhere. However, caution needs to be exercised when using these data. The time span of observation, methods of measurement, calculations and even definitions of terms (i.e. 'mean' and 'maximum') used in acquiring erosion rates differ among studies, complicating direct comparison. Furthermore, it is often those rivers that are actively migrating that are targeted for study. Although the mean migration rate for confined meanders used here does not include the stable bends, river sites were chosen based on their degree of confinement, not on observation of movement. In recognition of the fact the published rates may be biased towards the higher range of movement, the maximum migration rate for the confined meanders was included for comparison. It can be seen that these maximum rates also fall well within the general distribution of the published data (Figure 3.10). The reasons for the outlier with the lowest average migration rate (Clearwater River) are not known; see discussion in section 3.3.3.

Figure 3.10: Comparison of migration rates to published data

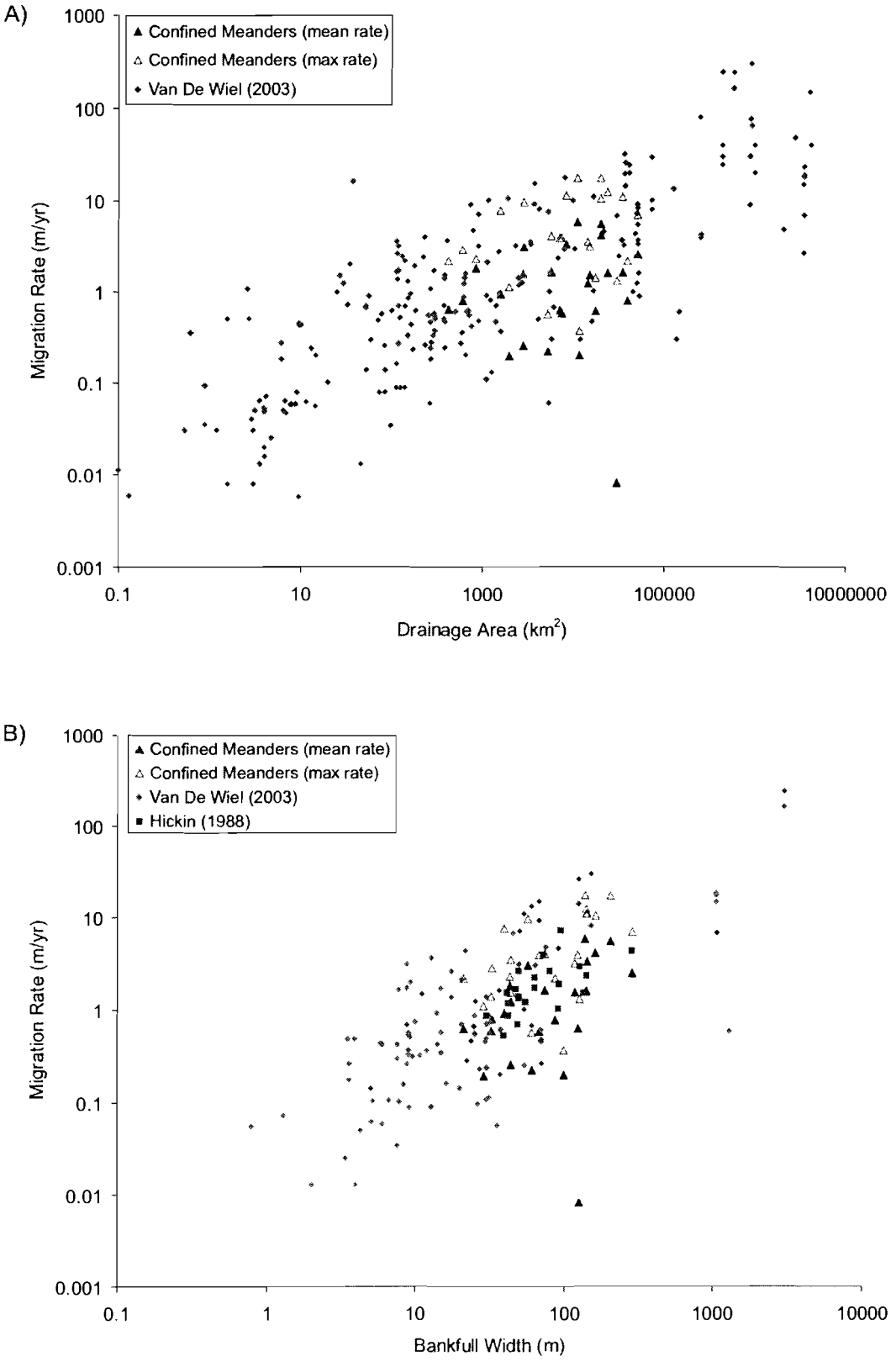

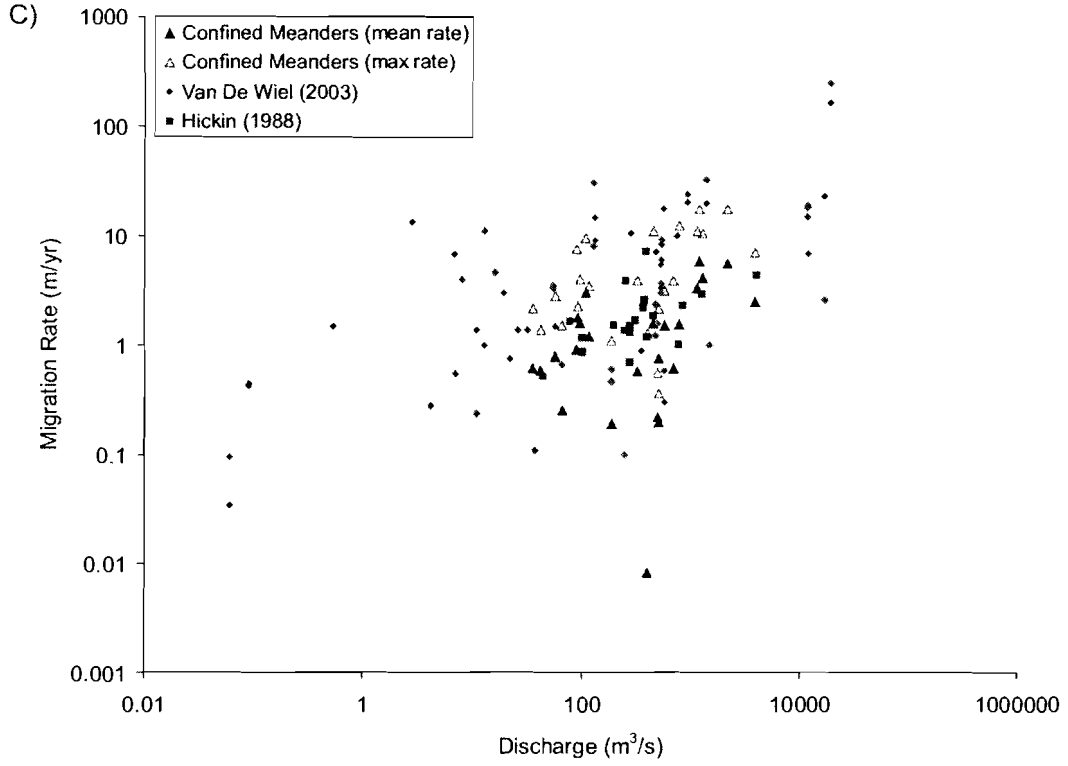

To allow comparison on a more regional scale, data were extracted from the Hickin (1988) compilation for rivers located in Alberta and British Columbia. Figure 3.11 plots the rates of these rivers with the mean and maximum rates for confined meanders observed in this study. Drainage area was not available for the published data; bankfull width and discharge are used for scaling purposes. The mean migration rates for the confined meanders are consistent with those of other rivers within the same region. Once again, a few of the mean migration rates appear to be lower than other rivers of the same scale, including the very low outlier for the Clearwater River. However, it should be noted the majority of the Alberta and British Columbia erosion rates used in these graphs were calculated for meanders with a Rc/w ratio between 2 and 4 (Nanson and Hickin, 1986), a range noted to contain the maximum migration rates observed for those

rivers. For this reason the maximum migration rates observed on the confined meanders were also plotted. With the exception of the Petitot River, the few sites with mean migration rates that appear to be lower than other rivers of the same scale have maximum migration rates that fall within the general distribution of the data. Overall, the maximum values generally plot on the high boundary of the distribution, although they do not appear to be abnormally high for the region. They may indicate an upper threshold for migration rates on comparably-sized rivers.

Figure 3.11: Regional migration rate comparison

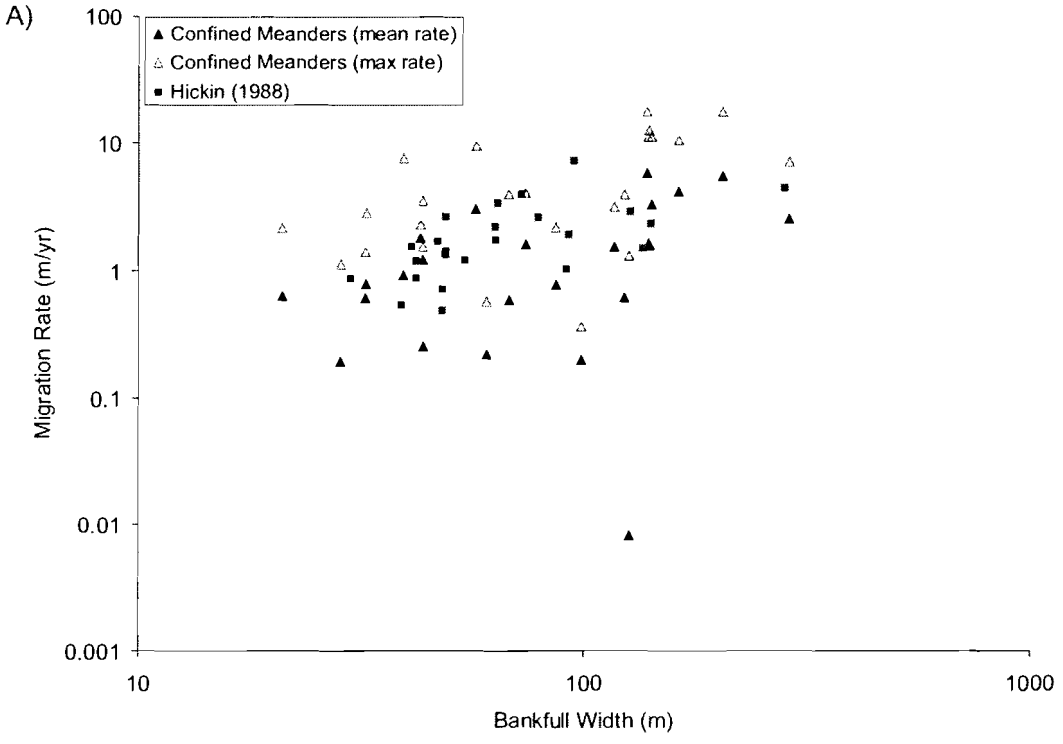

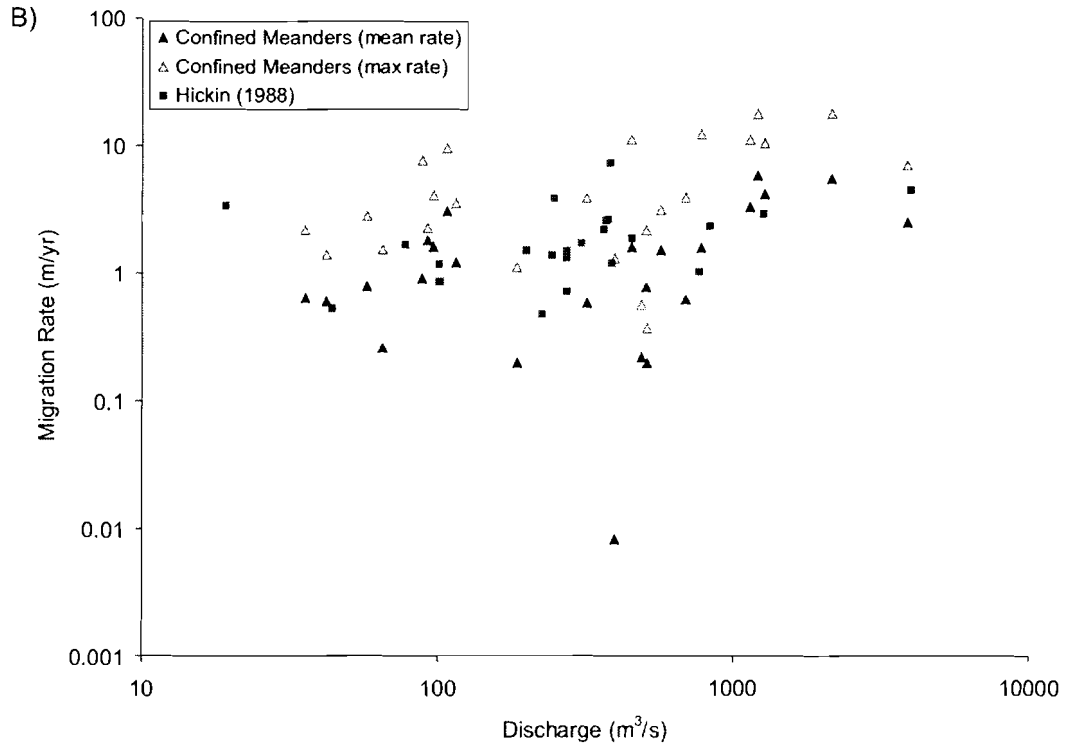

The confined meanders of this study do not appear to have migration rates that exceed those found in freely-meandering rivers of comparable scale. However, due to confinement, their movement is restricted to the downvalley direction. Therefore, a confined-meandering river with a lower average-migration rate than a comparably-sized freely-meandering river may actually be moving downvalley at a faster rate. This would have obvious implications for any infrastructure located on the floodplain. Due to the unique shape of confined meanders, the majority of the floodplain will be re-worked with a channel movement equal to one-half wavelength. The time it would take to re-work the floodplain based on both the mean and maximum migration rates for the study locations is presented in Table 3.4. These are first-order estimates; it is highly probable that the rates of migration will not remain constant through time.

Nevertheless, the time periods calculated likely will be within an order of magnitude of the true long-term average. The stability of streams such as the Clearwater River contrasts markedly with the relative mobility for the Clear, Wapiti and Muskwa River.

Table 3.4: Time required for the re-working of floodplain deposits

River	Wavelength (m)	Average Migration (m/year)	Time (years)	Maximum Migration (m/year)	Time (years)
Baptiste River	456	0.6	362	2.2	105
Battle River	991	0.6	822	1.4	356
Beaver River	757	1.2	313	3.5	108
Bow River	2098	1.5	693	3.1	334
Clear River	642	3.0	106	9.5	34
Clearwater River	1958	0.01	119493	1.3	752
Doig River	750	0.2	1923	1.1	338
Fontas River	1208	0.6	1039	3.9	154
Fort Nelson River (downstream)	4578	2.5	908	7.0	325
Fort Nelson River (upstream)	2036	4.1	246	10.4	98
Hay River (downstream)	1673	0.8	1078	2.2	385
Hay River (upstream)	627	0.3	1232	1.5	204
Klua Creek	663	1.8	185	2.3	146
Kootenay River	1825	0.6	1472	3.9	233
Milk River	1219	1.6	380	4.0	151
Muskwa River	2441	5.5	222	17.5	70
North Saskatchewan River	1612	0.2	3666	0.6	1426
Oldman River	2214	1.6	706	12.4	89
Petitot River	662	0.2	1678	0.4	903
Pinto Creek	591	0.8	376	2.8	105
Prophet River	2109	3.3	319	11.1	95
Red Deer River	3063	1.6	950	11.0	139
Wapiti River	2032	5.8	174	17.6	58
Wildhay River	571	0.9	312	7.6	38

3.3.2 Migration Rates Through Time

Although the average rates of migration presented here are based on the movement between the earliest and most recent aerial photography, migration rates were also calculated for at least one intervening time interval for the majority of study sites. Exceptions are the Fort Nelson (downstream), Klua and Petitot River sites where suitable photography was not available for an intervening time period. Of the 21 study sites with more than one time interval

examined, 12 had two intervals of photography examined while the remaining 9 sites had three time periods of photography. As expected, migration rates are not constant at all sites through the time period of photography. Indeed, there are four distinct trends: the migration rate increased over time, the rate decreased over time, the rate decreased then increased and the rate increased then decreased. These migration rates are averages for the reach; in some cases variation within the reach is significant as discussed below. The following sections discuss the study sites grouped according to the migration-rate trend observed. The data are presented graphically; numerical values for the average migration rates at each site are available in Appendix B. To illustrate the variance involved in the reach average, individual bend migration rates for each time interval are also available in Appendix B. An attempt is made to correlate the observed trends in migration rate to changes in mean annual flood for each photo period, calculated using available records of annual peak flow for the study sites. It is recognized that appreciable migration can occur with more moderate and more frequent events. However, use of mean monthly or daily discharge data tends to overlook the significant impact that the peak flow has on the level of bank erosion. Ideally, years with higher flow would also register higher peak flow. Use of peak flow data has its limitations but useful correlations can still be made.

Migration rate increase

Six of the 21 sites (Baptiste, Clear, Hay (downstream), Hay (upstream), North Saskatchewan, Kootenay) show an increase in migration rate in the later time interval of photography (Figure 3.12). Figure 3.13 displays the Water Survey

of Canada (WSC) peak flow data for the study sites with nearby gauges. Suitable data were not available for the Baptiste, Clear and Hay (upstream) river sites.

Figure 3.12: Study sites with migration rate increase

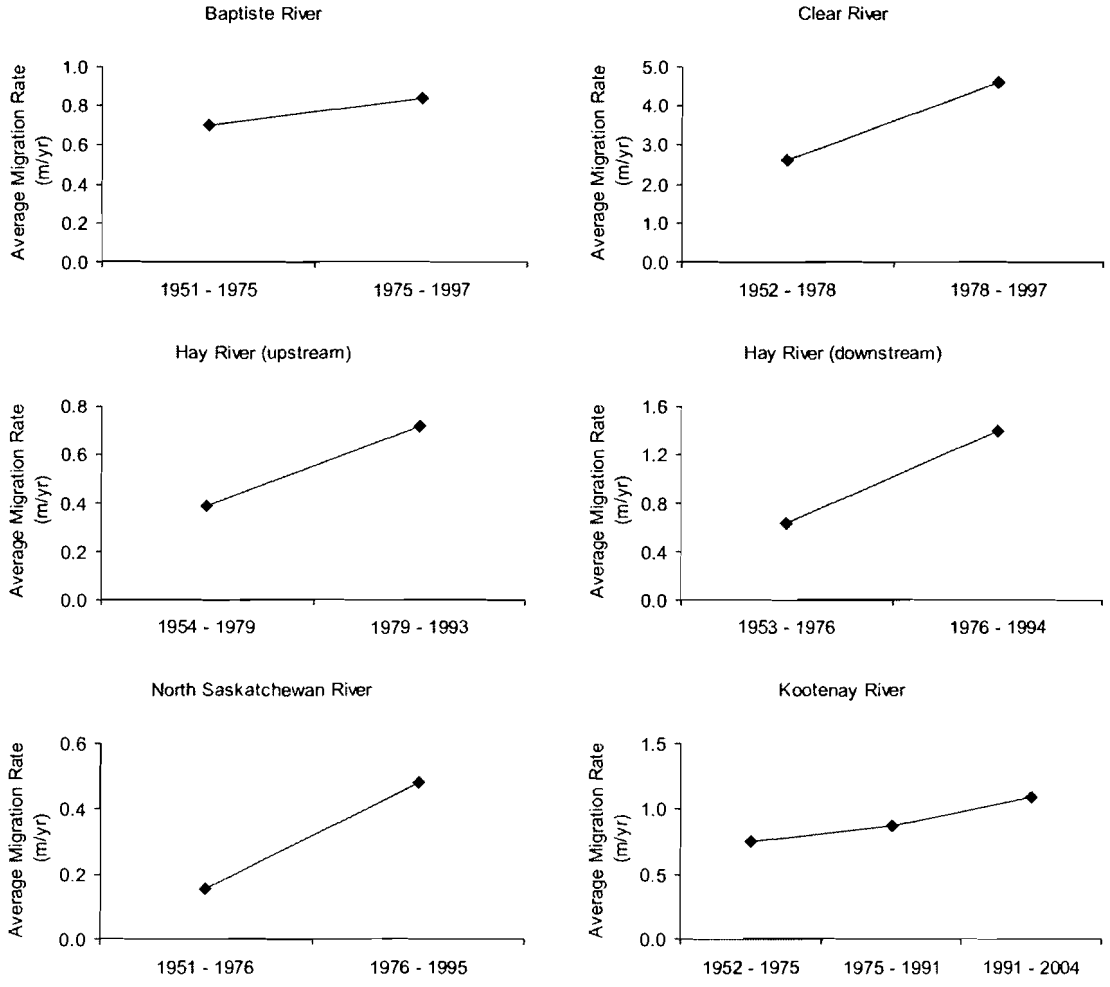

Figure 3.13: Peak flood data for study sites with migration rate increase (vertical lines indicate boundaries for air photo time intervals)

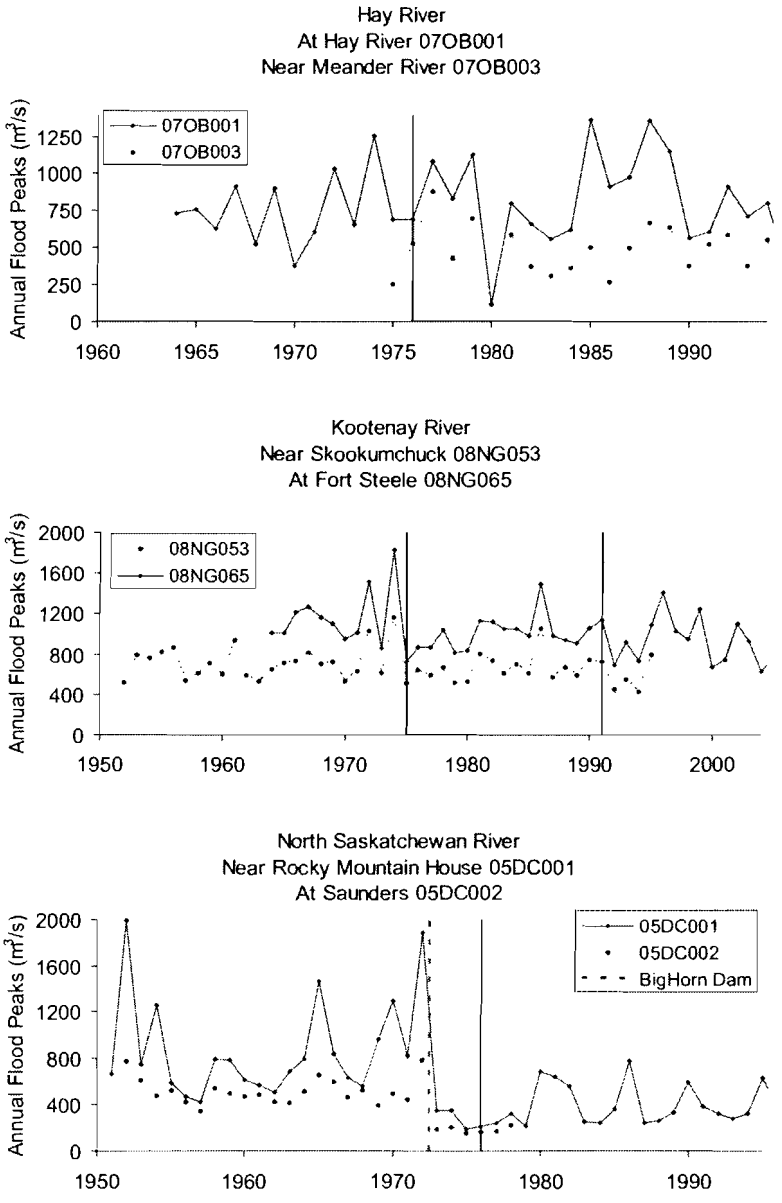

Of the six sites only two, the Clear River and Hay River (downstream), display an increasing trend in migration rate that is clearly beyond the magnitude of error involved in the measurement. The Baptiste, Hay (upstream), North Saskatchewan and Kootenay River sites have increases that are based on average differences of movement within each time interval of less than 5 m.

While the migration rates on these sites may be increasing, it is beyond the resolution of the methods in this study to determine this unequivocally. In the case of the Kootenay River it is interesting to note that the average of annual peak floods has actually decreased over the photo time intervals from 1138 to 1017 to 935 m^3/s as measured at the Fort Steele gauge, while the migration rate appears to either increase or at least remain relatively constant through time. At the North Saskatchewan River site, the completion of the Bighorn Dam (45 km upvalley) in 1972 has had an obvious effect on the annual peak flood. Pre-dam mean annual flood at Rocky Mountain House has dropped from 896 to 465 m^3/s in the years following dam closure. However, the results of this study indicate the migration rate of the reach has remained relatively constant, albeit at a very slow rate. Owing to the presence of the dam, it is not surprising that this reach of river is relatively stable in the later time interval. What is perhaps the more interesting question is why there is an apparent lack of significant movement in the years of higher flow before dam closure? It is one, however, that the present study is unable to resolve.

Migration rates of the Clear River and Hay River (downstream) have clearly increased in the later time interval. Unfortunately, the Clear River discharge record is too short to be of use; this river is a relatively steep tributary that has remained highly active throughout the time period of photography. The discharge records of sufficient length for the Hay River (downstream) site are located almost 160 km downvalley at Hay River, NWT. However, they do correlate well with the records available for the Meander River townsite gauge

45 km upvalley from the study site and so can be reasonably assumed to represent the trends in peak annual floods at the study site. The increase in migration rates for Hay River (downstream) site can be correlated to an increase in mean annual floods for the time periods of photography. The Hay River gauge records a slight increase in mean annual flood from 750 m^3/s before 1976 to 807 m^3/s after. The increase in the median peak flood is more significant from 692 to 799 m^3/s.

Migration rate decrease

Seven of the 21 sites (Battle, Bow, Doig, Fontas, Fort Nelson (upstream), Pinto, Prophet) show a decrease in migration rate in the later time interval of photography (Figure 3.14). Annual peak-flow data from the WSC were of sufficient length for the Battle River and Bow River study locations only (Figure 3.15).

Figure 3.14: Study sites with migration rate decrease

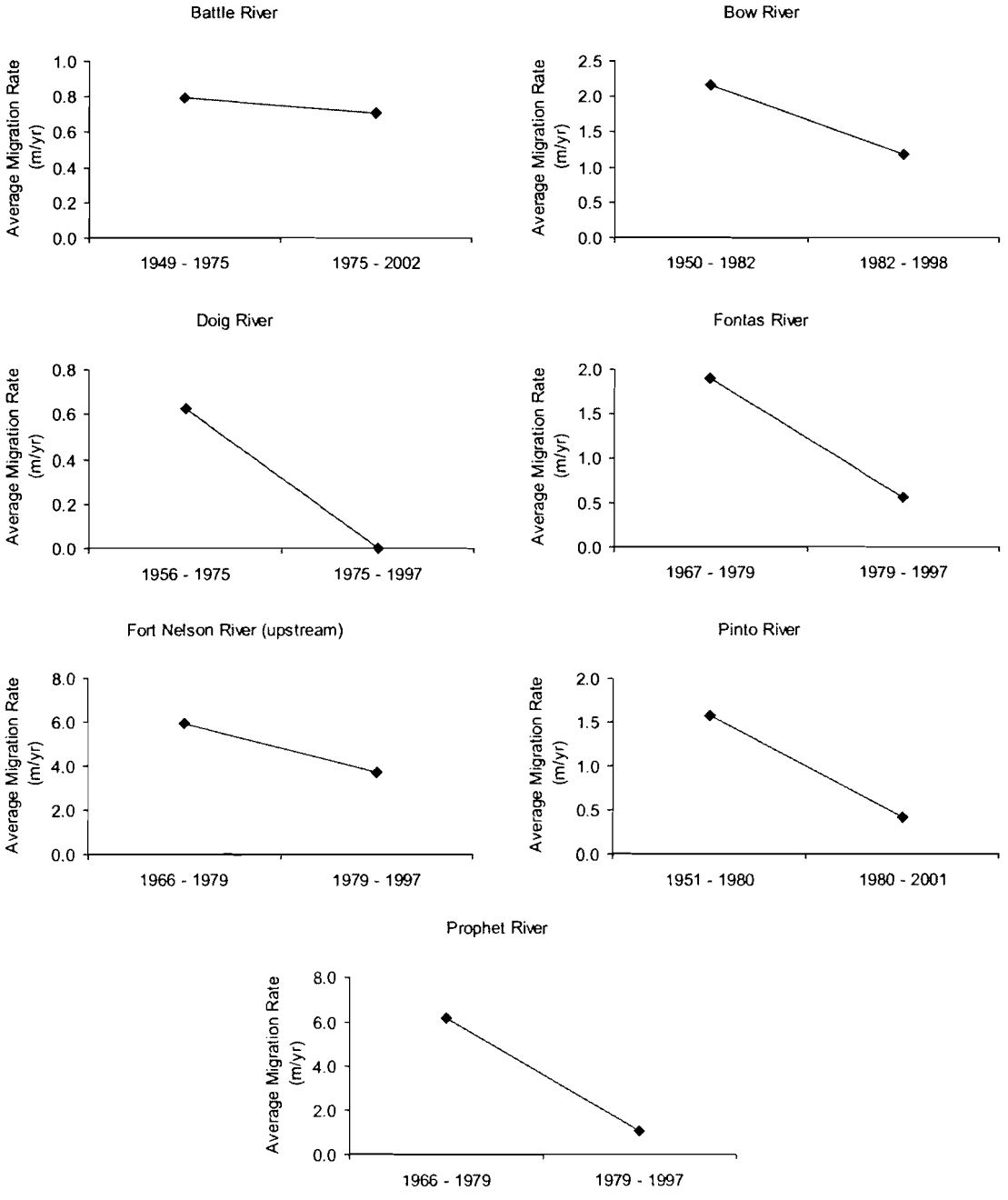

Figure 3.15: Peak flood data for study sites with migration rate decrease (vertical lines indicate boundaries for air photo time intervals)

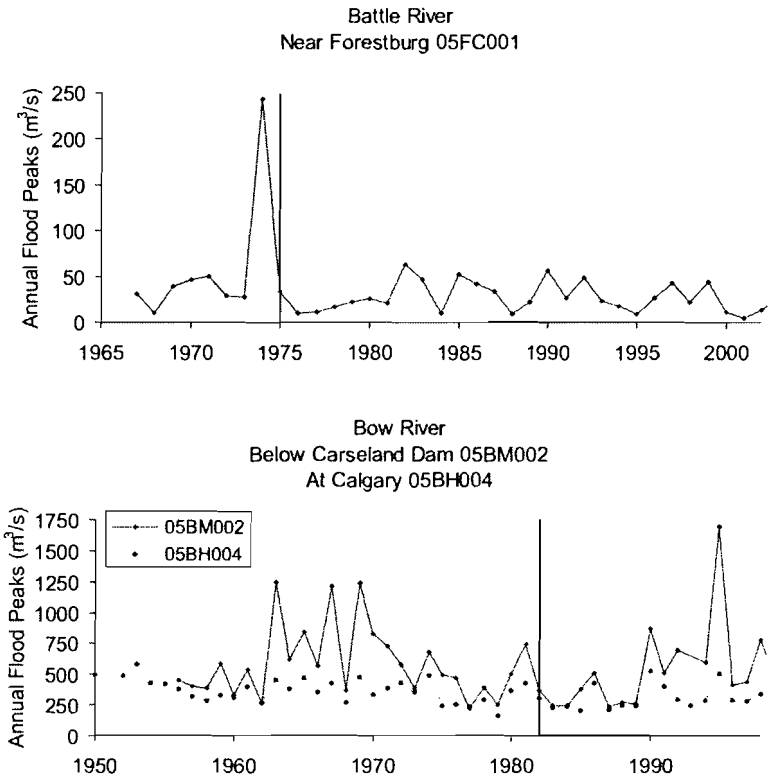

Of the seven sites only the decrease in rate for the Battle River site is below the magnitude of error associated with the methods in this study. There is no question that this river has migrated over time but its rate can be considered sensibly constant over the period of photography. The large flood in 1974 did not appear to significantly increase the migration rate; excluding this event the mean annual flood does not significantly change between the two time periods of photography.

The decrease in migration rate for the Bow River site can be correlated to a decrease in mean annual flood between the two photo periods. Mean annual floods at the Calgary and Carseland Dam gauges before 1982 were 367 and 581

m^3/s respectively. These decreased modestly to 307 and 541 m^3/s for the period after 1982. The Bow River does have numerous dams within its watershed; however, the Bearspaw Dam in 1954 was the last significant infrastructure built. Presumably, river regulation would have an unknown but equal effect on migration rates throughout the time periods examined.

The Doig, Fontas, Fort Nelson (upstream), Pinto and Prophet River sites had decreases in migration rate that is above the magnitude of potential error in this study. However, sufficient gauging records for possible correlation analysis are not available for any of these sites.

Migration rate decrease then increase

Four of the 21 sites (Beaver, Red Deer, Wapiti, Wildhay) show a decrease in migration rate for the second time interval of photography followed by an increase in migration rate (Figure 3.16). Annual peak flow data from the WSC is available for all sites and are shown in Figure 3.17.

Figure 3.16: Study sites with migration rate decrease then increase

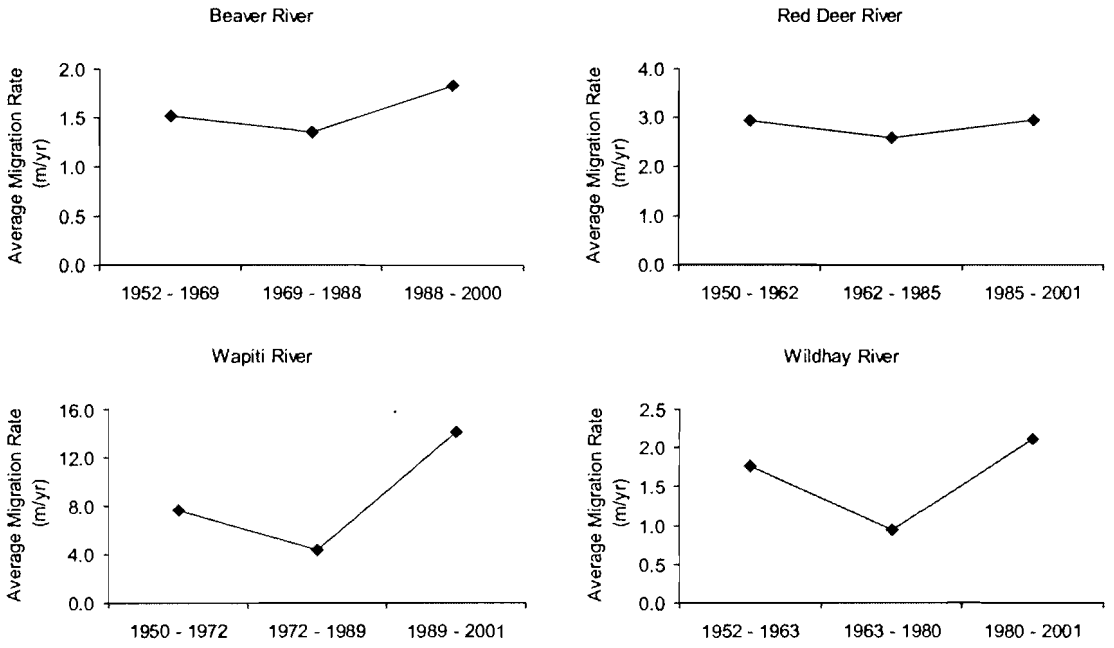

Figure 3.17: Peak flood data for study sites with migration rate decrease then increase (vertical lines indicate boundaries for air photo time intervals)

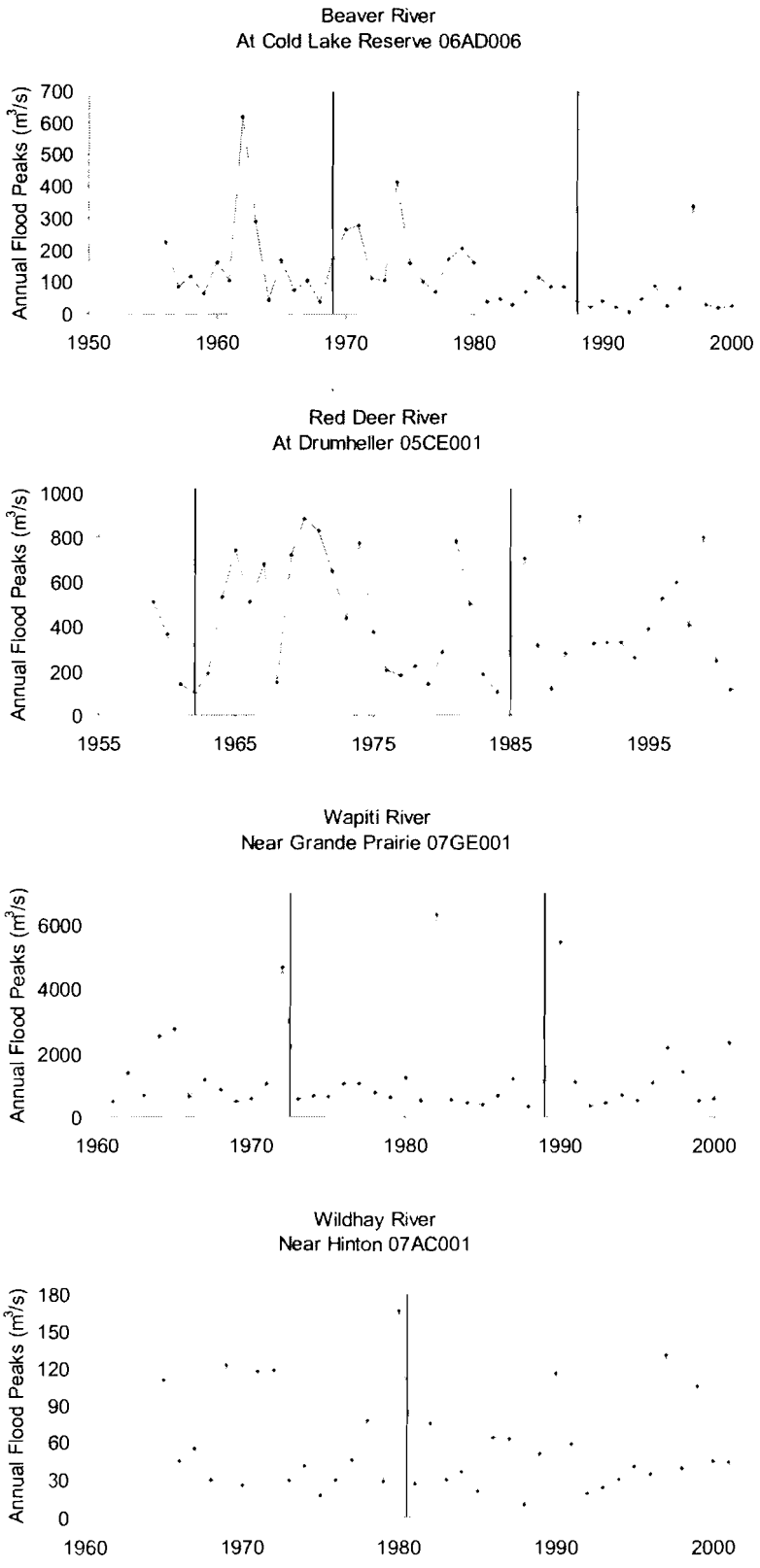

The Beaver River site is the only one of the four reaches where the migration-rate change is below the magnitude of error associated with the methods in this study. Similar to the Battle River site, there is no doubt that this river has migrated over time but its rate can be considered sensibly constant over the period of photography. Whether the apparent decreasing/increasing trends are reality, or the river migration rate has remained constant through time, is not possible to determine. Both tendencies are opposite to what would be expected; mean annual floods have actually been decreasing for the time intervals of photography, from 162 to 139 to 61 m^3/s.

Peak flow data are unavailable for the earliest time interval of photography on the Red Deer River. However, data for the subsequent two intervals indicate a decrease in the mean annual flood from 457 to 409 m^3/s at the Drumheller gauge. The observed increase in migration rate over the same time is thus opposite that expected from the peak flow-data alone. The Red Deer River has been regulated since 1908; the most recent large dam to be built is the Dickson Dam in 1983, located around 300 km upstream of the study site. The data do not indicate that this dam significantly affects the annual peak flow at the study site. Increased winter flows due to the dam may be part of the reason for the observed increase in migration rate although this is unlikely this far downstream. It is more probable that site-specific factors are responsible for the slight increase in migration rate observed for the most recent time interval.

The mean annual floods for the Wapiti River do appear to correlate to some extent with the observed trends in migration rate. In sequential order, the

mean annual floods calculated for the time periods are 1432, 1057 and 1382 m^3/s, correlating to the decrease and increase in the migration rate over time. However, the migration rate for the 1989 – 2001 photo time interval is 6.5 m/year greater than the migration rate for 1950 – 1972 yet there is a modest decrease in mean annual flood when compared to the earlier interval. The largest flood event on record occurred in 1982, within the period with the lowest migration rate. It is possible that the 1982 event somehow 'prepared' the river for the large 1990 event, causing this event to be more substantial with regards to channel migration than it otherwise would have been and greatly increasing the migration rate for the most recent time interval. Examination of photography from the early 1990s would be required to substantiate this hypothesis.

Peak flow data are not available prior to 1965 for the Wildhay River site. However, the data available for the later two photography time intervals do not offer an explanation for the observed increase in migration rate. The mean annual flood at the upstream gauging site decreased slightly over these periods, from 66 to 50 m^3/s, while the median peak flood remained relatively constant at 45 and 41 m^3/s.

Migration rate increase then decrease

Four of the 21 sites (Clearwater, Milk, Muskwa, Oldman) display an increase in migration rate for the second time interval of photography followed by a decrease in migration rate (Figure 3.18). Annual peak flow data from the WSC is available for all sites and is shown in Figure 3.19.

Figure 3.18: Study sites with migration rate increase then decrease

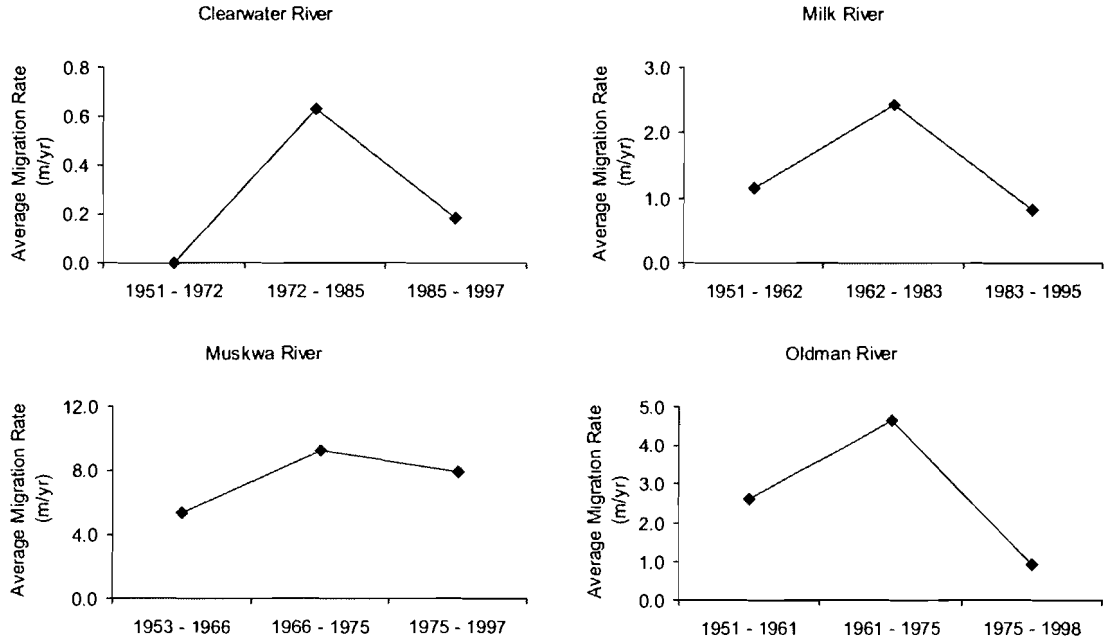

Figure 3.19: Peak flood data for study sites with migration rate increase then decrease (vertical lines indicate boundaries for air photo time intervals)

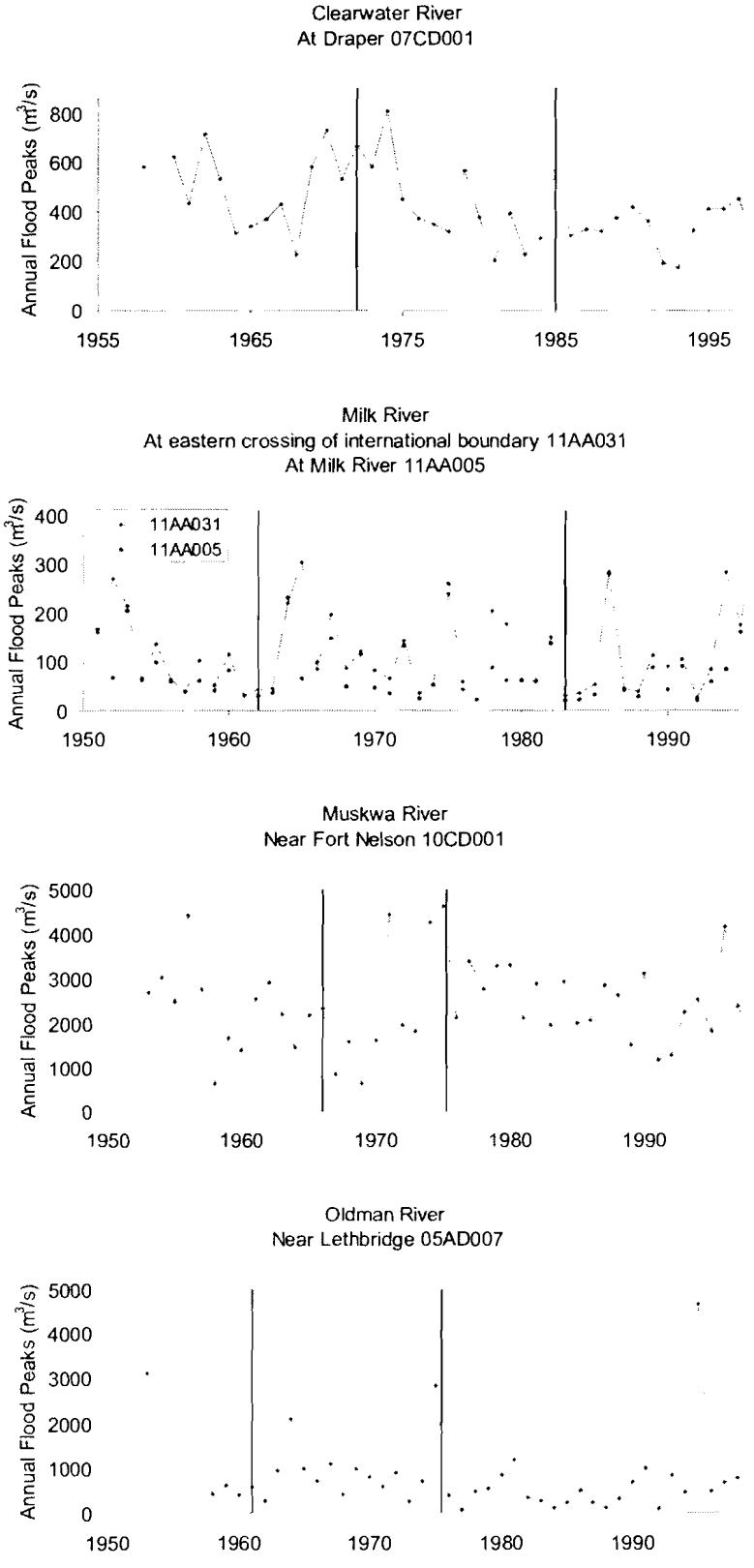

The change in migration rate for the Clearwater River site is below the magnitude of error associated with the methods in this study; the migration rate therefore is regarded as constant. In fact, this is the one river in the study set where evidence for movement at the level of resolution of the study methods is sparse. There is evidence of bar stabilization throughout the air photo period but the majority of bends display zero movement. The relatively high migration rate for the 1972 – 1985 photo period is primarily based on the movement of one bend. Examination of the gauging station data reveals the mean annual flood has been steadily declining in each photo period from 502 to 420 to 336 m^3/s, suggesting a cause for bar stabilization.

The mean annual floods for the Milk River do appear to correlate with the observed trends in migration rate. In sequential order, the mean annual floods calculated for the time periods are 107, 120 and 105 m^3/s as measured at the east international boundary crossing, correlating to the increase and decrease in the migration rate over time. A similar trend in mean annual flood can be calculated for the Milk River townsite gauge. However, the increase in mean annual flood for the 1962 – 1983 photo period is rather modest yet led to a 1.3 m/year increase in migration rate; other factors are likely involved in the increase.

The trends in migration rate for the Muskwa River do not correlate well with the change in mean annual flood for the time periods. Mean annual floods have actually continually increased with the time periods from 2335 to 2415 to 2569 m^3/s. However, Figure 3.19 depicts three large flood events within the later

half of the 1966 – 1975 photo interval which may explain the high migration rate during this time. The most recent photo period has seen frequent events of moderate magnitude which may have kept the migration rate relatively high.

The Oldman River is another highly regulated watershed, in this case since 1910. The only significant structure to be built within the period of aerial photography was the Oldman Dam, completed in 1992 about 170 km upstream of the study site. With the dam completion close to the end date of photography, taken together with the large flood of 1995, the impact of this dam on the migration rate calculated within this study is probably negligible. There are only 5 years of peak-flow data for the 1951 to 1961 photo interval. These show a large flood in 1953 with smaller peak flows for the remaining years. These smaller peak flows are larger than the low flows recorded within the most recent air-photo interval, possibly correlating to the intermediate migration rate of this early period. There is a significant decrease in mean-annual flood within the next two photo time periods from 964 m^3/s for 1961 – 1975 to 661 m^3/s in 1975 to 1998. This decrease probably explains much of the decrease in migration rate seen between these two time periods. The Oldman River flows through the dry lands of southern Alberta, consequently demand for water is high. Between 1960 and 2000 water allocation in the basin increased from 30 – 40% of natural flow to almost 70% (Alberta Environment, 2006). Although this amount of water is not necessarily used each year it almost certainly has an effect on overall discharge levels and accordingly, on migration rate.

Regional trends in migration rate

The previous section subdivided the river sites based on trends in migration rates; however, whether overall regional trends exist was not investigated. Although three photo time-intervals were examined for many sites, the majority of sites had a photo interval start/end in the late 1970s and early 1980s. To enable comparison across sites, this section examines the migration trends displayed before and after this interval. Following discussion in the previous section a summary table of migration-rate trend is presented (Table 3.5). Table 3.5 depicts the Red Deer River site as spanning two categories. This is due to the fact it has a late photo interval break in 1985 combined with a relatively low increase in migration rate. Figure 3.20 uses the summary table to present a regional overview map of the trends in migration rates.

Table 3.5: Summary table of trends in migration rate

Decrease over time	Constant through time	Increase over time
Bow (Bw)	Baptiste (Bp)	Clear (C)
Doig (D)	Battle (Bt)	Hay (downstream) (Hd)
Fontas (F)	Beaver (Bv)	Wapiti (Wa)
Fort Nelson (upstream) (Fnu)	Clearwater (Cw)	Wildhay (Wh)
Milk (Mi)	Hay (upstream) (Hu)	
Muskwa (Mk)	Kootenay (K)	
Oldman (O)	North Saskatchewan (N)	
Pinto (Pi)	Red Deer (R)	
Prophet (Pr)		

Figure 3.20: The geography of channel migration rate

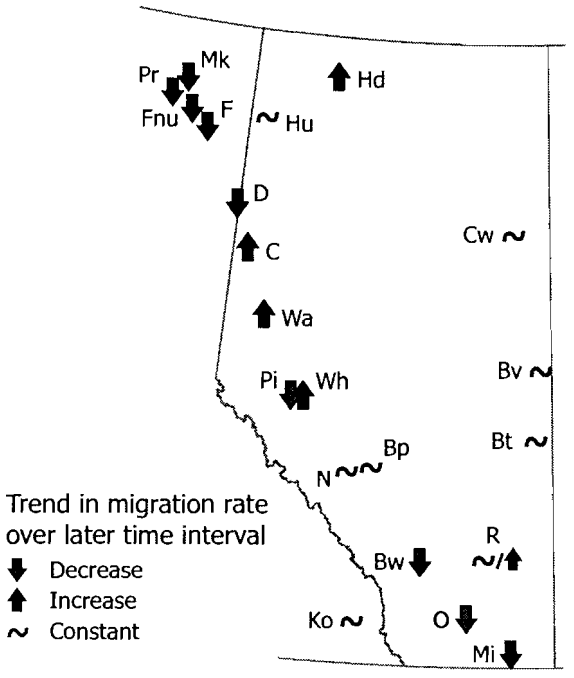

There does appear to be a geographic dimension of migration rate. Rivers in northeastern British Columbia have all recorded a drop in migration rate for the most recent interval of aerial photography. This suggests that there has been a regional decrease in discharge. Unfortunately, the lack of extended gauging records for this area of Canada precludes investigation of this speculation. Furthermore, the only lengthy records for peak flow available are for the Muskwa River. These records indicate the later time period has actually experienced a slight increase in mean annual flood. If this trend applies to the other rivers of the region then other factors must explain the decrease in migration rate. These rivers are still in a relatively pristine state with respect to development so it is unlikely the decrease is due to human influence.

The study sites displaying a definitive increase in migration rate for the later time interval are all relatively pristine rivers located in the

northcentral/northwest of Alberta. The Clear and Wapiti River sites are within the Peace River region of northwest Alberta. These sites are relatively steeply-sloping sites and both have been highly active throughout the time period of observation. The Doig River, also located within the Peace River region, differs in character with its low-slope flow through muskeg. Available discharge records for the Wapiti River do not indicate a significant increase in peak flows to explain the jump in migration rate but it is expected that both this site and the Clear River site would be more responsive to any change in discharge than the Doig River site would be. The increase in migration rate at the Wildhay site is remarkable in that the neighbouring Pinto River study site actually recorded a significant decrease in migration rate over the exact same time period. These study sites are within 11 km of each other and have similar slopes and bankfull widths. The Wildhay River study site does have an appreciably larger drainage area but it is unclear from this study what would account for the difference in rates seen between the two sites.

With the possible exception of the Red Deer River site, migration rates for study sites located throughout the south-central, southern and eastern portions of Alberta have all remained constant through time or decreased. This is not surprising given that available peak flow data for these sites all indicate a decrease in mean annual flood for the later time interval. Many of these rivers flow through highly populated areas and are impacted to some degree by regulation. Predictions of increased dryness throughout much of Alberta combined with increased population pressure will probably maintain the observed

temporal trends in migration rate. Indeed, it would not be surprising if those rivers that have thus far displayed a constant rate of migration would start to exhibit declining rates over the next several decades.

3.3.3 Correlations to Migration Rate

An important objective of this study is to provide a statistical description of confined meanders that provides the basis for the prediction of migration rates. To achieve this objective, relationships among migration rate and factors such as planform geometry, mean annual flood, drainage area, channel slope, valley slope, stream power and bed material were examined. The measurements of planform geometry for the study sites have been presented earlier; Table 3.6 displays the values for the remaining variables that are used in the analysis. Graphs within this section have study sites labelled in accordance with those in Table 3.6. While this table presents bed-material data it should be noted that these data are estimates of the actual conditions at the site. Information on bed material was obtained through a combination of previously published material (Burge and Smith, 1999; Hickin and Nanson, 1984; Kellerhals et al., 1972) and from field visits to seven of the study sites.

Table 3.6: Environmental data used in analysis

River	Label	Mean Annual Flood (m^3/s)	Drainage Area (km^2)	Channel Slope	Valley Slope	Stream Power (Wm^{-1})	Specific Stream Power (Wm^{-2})	Bed Material
Baptiste	Bp	36	420	0.0028	0.0037	964	45.7	Gravel
Battle	Bt	42	17800	0.0003	0.0004	128	4.0	Sand
Beaver	Bv	115	14500	0.0002	0.0005	265	6.1	Gravel to sand transition; mostly sand
Bow	Bw	569	15370	0.0018	0.0019	10107	86.4	Gravel
Clear	C	108	2880	0.0030	0.0038	3163	55.4	Gravel
Clearwater	Cw	399	30800	0.0002	0.0008	782	6.2	Sand
Doig	D	186	1940	0.0001	0.0004	192	6.8	Gravel to sand transition; mostly gravel
Fontas	F	320	7400	0.0001	0.0004	173	2.6	Sand
Fort Nelson (downstream)	Fnd	3867	52230	0.0003	0.0004	12365	42.9	Gravel to sand transition; mostly gravel
Fort Nelson (upstream)	Fnu	1276	20320	0.0005	0.0009	6097	37.4	Gravel to sand transition; mostly gravel
Hay (downstream)	Hd	506	39680	0.0002	0.0003	860	10.0	Gravel to sand transition; mostly sand
Hay (upstream)	Hu	65	2830	0.0003	0.0006	214	4.9	Sand
Klua	Kl	92	840	0.0013	0.0019	1182	27.5	Gravel
Kootenay	Ko	690	7120	0.0001	0.0002	974	7.9	Gravel to sand transition; mostly sand
Milk	Mi	97	5730	0.0007	0.0009	625	8.5	Gravel to sand transition; mostly sand
Muskwa	Mk	2161	20300	0.0003	0.0004	6366	31.1	Gravel
North Saskatchewan	N	492	5160	0.0023	0.0026	11056	183.3	Gravel
Oldman	O	778	23820	0.0007	0.0009	5065	36.1	Gravel
Petitot	Pe	511	11830	0.0013	0.0013	6331	64.0	Gravel

River	Label	Mean Annual Flood (m^3/s)	Drainage Area (km^2)	Channel Slope	Valley Slope	Stream Power (Wm^{-1})	Specific Stream Power (Wm^{-2})	Bed Material
Pinto	Pi	58	610	0.0024	0.0026	1348	41.3	Gravel
Prophet	Pr	1141	8450	0.0008	0.0015	9310	65.6	Gravel
Red Deer	R	454	35280	0.0003	0.0005	1188	8.5	Gravel to sand transition; mostly sand
Wapiti	Wa	1205	11300	0.0012	0.0013	13788	99.4	Gravel
Wildhay	Wh	89	1560	0.0026	0.0039	2235	56.8	Gravel

Numerous authors have recognized a relationship between bend curvature and migration rate in which the maximum rates are generally found with Rc/w ratios of 2 to 3 (Hickin and Nanson, 1984, Hooke, 2007). Essentially the same association is found with the confined meanders in this study. Figure 3.21 plots the average of the migration rates for each time interval for each bend examined in the study. The envelope curve is of much the same shape as the distributions reported in previously mentioned work. There is a sharp increase in migration rate to a maximum for Rc/w ratios between 2 and 4, followed by a general decline in rate for larger bend curvatures. Normalizing the measurements to bankfull width keeps the same general shape of curve but with increased scatter (Figure 3.21b). Both graphs show a large amount of scatter within the relation; very low rates of migration are also found between Rc/w of 2 to 4.

Figure 3.21: The relation between average migration rate and Rc/w for all bends in the study

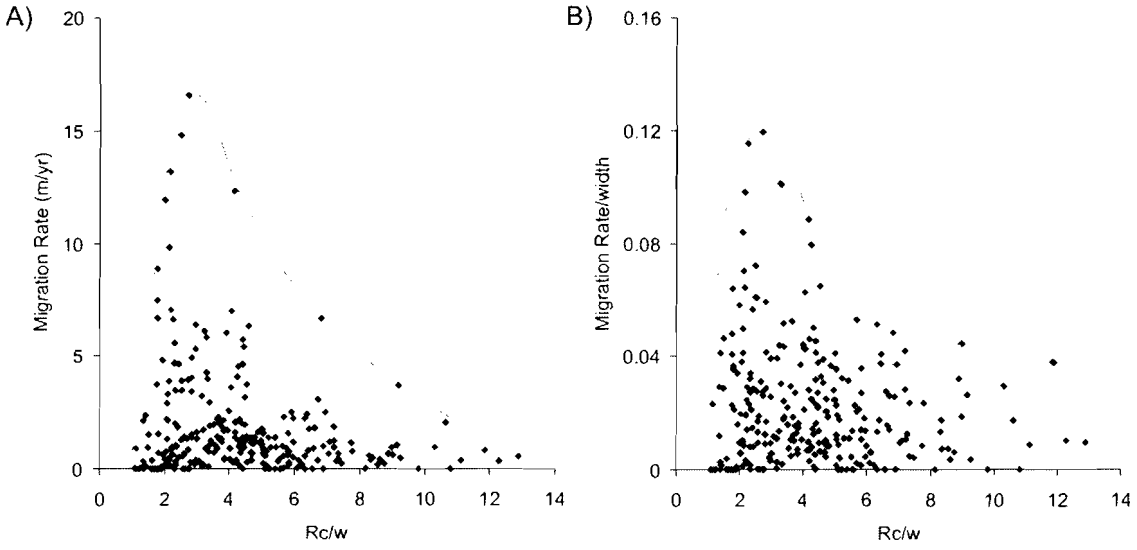

Part of the reason for the scatter becomes apparent when the same curvature-migration rate relation is plotted for the individual study sites (Figure 3.22). A few of the study sites such as those on the Kootenay, Wapiti and Wildhay rivers show what could be deemed expected behaviour based on published findings – migration rate maximums at Rc/w ratios between 2 and 4 followed by declining rates. Other study reaches, notably the Battle and North Saskatchewan sites, have bends with relatively high bend curvature displaying the highest rates of migration. Other sites may display the suggestion of a curve with a maximum between 2 and 4 but migration rates vary greatly over a small range of bend curvature. Taken as a whole, the results indicate bend curvature does play a part in determining migration rate; however, it obviously is not the only factor.

Figure 3.22: The relation between average migration rate and Rc/w for each bend

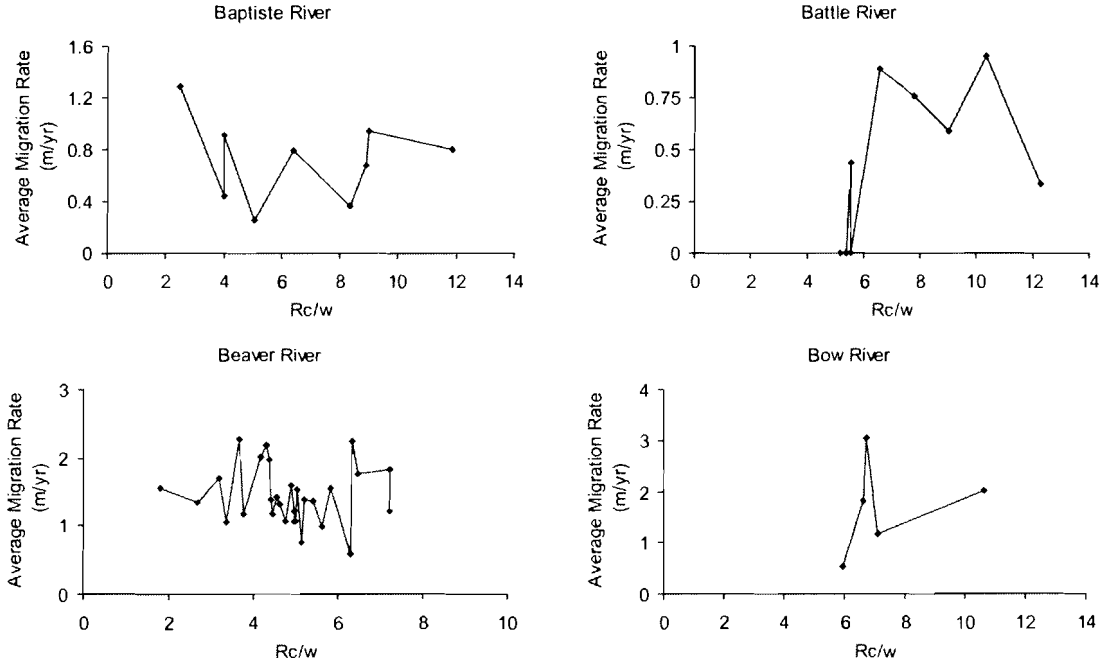

Clear River

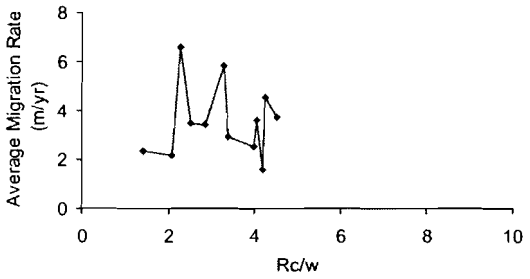

Clearwater River

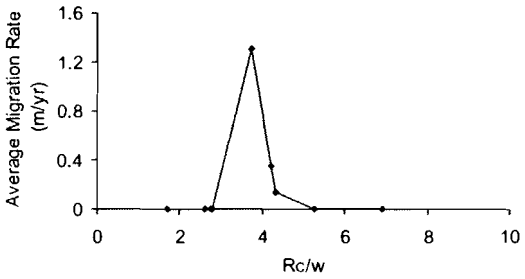

Doig River

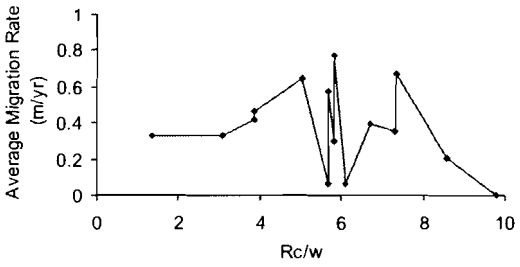

Fontas River

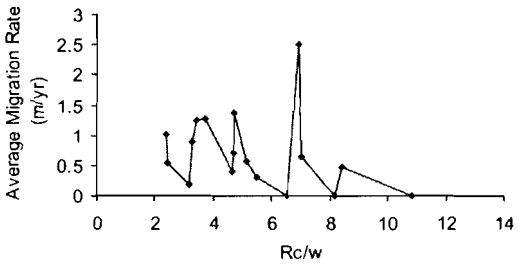

Fort Nelson River (downstream)

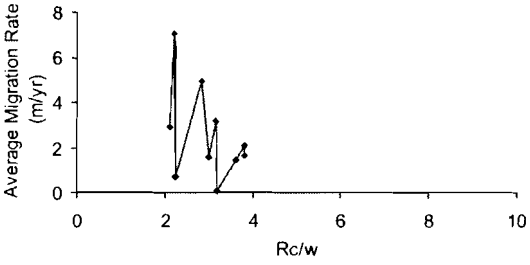

Fort Nelson River (upstream)

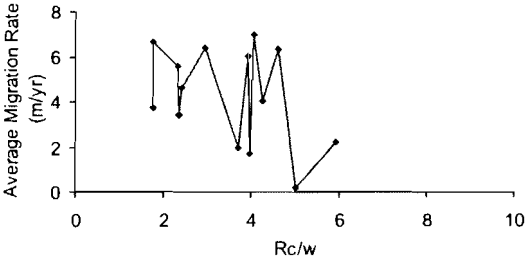

Hay River (downstream)

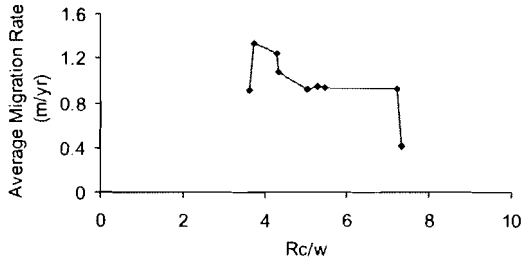

Hay River (upstream)

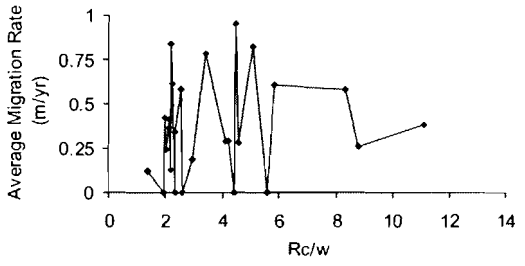

Klua River

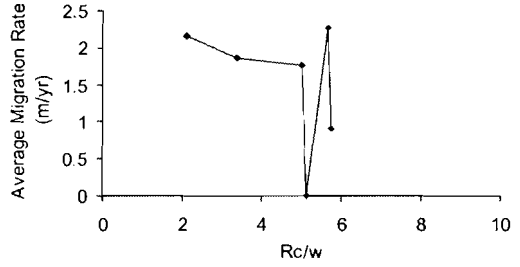

Kootenay River

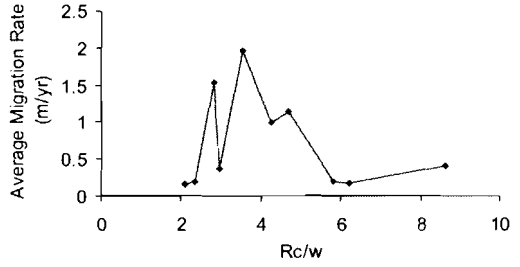

Milk River

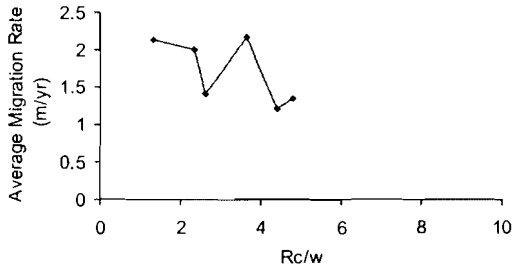

Muskwa River

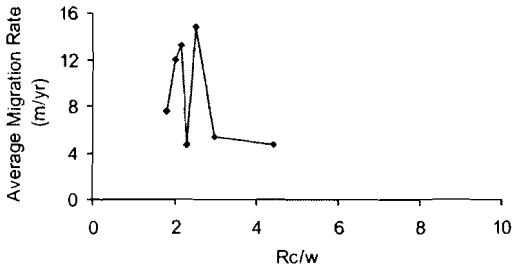

North Saskatchewan River

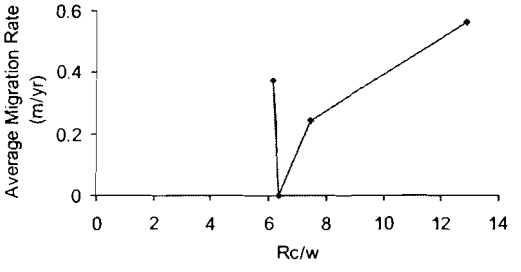

Oldman River

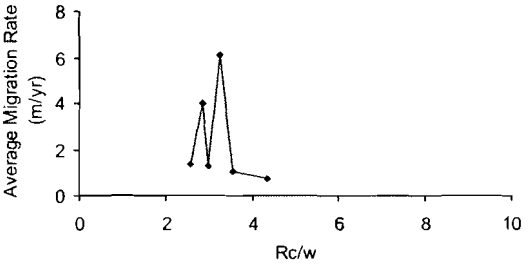

Petitot River

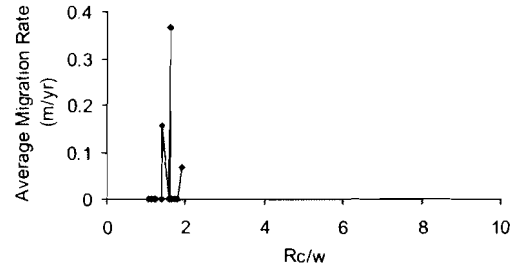

Pinto River

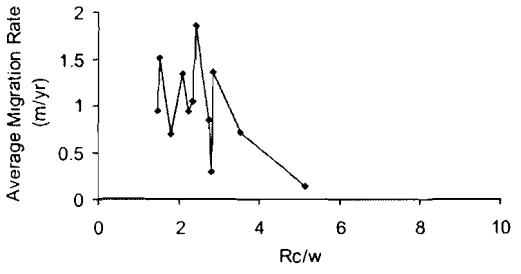

Prophet River

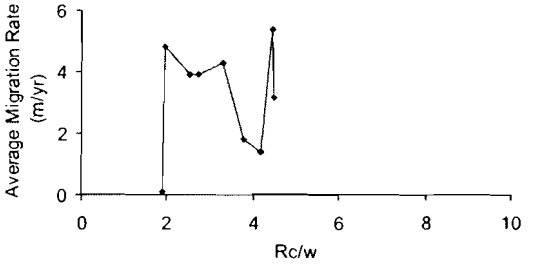

Red Deer River

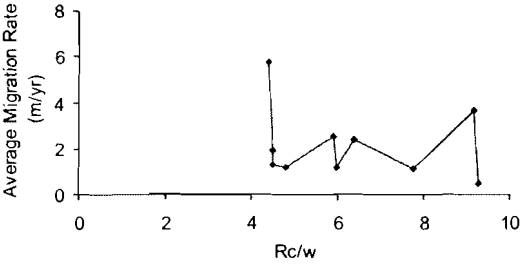

Wapiti River

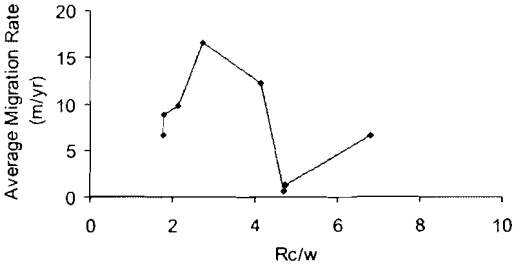

Wildhay River

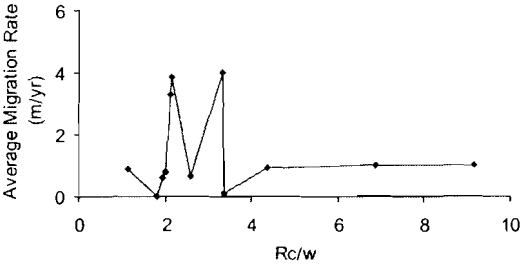

Migration rates have been shown to be closely related to drainage area (Brice, 1984; Hooke, 1980). Hooke (1980) found a high percentage of variation in erosion rate, 53%, could be explained using catchment area alone. Such a strong relation was not found in this study but generalities do exist. The largest migration rates are associated with the larger drainage areas, although low migration rates were also observed in drainage areas of relatively large size (Figure 3.23). When the migration rate is normalized to bankfull width the trend reverses; the largest migration rates per unit width are located in smaller watersheds. Many of these rivers are small, active rivers; a comparatively small absolute movement will have a proportionally larger impact on the normalized migration rate as compared to larger rivers. The lack of a strong relation between drainage area and migration rate in this study is likely due to the relatively small range of drainage areas present. This inference is also supported by Figure 3.10, where the data from this study are plotted with previously published rates. In this case a strong relation between drainage area and migration rate is observed. Hickin (1988) has also noted that the relation between drainage area and migration rate can be lost amongst data scatter for data sets spanning less than a few orders of magnitude in drainage area.

Figure 3.23: Relationship between drainage area and migration rate

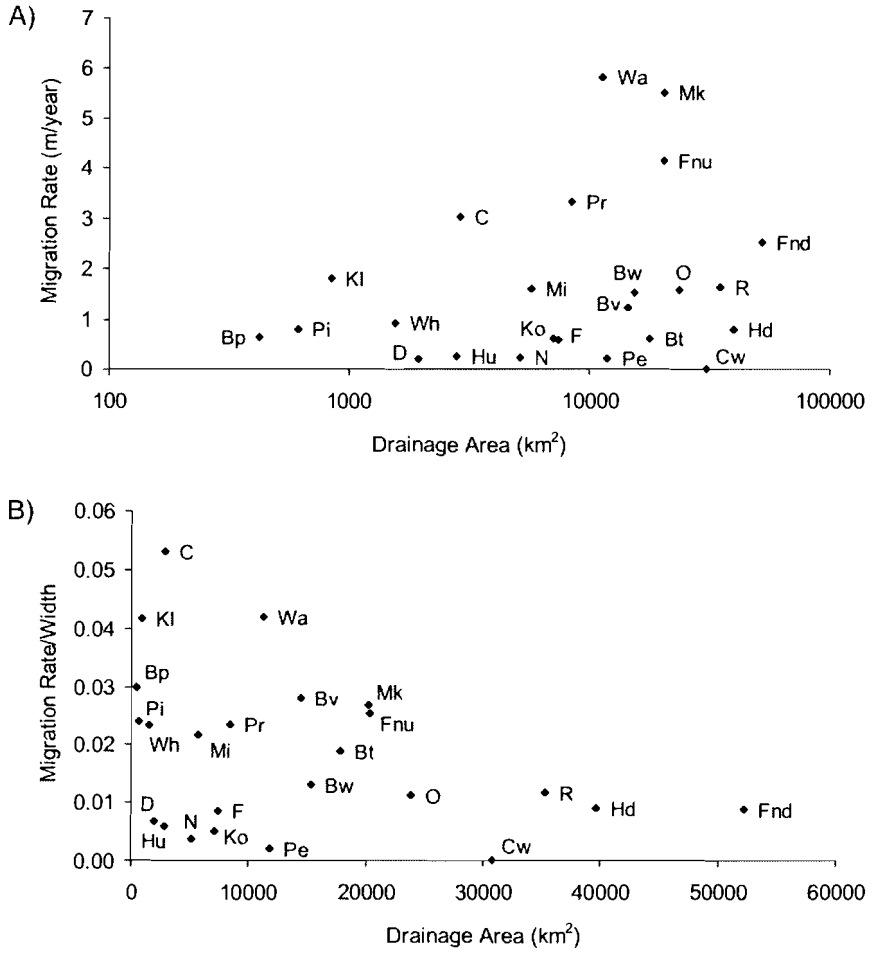

Previous studies have shown channel width to have a strong relationship with migration rate. In a study of Rio Grande migration, width statistically explains over 50% of variation in migration rate (Richard et al., 2005); Nanson and Hickin (1986) found width explained 44% of variance in erosion rates in western Canadian rivers. For this study the relationship between width and migration rate is one of the strongest calculated; however, the level of explanation offered is somewhat less than in the previously mentioned work. In general, migration rate increases linearly with bankfull width (Figure 3.24). Simple linear regression

indicates bankfull width explains 32% of the variance in migration rates observed. Many of the study sites, particularly the North Saskatchewan, Petitot and Clearwater rivers, had relatively slow migration rates for their size. To improve the percentage that could be explained by bankfull width the maximum migration rate was used as a substitute for the average rate but found to increase the percentage explained only slightly, to 33%. Sites with low average-migration rates also had low maximum rates, resisting any strengthening in the relation.

Figure 3.24: The relation between bankfull width and migration rate

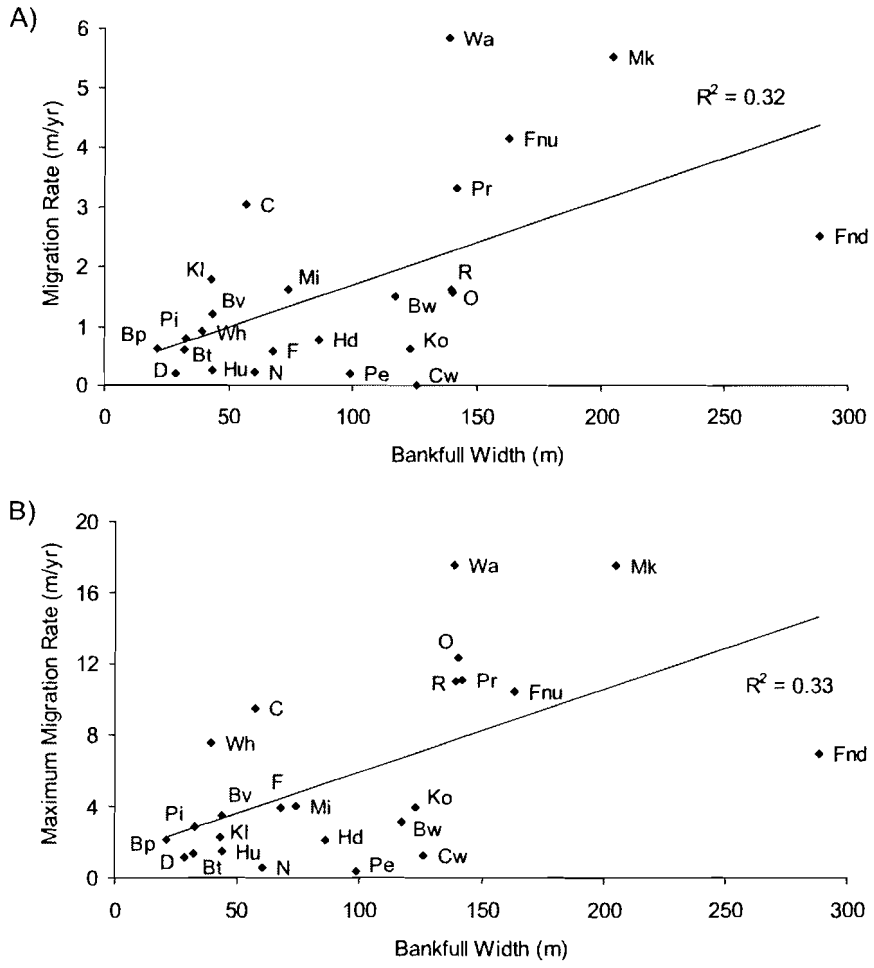

The amount of discharge will obviously have an impact on the rate of migration for a river. If discharge is insufficient the river will be incapable of entraining and transporting sediment and channel movement will not occur. For this study, the discharge used in analysis is the mean annual flood. Figure 3.25 presents semi-log plots of both average migration rate (a) and migration rate per unit channel width (b) versus the mean annual flood. Overall, absolute migration rate increases linearly with discharge and explains 30% of the variation in migration rate. If the study sites are split into their respective bed material types a

strong relationship between the migration rates of gravel-bed rivers and mean annual flood is evident; the explanation of variance in migration rate jumps to 58%. However, most of this increase is due to the Fort Nelson (downstream) site having a bed material classification of transitional gravel. Due to its very large mean annual flood and relatively slow absolute migration rate, the Fort Nelson (downstream) site has a significant influence on the trend lines drawn in this plot. If gravel and transitional gravel sites are combined into one classification the level of explanation drops to 26%. Sites with bed material classifications of sand and transitional sand have average migration rates that are in the lower range of the data but no strong linear relation is evident for these sites. Although only nine sites are sand-bedded to some extent, when comparing sites having similar mean annual floods it can be seen that the transitional sand-bedded rivers consistently display higher rates of migration than those that are fully sand-bedded. There is no general trend observed for average migration rates of sand-bed rivers when examining absolute migration rates; similar migration rates are found over a range of mean annual floods. Once scaled to bankfull width the sand-bedded rivers display a general decrease in migration rate per unit width with increases in mean annual flood. This decrease is linear and a trend line through this subset of the data has an $R^2 = 0.354$. The sand-bed rivers still generally plot in the lower range of the data after scaling.

If the square root of mean annual flood is used in place of mean annual flood the overall percentage of explained variance in migration rate increases slightly (to 35%) and the percentage for fully gravel-bedded rivers decreases (to

48%). However, the percentage of variance explained for gravel-bedded rivers including those with transitional-gravel beds increases to 35%. Use of the square root of mean annual flood has no influence on the percent of variance that can be explained when migration rate is scaled to bankfull width.

Figure 3.25: Migration rate and mean annual flood

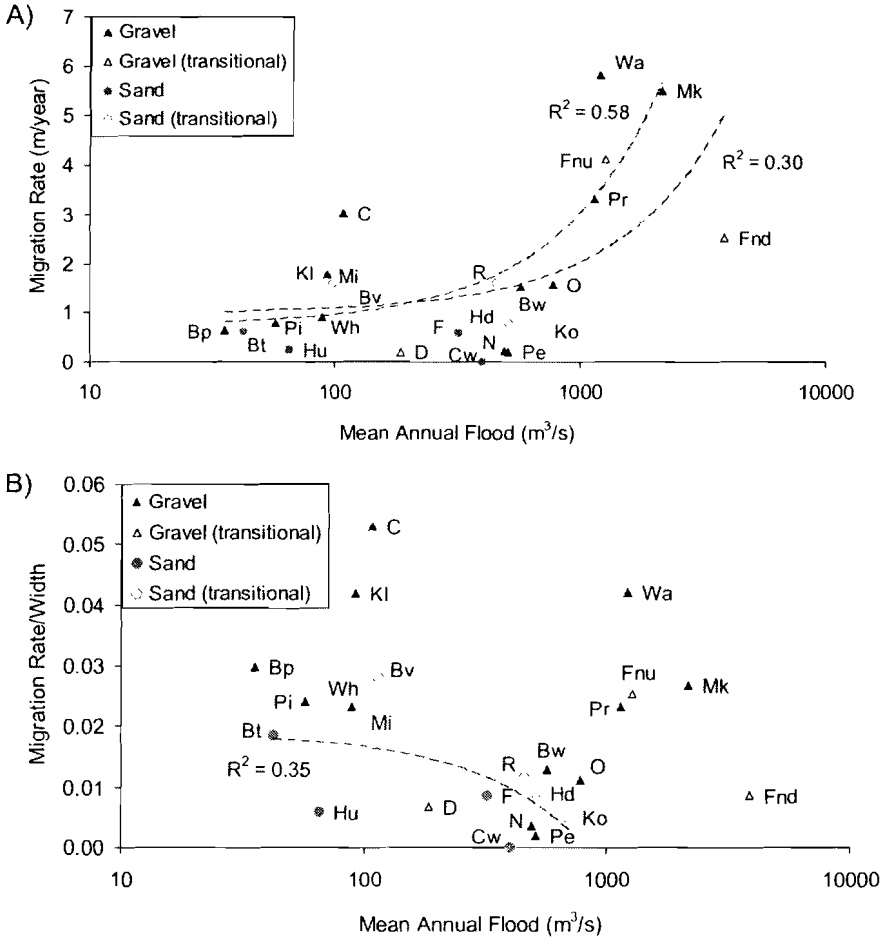

Physical reasoning suggests that increasing slope should increase migration rate, all else being equal. Figure 3.26 plots the relation between slope and migration rate for the study sites, with migration scaled to bankfull width. Study sites with relatively high slopes do display higher migration rates. Overall,

channel slope explains 22% of variation in migration rate; this increases slightly (to 25%) when valley slope is used. However, there is significant scatter within this relation and slope is obviously not the only factor influencing the migration rate of these rivers.

Figure 3.26: The relation between slope and migration rate

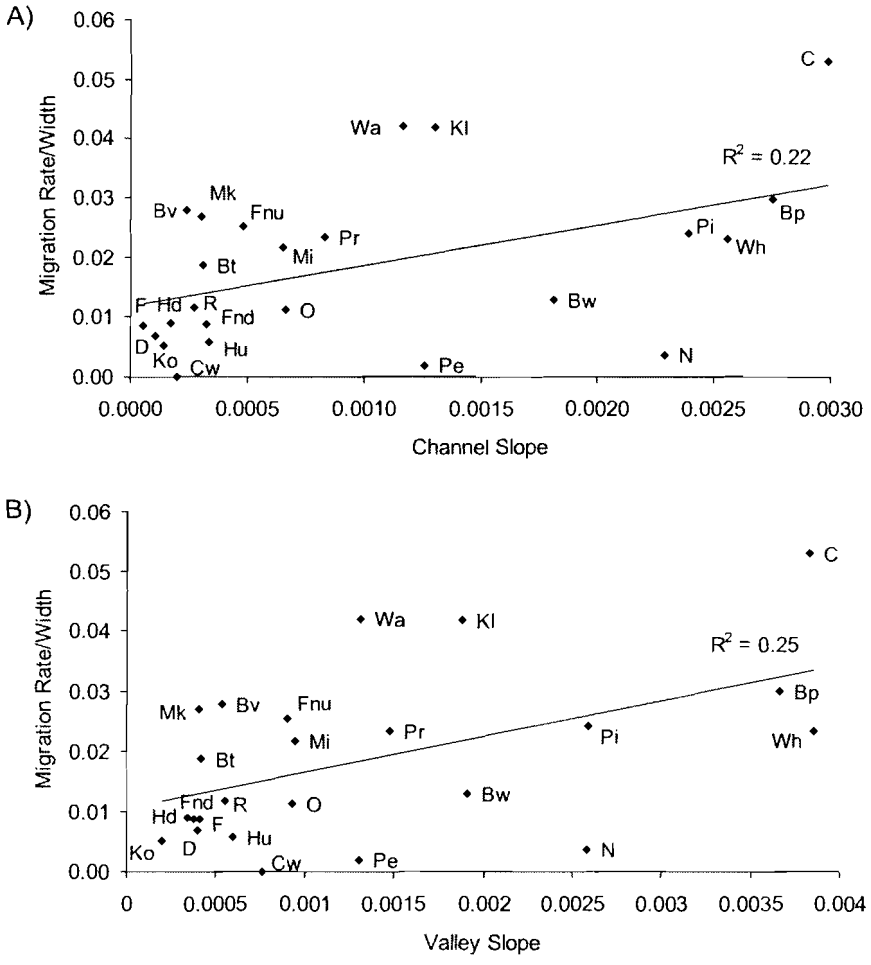

Perhaps a better measure for seeking an explanation of migration rate is stream power because it incorporates both discharge and slope. Stream power is the rate of potential energy expenditure per unit channel length, expressed as a

product of discharge and channel slope. Previous work has shown stream power to be very important in for explanation of variance in migration rates. Studies by both Nanson and Hickin (1986) and Richard et al. (2005) found stream power explained 48% and 52% respectively of the variation in migration rate. The relationships between slope and migration rate were shown previously to be slightly stronger when valley slope was utilized. Thus stream power was calculated using valley slope in place of channel slope for this study. Specific stream power, the stream power per unit width, is also calculated using the valley slope.

Figure 3.27: The relation between migration rate and stream power

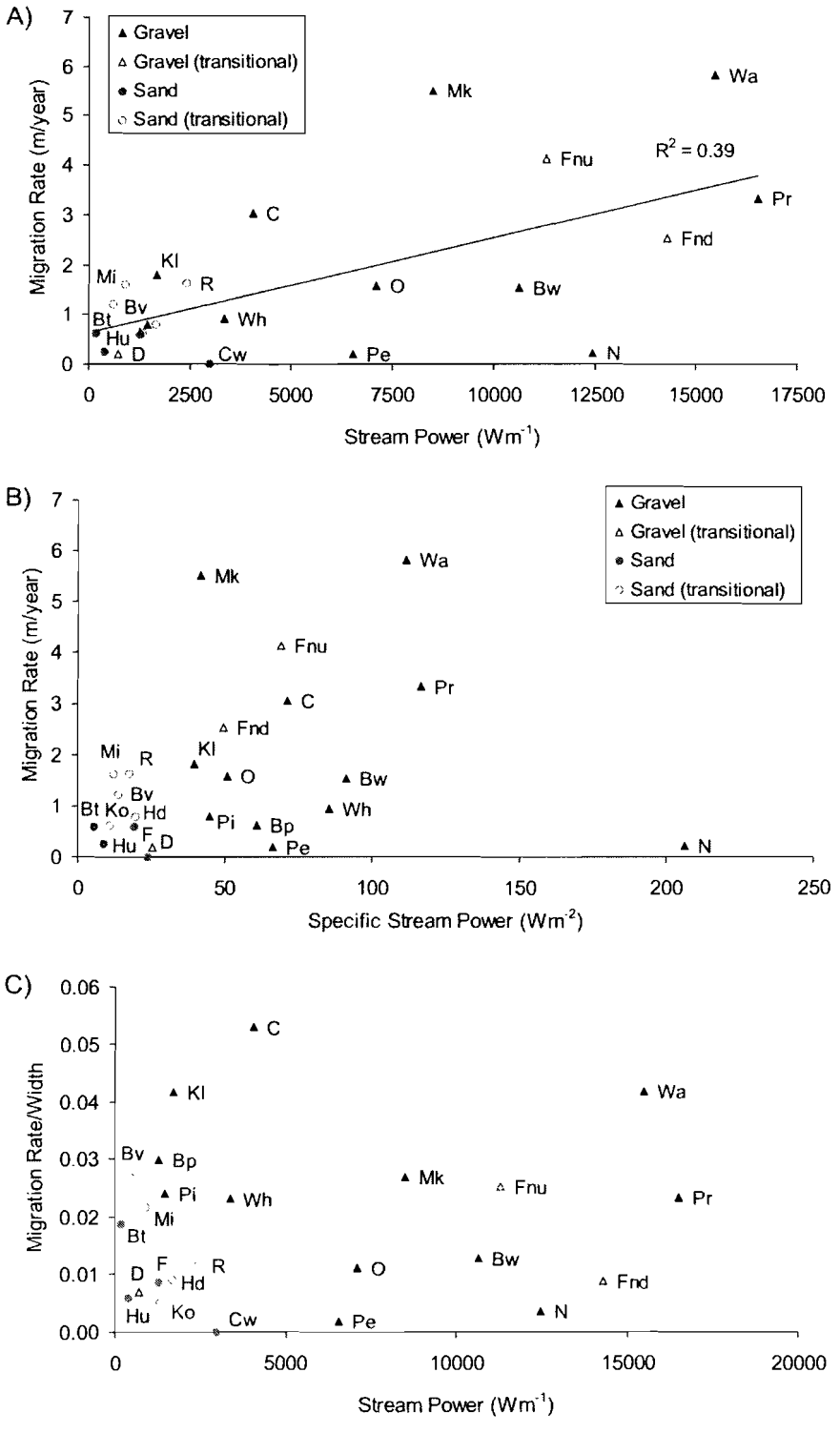

Stream power provided the best explanation for variation in migration rate of any factor examined within this study (Figure 3.27). Stream power alone explains 39% of the variation, slightly higher than the 32% provided by bankfull width and the 30% by mean annual flood. No improvement in this percentage can be achieved by separating the study sites by their bed-material type. Using exclusively gravel-bedded rivers the percentage of variation explained decreases to 30%; no trend exists when the sand-bed rivers are considered separately. It is apparent in Figure 3.27 that the sand-bed rivers within this study have relatively low stream power and somewhat lower migration rates overall. When migration rate is scaled to bankfull width only two of the transitional sand-bed study sites are migrating at a rate greater than 2% of their bankfull width per year. In comparison, a large proportion of gravel-bedded rivers are migrating at rates greater than 2%.

Certain study reaches, notably the Clearwater, North Saskatchewan and Petitot river sites, have recorded much lower migration rates than may be expected for their available stream power. The Clearwater and Petitot river sites are unregulated and it is likely other site-specific factors that cannot be resolved within this study are responsible for their low migration rates. However, discharge at the North Saskatchewan River location is significantly affected by the building of the Bighorn dam within the time period of photography. As such, its migration behaviour may be suspect. If this one site is taken out the plots, the explanation of variance in migration rate provided by stream power jumps to 52%, consistent with the results of previous studies. While the complete removal of the North

Saskatchewan River site from the dataset may not be justified, it should be noted that this site does have a significant effect on the robustness of the relations.

While stream power does provide a reasonable predictor for migration rate, at best it still leaves 48% of the variation in rate unexplained. Although it is unreasonable in a natural science study to expect 100% explanation, an explanatory component shown elsewhere to be important (Hickin and Nanson, 1984) is the resistance to erosion of the boundary sediment within the meanders. While Nanson and Hickin (1986) found sediment size at the base of the outer bank to be the best measure of erosion resistance, other studies placed more importance on percentage of silt/clay in the banks (Hooke, 1980), presence of vegetation (Burckhardt and Todd, 1998) and height of the outer bank (Hickin and Nanson, 1984). While the importance of each may vary between sites the commonality between them is the estimate of resistive forces they provide. Due to the remote nature of many of the study reaches and lack of published data, quantitative estimates of boundary-sediment resistance at the study sites is beyond the means of this study. Yet it is likely that these missing elements explain a significant proportion of the statistically unexplained variation in migration rate. Supporting this suggestion are the probable bank characteristics of five of the six sites recording the lowest absolute migration rates: the Clearwater, Doig, Petitot, Hay (upstream) and Fontas river sites. Each of these rivers is to some extent flowing through areas of muskeg. Banks would likely have significant proportions of fine-grained sediment and dense root mats, making them highly resistive to erosion and thereby lowering migration rate. The

North Saskatchewan site is the sixth site and as noted, regulation may be the main reason for its slow migration rate. Although factors to explain resistance of boundary sediment to erosion would likely improve the level of explanation provided by any relation, there are undoubtedly also local, site-specific factors that are influencing migration rate at individual sites that will always weaken simple linear relations derived from the data. The intermittent nature of migration will further confound attempts at correlating migration rate to controlling factors. Past studies have used multiple regression techniques to further improve explanation of variance in migration rate. Multiple regression was attempted in this study using various combinations of slope, mean annual flood and width as independent variables but these provided no improvement in the level of explanation that could be achieved by simple bivariate correlation.

3.3.4 Regional Trends in Migration Rates

Figure 3.28 is a map of average migration rate scaled to bankfull width for the study sites. Sites are classified according to the estimate of bed material; study sites marked as having transitional gravel or sand have been classified based on which category best describes the bulk of the bed material.

Figure 3.28: Regional trends for average migration rates classified by bed material type

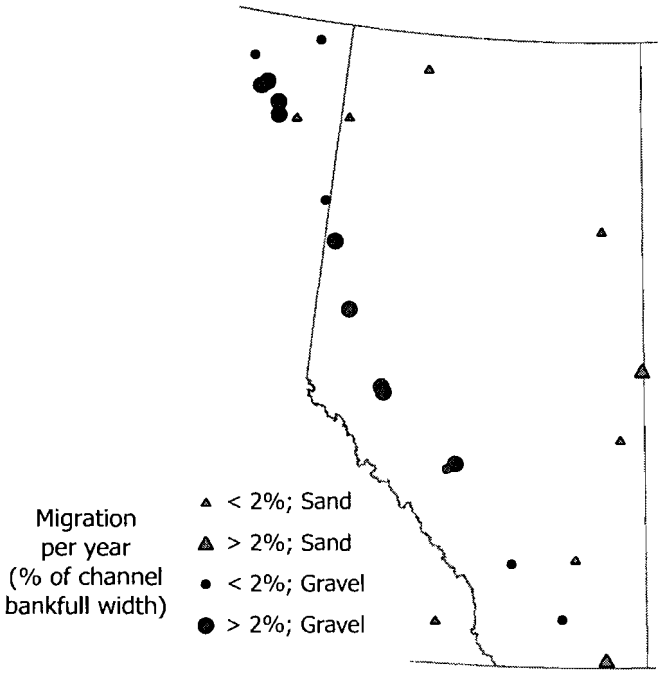

With the exceptions of the Milk River in southern Alberta and the Beaver River on the border of Saskatchewan, study reaches that are migrating on average greater than 2% of their channel width are gravel-bed rivers located in the west of the study region, paralleling the Rocky Mountains. In general, rivers with primarily sand-beds are found in the eastern half of Alberta, although exceptions do exist, such as the Fontas River in northeastern B.C. and the Kootenay River in southeastern B.C. The Milk River is the only site in the southern portion of the study region with a high migration rate per channel width, although at a rate of 2.1%, it is very close to the cut-off for this grouping.

3.4 Summary

In general, relationships in planform geometry that have been found for freely-meandering rivers appear to apply to confined meanders as well.

Wavelength is proportional to bankfull width; both variables are proportional to the square root of discharge. Wavelength for confined meanders is generally around 15 times the bankfull width, slightly higher than the 8 – 12 times that is commonly given for other rivers. The median Rc/w of 4.1 calculated in this study is also slightly higher when compared to the median Rc/w between 2 and 3 that is generally reported for freely-meandering rivers.

Absolute migration rates for the confined meanders fall within the general distribution of rates published for other rivers, both in a global and regional context. Although rates for study sites such as the Wapiti River at 5.8 m/year may seem very high, they are not abnormally so when compared to those measured elsewhere. Migration rates for the study sites varied over time; during the most recent photo interval most rates declined or remained constant although four study sites did show a clear increase in migration rate during this same period. Generally, trends in migration rates could be linked to corresponding changes in mean annual flood where such records are available, though sites such as the Wildhay River and the Muskwa River are exceptions to this. It is clear that, while the observed trends in migration rate are likely linked to discharge patterns, there are other factors influencing rate changes at each site that have not been captured in this study. Regionally, migration rates have decreased in northeastern B.C. and remained constant or decreased in central and southern Alberta. However, absolute migration rates for most rivers in northeastern B.C. remain among the highest measured in this study.

Attempts to link controlling factors to migration rate are modestly successful. Similar to other studies, the highest migration rates are found with bend curvatures between 2 and 4; however, this relation has a good deal of scatter within it. In general, migration rate increases with drainage area although this relation is much more apparent when drainage areas range over several orders. Slope displays the same sort of broad relation; high rates of migration are associated with steeper slopes. The use of width and mean annual flood as controlling factors is modestly successful with 32% and 30% respectively of variation in migration rate explained by using these factors alone. Stream power offers the best predictor of migration rate by providing explanation for 39% of variance in migration rate. This percentage increases to 52% with the exclusion of the study site on the North Saskatchewan River, one affected by a nearby dam. These levels of explanation are comparable to those found by other others (Nanson and Hickin, 1986; Richard et al., 2005). Changes in migration behaviour that could be clearly attributed to bed material type were absent; however, sand-bed rivers were noted to have lower stream power and to generally have lower migration rates as compared to similar-sized gravel-bed rivers.

Planform appearance notwithstanding, the behaviour and characteristics of the confined meandering rivers in this study appear to be consistent with those observed for their freely-meandering counterparts. While there may be slight differences in the specifics of the relationships between variables of planform geometry, the same common relationships exist. Migration rates fall within the general distribution of published migration rates and the levels of explanation for

the varying rates of migration that can be achieved by statistical analysis are also similar to published studies that have examined freely-meandering rivers.

CHAPTER 4: BEDLOAD TRANSPORT

4.1 Introduction

This chapter presents the bedload-transport estimates based on the channel morphodynamics determined for five of the study sites within this project. A basic description for each site is provided as well as the cross-sections used for calculations of the thickness of bedload material in the floodplain. Although there are no direct measurements of bedload transport for these five sites for comparison, the morphology-based rates are set in the context of published rates for other rivers. Furthermore, the present data provide an opportunity to assess the utility of a widely-used bedload transport formula (Meyer-Peter and Müller, 1948).

4.2 Bow River

The Bow River is a tributary of the South Saskatchewan River; flow eventually drains into Hudson Bay via Lake Winnipeg. The total watershed area for the Bow River is slightly greater than 25 000 km^2; the drainage area at the

study site is 15 370 km^2. The study site is located 22 km downstream of Calgary, 2 km from the Highwood River confluence.

Clasts were measured on four separate bars within the study reach. Grain-size distribution is shown in Figure 4.1; the median grain-size measured over all four bars is 36 mm.

Figure 4.1: Grain-size distribution at Bow River site

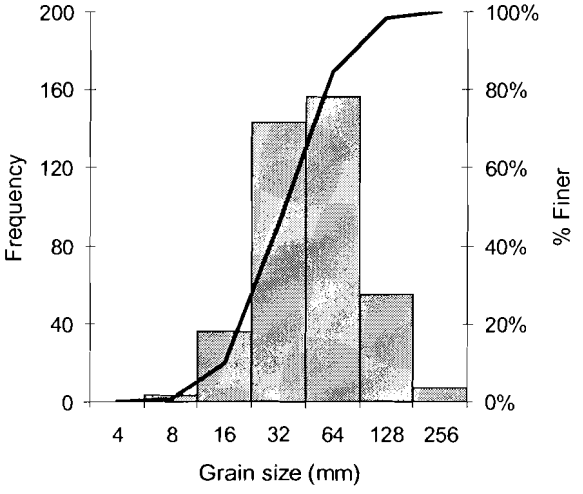

At the cross-section locations the confining valley walls rise above the floodplain approximately 80 m; the valley bottom is about 400 m in width at these locations. Two separate bends were examined in the field with three cross-sections measured on each bend. Figure 4.2a shows a typical view of the Bow River at the second cross-section; the following photo (Figure 4.2b) depicts the rather sharp delineation between the coarse bedload layer and finer sediments within the bank at the same cross-section.

Figure 4.2a: Bow River site (2 km east of the Highwood River confluence)

Figure 4.2b: The upper boundary of the coarse basal layer at Bow River site

The height of the gravel layer in the bank was surveyed at each cross-section. The average thickness of the coarse layer for each of the upstream and downstream bends is used in the bedload-transport calculation. One cross-section on the downstream bend is not used in the calculations of bedload transport because of the difficulty in delineating the coarse bedload layer in the bank. Average thickness of the gravel layer (h) for the downstream bend is therefore based on the two remaining cross-sections. The actual cross-sections

and thickness of the gravel layer are presented in Figure 4.3. For all cross-sections within this chapter the solid line represents the water level at the time of survey while the dashed line indicates the height of the gravel layer in the bank. Cross-sections 1 to 3 are located on the upstream bend; cross-sections 4 and 5 are located on the downstream study bend. Regardless of which bend is examined, the value for h varies only slightly, from 3.4 m to 3.8 m.

Figure 4.3a: Cross-sections for the upstream bend of Bow River

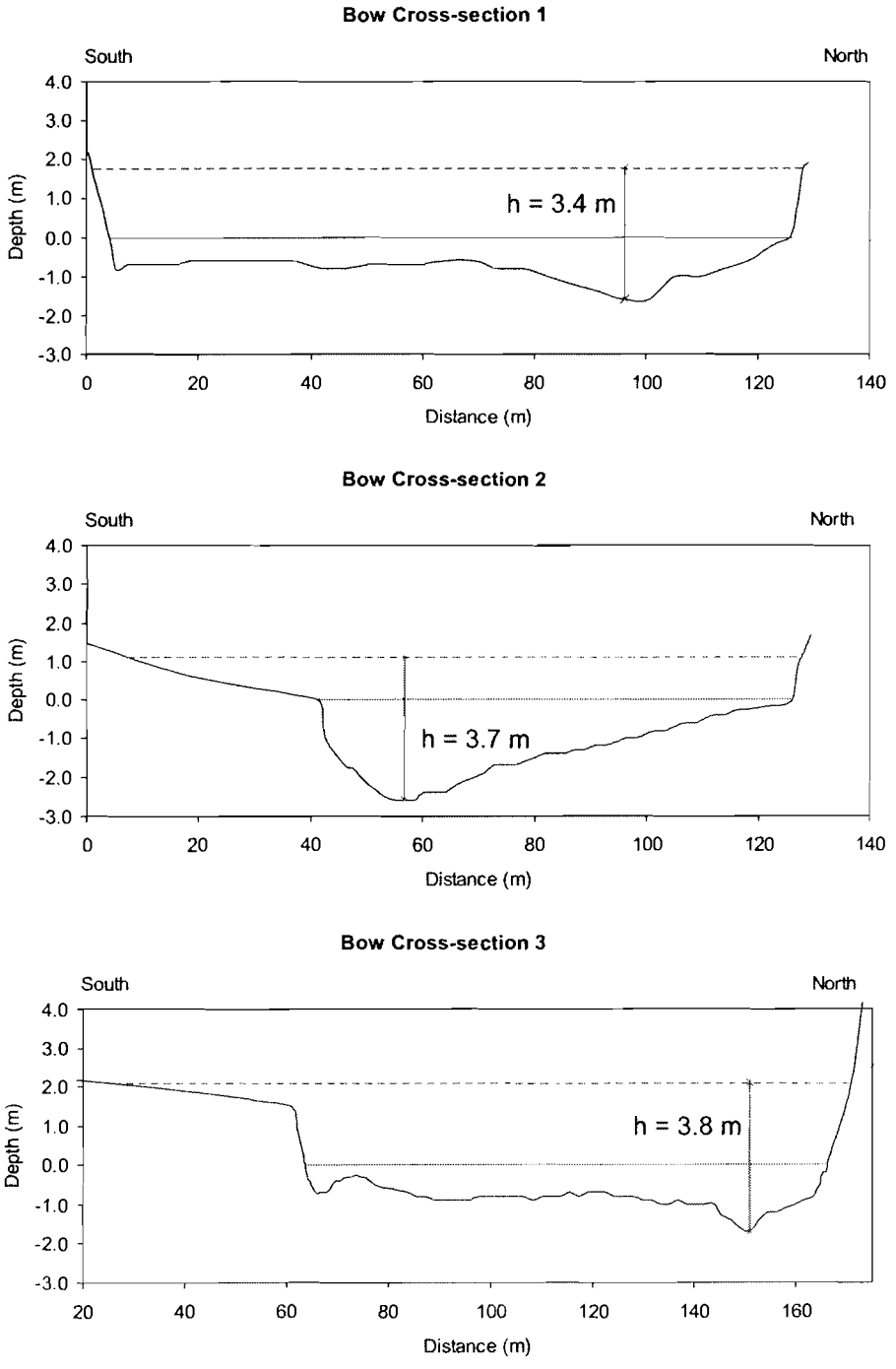

Figure 4.3b: Cross-sections for the downstream bend of Bow River

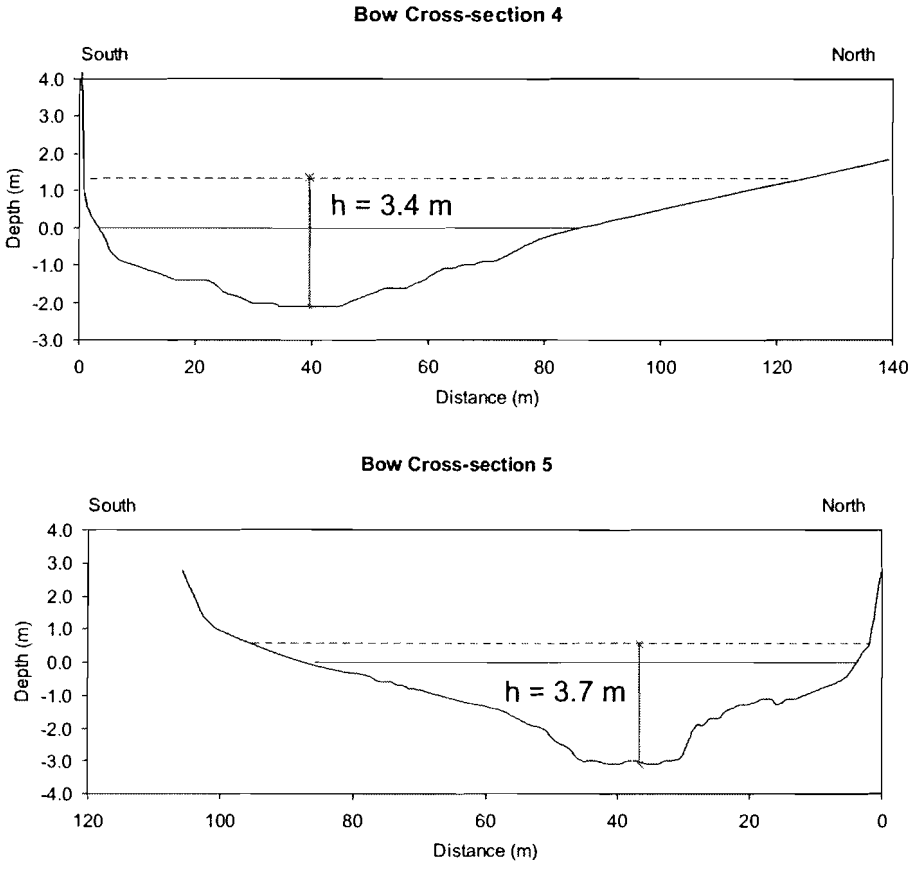

Following the methodology discussed in Chapter 2, an average volumetric bedload-transport rate was calculated using the following equation:

$$Q_s = \frac{Ah}{t} \qquad (2.1)$$

where Q_s is the bedload transport rate, A is the area eroded over the time period of observation, h is the height of the mobilized bed material layer, and t is the time period of observation in years. Using the average thickness of the gravel layer at each bend and the 48-year time period of aerial photography provides an

average volumetric bedload transport rate for the Bow River of 1500 m^3 per year (Table 4.1).

Table 4.1: Morphologic bedload transport rate for the Bow River site

Bow River	Average h (m)	Area Eroded (m^2)	Bedload Transport Rate (m^3/year)
Upstream Bend	3.7	16 300	1200
Downstream Bend	3.6	23 400	1700
		Average Rate	**1500**

4.3 Red Deer River

The Red Deer River basin is the major watershed bordering the north of the Bow River basin. The Red Deer River also flows into the South Saskatchewan River, joining this river just over the Saskatchewan border. The total drainage area of the Red Deer River basin is close to 50 000 km^2; the drainage area at the study site is 35 280 km^2. The study site is located approximately 70 km downstream of the town of Drumheller, 3 km upstream of the Highway 36 bridge crossing.

Clasts were measured on two bars within the study reach. Grain-size distribution is shown in Figure 4.4; the median grain-size of clasts measured on the two bars is 38 mm.

Figure 4.4: Grain-size distribution for Red Deer River site

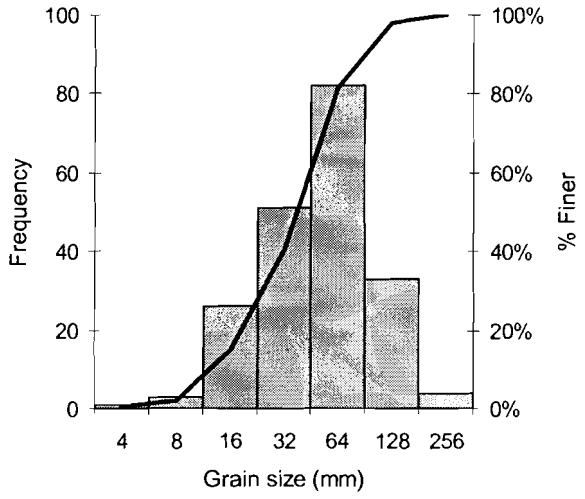

The valley walls are approximately 65 m high at the study site; the valley bottom is about 750 m wide at the location of the cross-sections. Three cross-sections were taken along one river bend. At this bend the confining valley walls are somewhat set back from the river and the river is flowing against an approximately 15 m-high terrace at the outside bank. Slumping of this bank is very common and this colluvium, together with small ephemeral streams which cut through the terrace, appear to be sources for much of the gravel present in this section of the river. Figure 4.5a shows a typical view at the study bend with the terrace on the left; Figure 4.5b illustrates the upper boundary of the coarse gravel layer. Cross-sections showing the thickness of the gravel layer are presented in Figure 4.6.

Figure 4.5a: Red Deer River site (3 km upstream of the Highway 36 bridge crossing)

Figure 4.5b: The upper boundary of the coarse basal layer just above the water line at the Red Deer River site

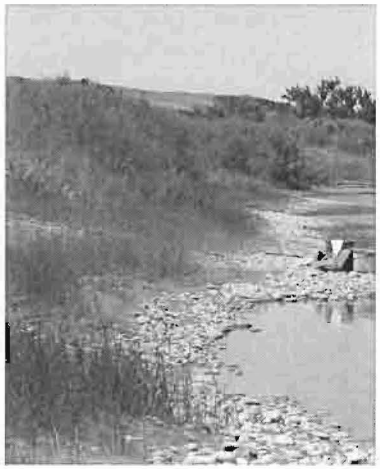

Figure 4.6: Cross-sections for the study bend on Red Deer River

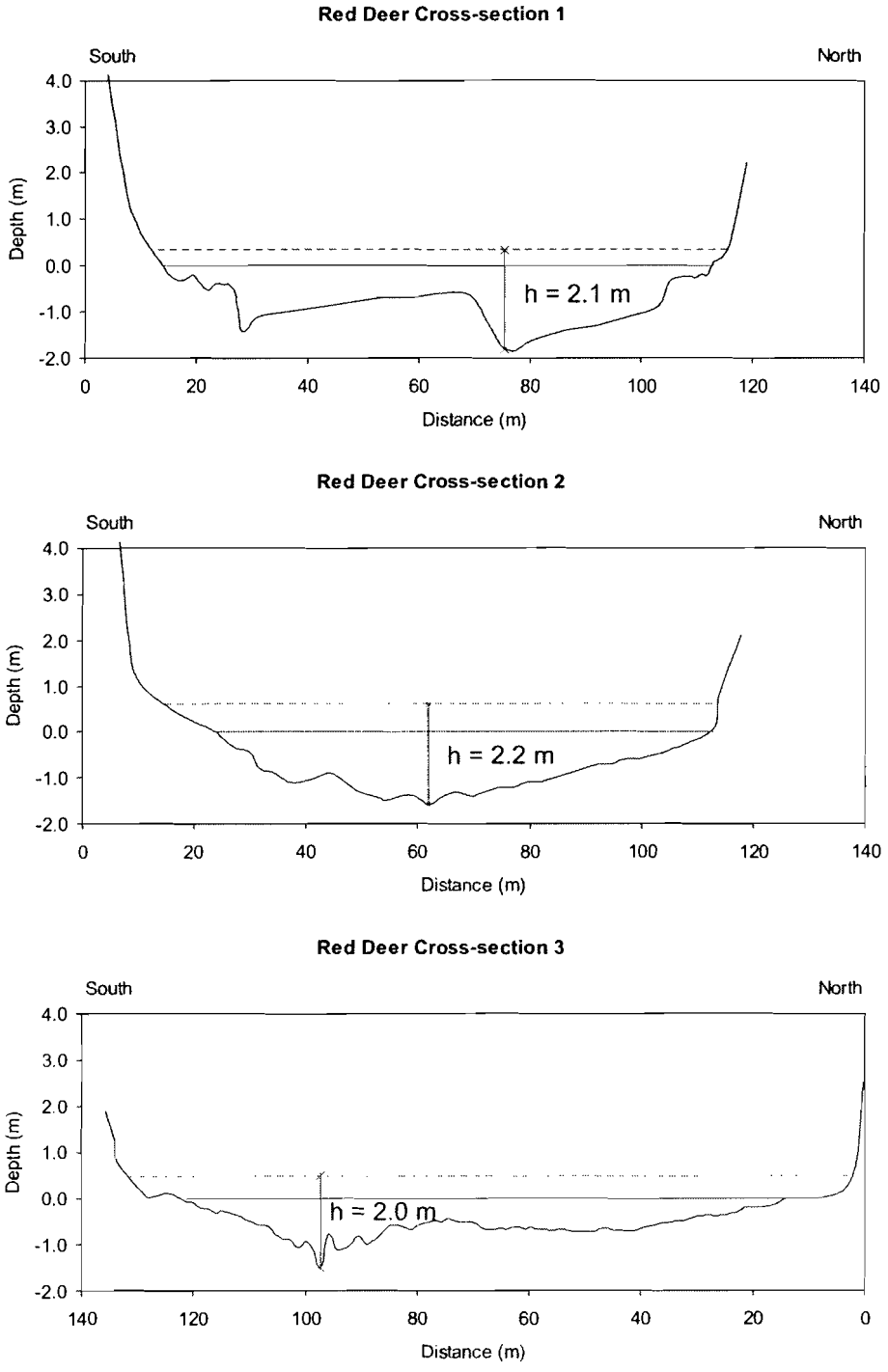

Combining the average thickness of the gravel layer with the area eroded for these bends during the 51 year period of aerial photography provides an average volumetric bedload transport rate of 2600 m^3 per year (Table 4.2).

Table 4.2: Morphologic bedload transport rate for the Red Deer River site

Red Deer River	Average h (m)	Area Eroded (m^2)	Bedload Transport Rate (m^3/year)
	2.1	62 800	2600

4.4 Fort Nelson River

The Fort Nelson River is a major tributary of the Liard River, itself a tributary of the Arctic-bound Mackenzie River. The drainage area at the site is 52 230 km^2, the largest of any study site within this project. The site is located 65 km downstream of the town of Fort Nelson, 3 km upstream of the Liard Highway bridge crossing.

Clasts were measured on three separate bars within the study reach. Grain-size distribution is shown in Figure 4.7; the median grain-size of clasts measured on the three bars is the finest of the study sites at 20 mm.

Figure 4.7: Grain-size distribution at the Fort Nelson River site

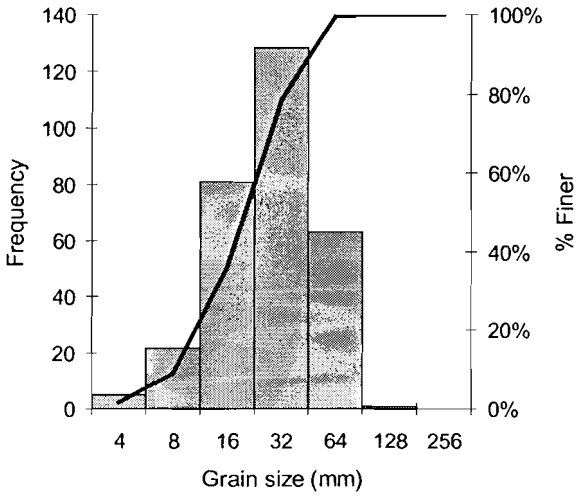

At the cross-section locations the confining valley walls rise above the floodplain approximately 65 m; the valley bottom is around 1240 m wide at these locations. Two separate bends were examined in the field and three cross-sections measured on each bend. At the study sites the river is characterized by high confining valley walls that commonly slump into the channel and well-developed point bars on the opposite bank which grade into concave-bank benches near the point of channel impingement on the valley walls (Figure 4.8a). The boundary of the coarse gravel layer is generally well-defined in the bank (Figure 4.8b).

Figure 4.8a: Fort Nelson River site
(3 km upstream of the Liard Highway bridge crossing)

Figure 4.8b: The upper boundary of the coarse basal layer at the Fort Nelson River site (bear spray for scale)

One cross-section on the upstream study bend is not used in the calculations of bedload transport; excessive slumping on the concave bank concealed the boundary of the coarse bedload-layer at this cross-section. The average thickness of the gravel layer (h) for the upstream bend is therefore based on the data of the two remaining cross-sections. Cross-sections and thickness of the gravel layer are presented in Figure 4.9.

Figure 4.9a: Cross-sections for the upstream bend of Fort Nelson River

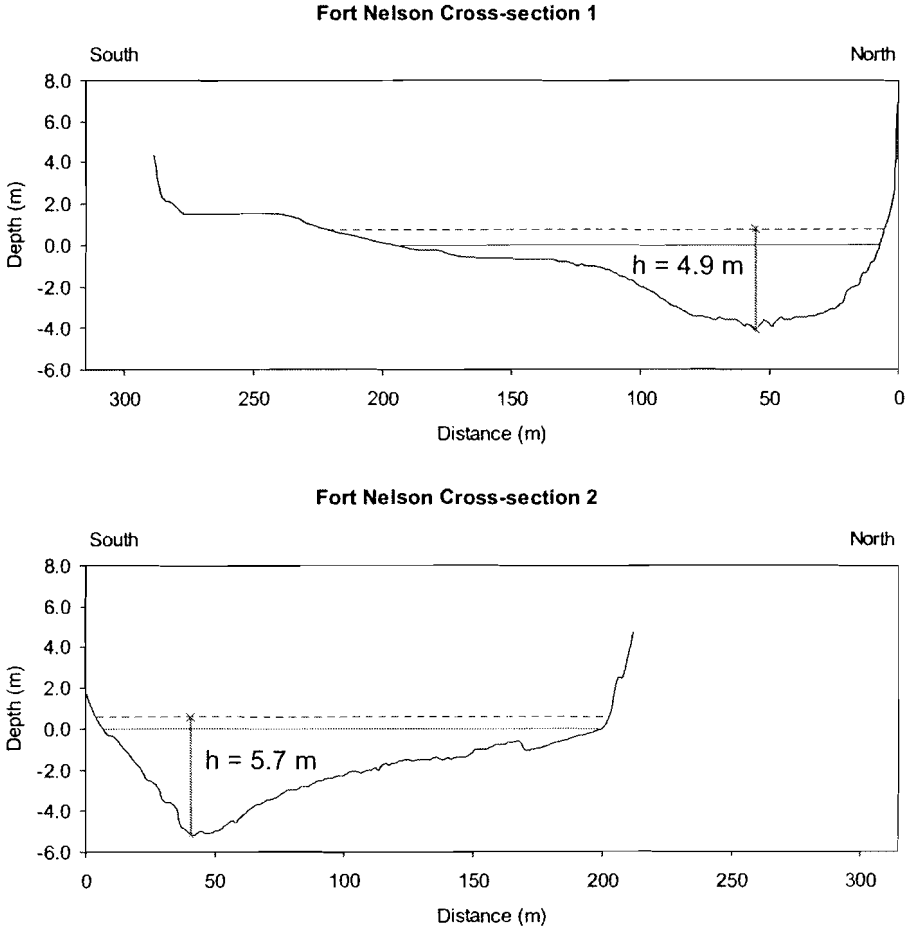

Figure 4.9b: Cross-sections for the downstream bend of Fort Nelson River

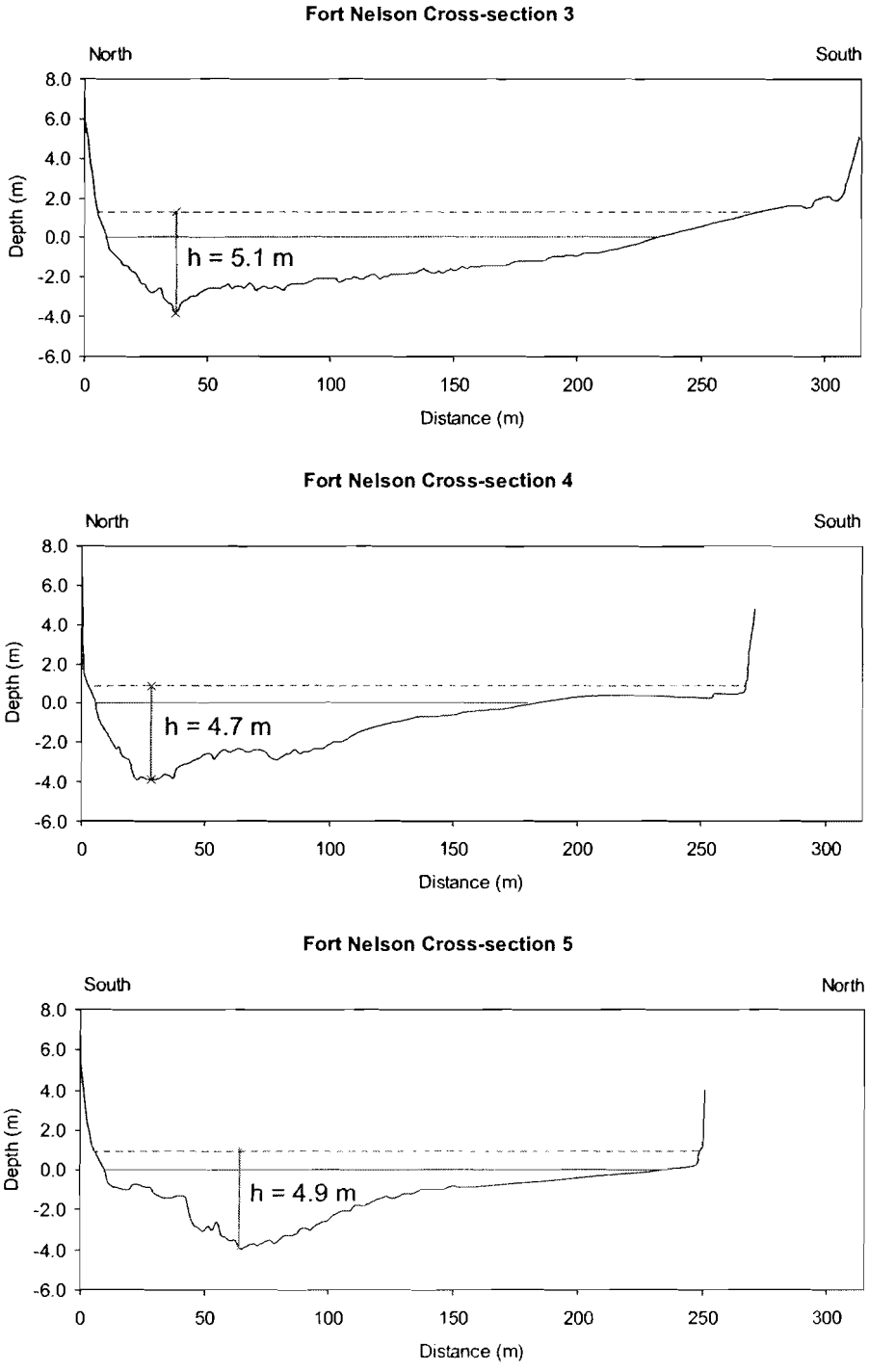

Combining the average thickness of the gravel layer with the area eroded for these bends during the 30 year period of aerial photography provides an average volumetric bedload transport rate of 22 300 m^3 per year (Table 4.3).

Table 4.3: Morphologic bedload transport rate for the Fort Nelson River site

Fort Nelson River	Average h (m)	Area Eroded (m^2)	Bedload Transport Rate (m^3/year)
Upstream Bend	5.3	133 200	23 600
Downstream Bend	4.9	128 200	20 900
		Average Rate	**22 300**

4.5 Muskwa River

The Muskwa River drains the foothills of the Rocky Mountains, joining the Fort Nelson River about 8 km northeast of the town of Fort Nelson. The drainage area at the site is 20 300 km^2. The study site is located directly south of the town of Fort Nelson, less than 2 km upstream of the Alaska Highway bridge crossing.

Clasts were measured on four separate bars within the study reach. The grain-size distribution is shown in Figure 4.10; the median grain-size of clasts measured on the three bars is 37 mm.

Figure 4.10: Grain-size distribution at the Muskwa River site

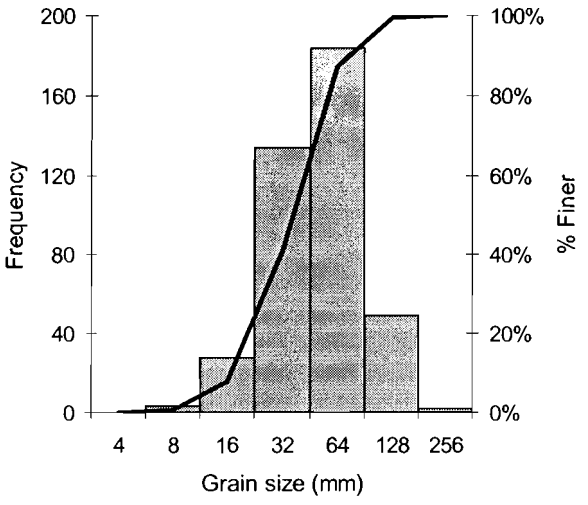

The confining valley walls rise above the river approximately 90 m; the valley bottom is about 1100 m wide at these locations. Two separate bends were examined in the field with three cross-sections measured on each bend. As with the Fort Nelson River sites, the Muskwa River is characterized by high confining valley walls that commonly slump into the channel and well-developed point bars and concave-bank benches (Figure 4.11a). Figure 4.11b is a continuation of the previous view showing the upper boundary of the coarse gravel layer in the bank. The cross-sections and the surveyed thickness of the gravel layer are presented in Figure 4.12.

Figure 4.11a: Muskwa River site (3 km south of town of Fort Nelson, B.C.)

Figure 4.11b: The upper boundary of the coarse basal layer at the Muskwa River site

Figure 4.12a: Cross-sections for the upstream bend of Muskwa River

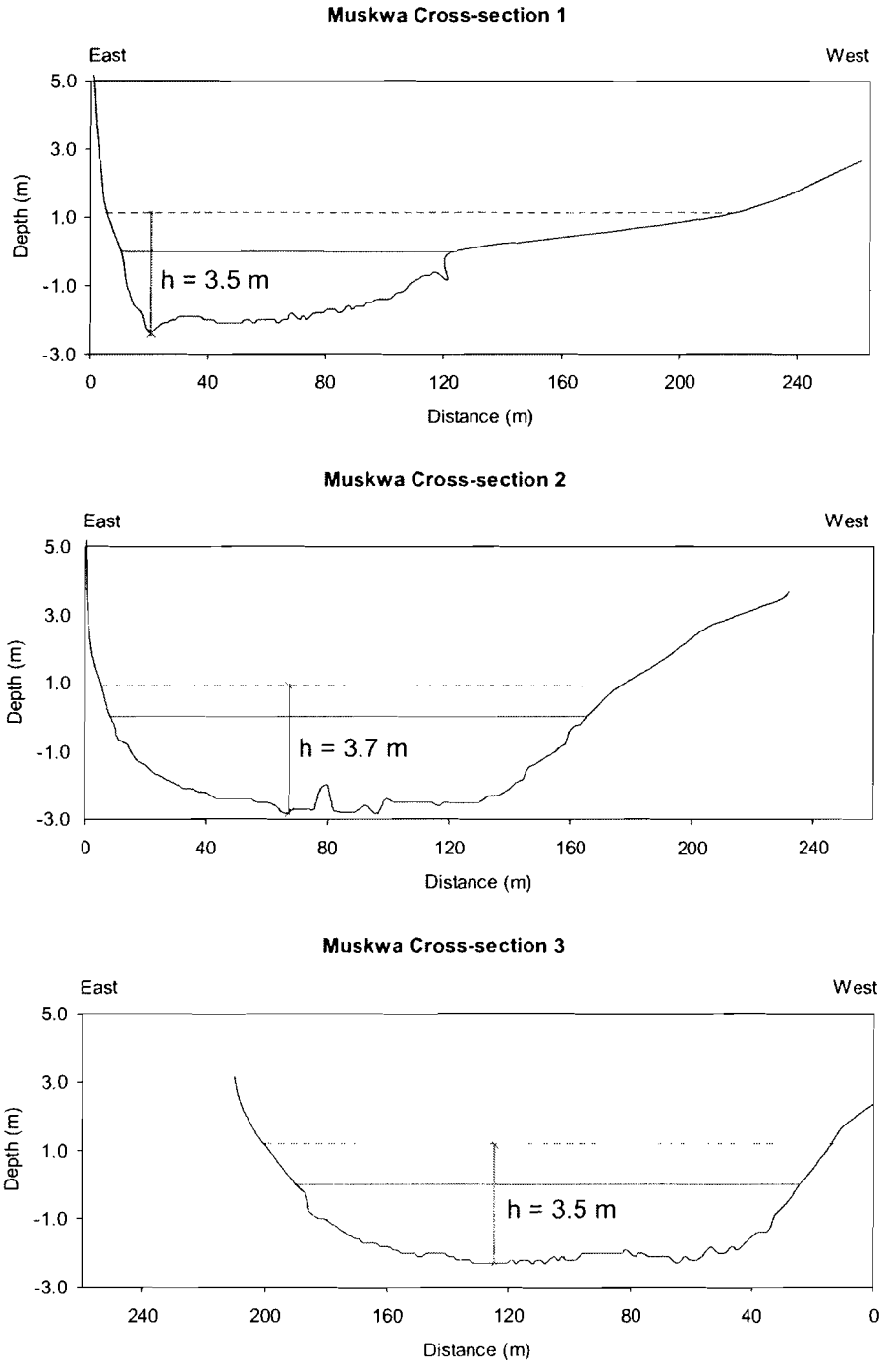

Figure 4.12b: Cross-sections for the downstream bend of Muskwa River

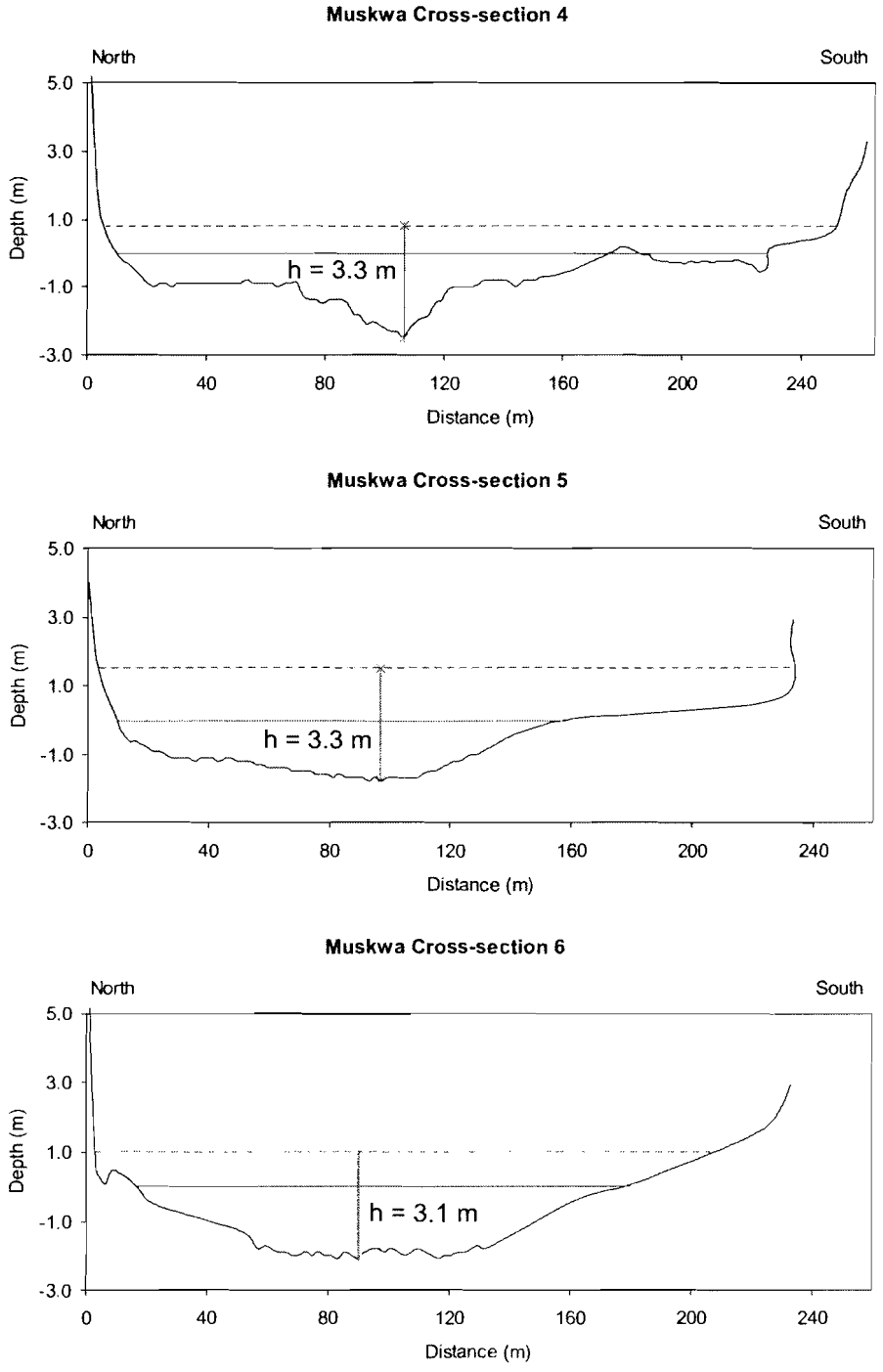

Combining the average thickness of the gravel layer with the area eroded for these bends during the 31 year period of aerial photography yields an average volumetric bedload transport rate of 23 300 m^3 per year (Table 4.4).

Table 4.4: **Morphologic bedload transport rate for the Muskwa River site**

Muskwa River	Average h (m)	Area Eroded (m^2)	Bedload Transport Rate (m^3/year)
Upstream Bend	3.6	270 300	31 000
Downstream Bend	3.2	148 300	15 500
		Average Rate	**23 300**

4.6 Wapiti River

The Wapiti River is a major tributary of the Smoky River, joining the Smoky River approximately 55 km downvalley on its way to the Peace River. The drainage area at the site is 11 300 km^2. The study site is located 1.5 km downstream of the Pipestone Creek confluence, 18 km upstream of the Highway 40 bridge crossing south of the city of Grande Prairie.

Clasts were measured on five bars within the study reach. Grain-size distribution is shown in Figure 4.13; the median grain size of clasts measured on the five bars is the largest of the study sites, at 44 mm.

Figure 4.13: Grain-size distribution at the Wapiti River site

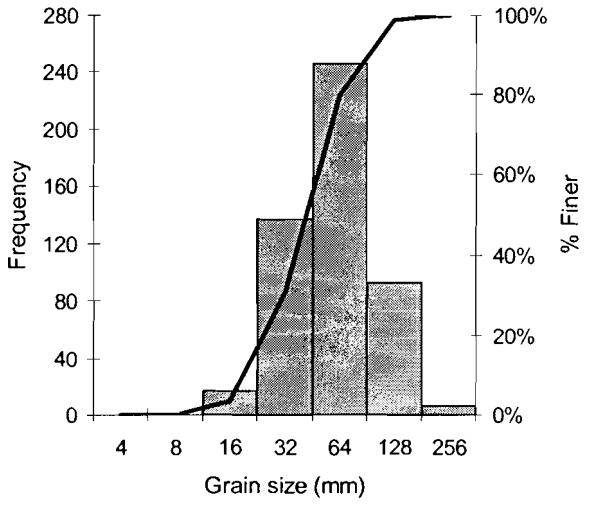

The confining valley walls are approximately 144 m above river level; the valley bottom is about 436 m wide at these locations. Two bends were examined in the field; four cross-sections were measured on the upstream bend and three on the bend located downstream. Typically, one bank on the study sites is bounded by the high confining valley wall with well-developed point bars on the opposite bank (Figure 4.14a). The boundary between the coarse gravel layer and overlying finer material is, in general, sharply delineated in the banks (Figure 4.14b). The cross-sections and the surveyed thickness of the gravel layer are presented in Figure 4.15.

Figure 4.14a: Wapiti River site (20 km southwest of Grande Prairie, AB)

Figure 4.14b: The upper boundary of the coarse basal layer at the Wapiti River site

Figure 4.15a: Cross-sections for the upstream bend of Wapiti River

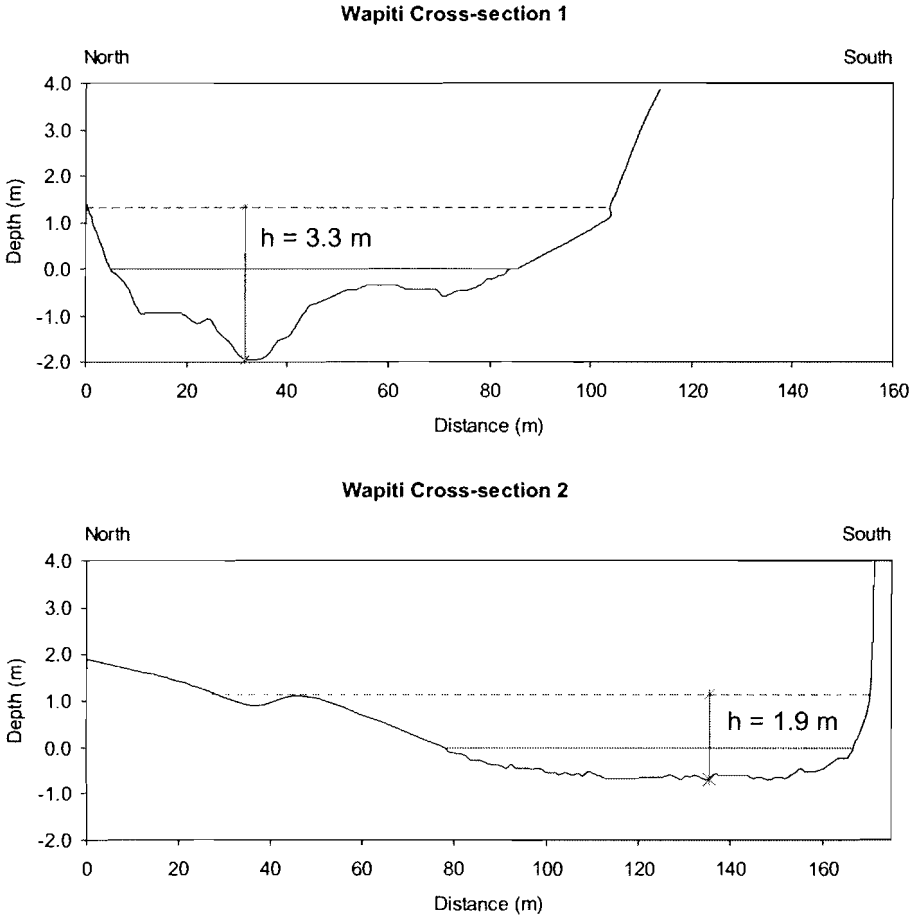

Wapiti Cross-section 3

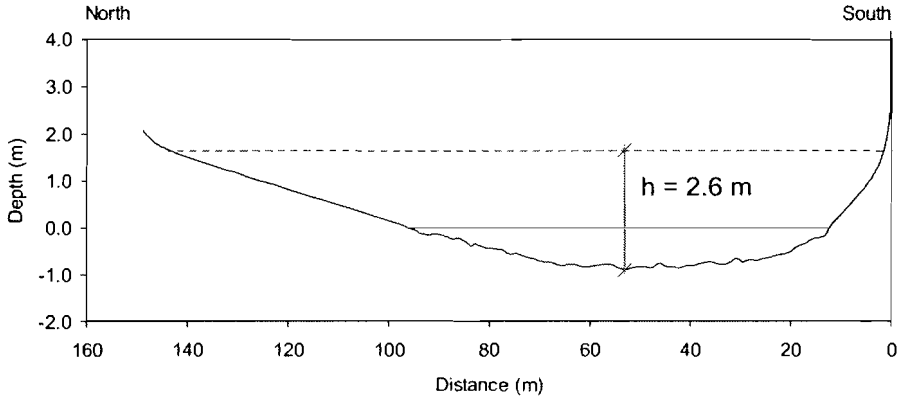

Wapiti Cross-section 4

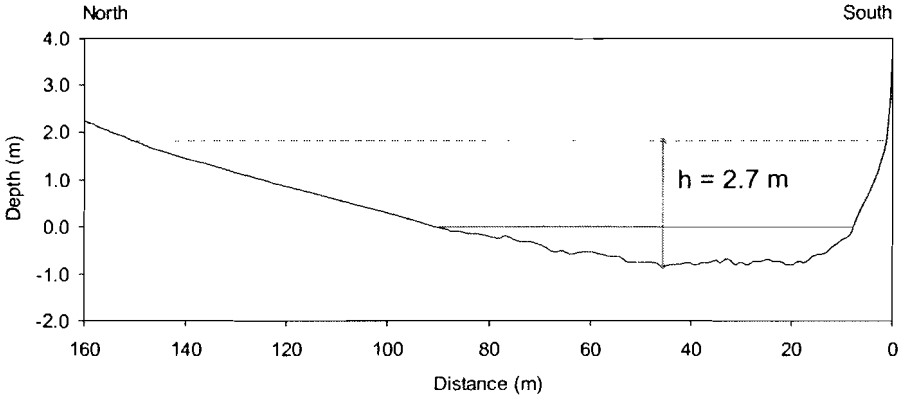

Figure 4.15b: Cross-sections for the downstream bend of Wapiti River

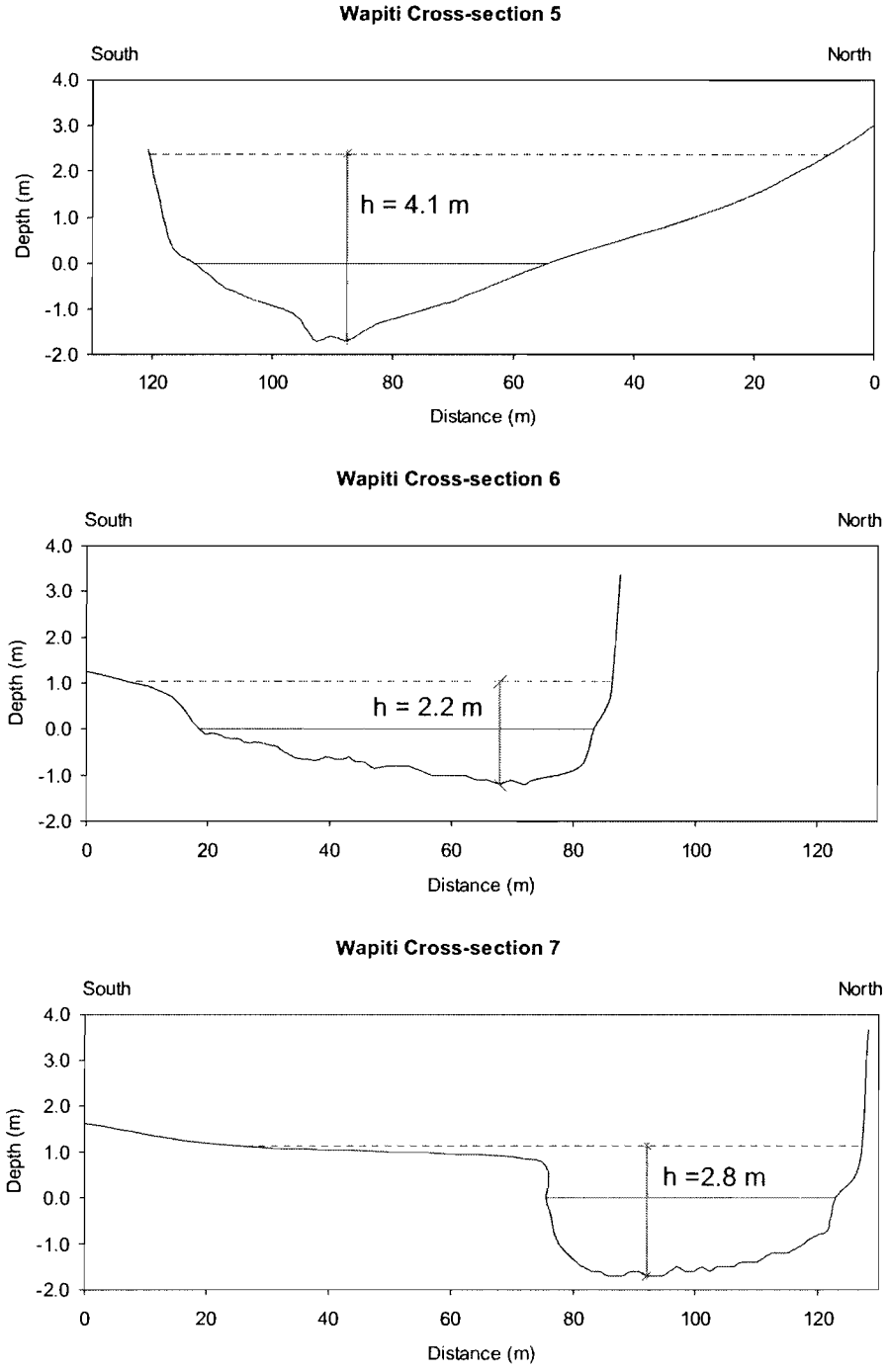

Combining the average thickness of the gravel layer with the area eroded for these bends during the 51 year period of aerial photography provides an average volumetric bedload transport rate of 7200 m^3 per year (Table 4.5).

Table 4.5: Morphologic bedload transport rate for the Wapiti River site

Wapiti River	Average h (m)	Area Eroded (m^2)	Bedload Transport Rate (m^3/year)
Upstream Bend	2.6	51 600	2600
Downstream Bend	3.1	195 300	11 700
		Average Rate	**7200**

4.7 Concave-Bank Benches on the Fort Nelson and Muskwa River

One factor that has not been considered thus far is the presence of well-developed concave-bank benches on two of the rivers in this study, the Fort Nelson and Muskwa Rivers (Figure 4.16).

Figure 4.16: Aerial view of a concave-bank bench on the Fort Nelson River (A) and at river level (B)

A) 

B) 

(Photo credit: E.J. Hickin)

Concave-bank bench deposits can be quite extensive and account for up to one-third of the total floodplain area (Page and Nanson, 1982). Much of the material within these fine-grained deposits would likely move in suspension

rather than along the bed, consequently an argument can be made for excluding this portion of the floodplain from the transport estimates. On the Fort Nelson and Muskwa Rivers concave-bank bench deposits appear to account for, respectively, 20% and 30% of the floodplain area, correspondingly reducing the calculated morphologic transport rate by the same proportion (Table 4.6).

Table 4.6: Calculated bedload transport rates for Fort Nelson and Muskwa River that account for presence of concave-bank benches

River	Morphologic bedload transport rate (m^3/y)	Rate after accounting for concave-bank bench deposits
Fort Nelson	22 300	17 800
Muskwa	23 300	16 300

However, although these deposits are predominantly fine-grained the presence of sand-sized material and isolated gravel within these deposits (see Burge and Smith, 1999; Page and Nanson, 1982) indicate that at least a portion of this material was transported as bedload. Furthermore, the morphologic method of calculating bedload transport in this study relies on the measurement of the area eroded at the concave-bank on the downstream limb of a meander. Presumably, this location would represent the oldest remaining concave-bank bench deposit on the floodplain deposited by the meander upstream. However, by this point the original concave-bank bench level has been greatly augmented through overbank accretion and become highly vegetated. Erosive processes here likely involve progressive undermining of this bank through bedload transport processes, leading to collapse of the upper bank, a supposition that is

supported by the prevalence of slumping banks in both the Fort Nelson and Muskwa Rivers. Although the sediment within the concave-bank benches may be partially derived from suspended sediment load, the process of eroding this deposit almost certainly includes a component of bedload transport. For these reasons the following sections will present the original calculations of bedload-transport rates for the Fort Nelson and Muskwa River.

4.8 Comparison to Published Gravel Transport Rates

Although data on gravel-transport rate is relatively scarce, there are several datasets that can be used to provide context for the morphology-based rates. Using various sources, Collins and Dunne (1990) compiled annual gravel loads for rivers located in the Pacific Northwest (including British Columbia, Oregon and Washington), Alaska, and one New Zealand site, ranging in drainage area from 300 to 250 000 km^2. Data for Fitzsimmons Creek in British Columbia (Pelpola and Hickin, 2004; drainage area of 100 km^2) has been added to the Pacific Northwest grouping. Data are also available for headwater streams in both Idaho (Whiting et al., 1999; drainage area < 381 km^2) and Switzerland (Rickenmann, 1997; drainage area < 2 km^2). A plot of these data shows that gravel transport can be roughly scaled to drainage area (Figure 4.17).

Figure 4.17: Comparison of calculated bedload transport rates to published data

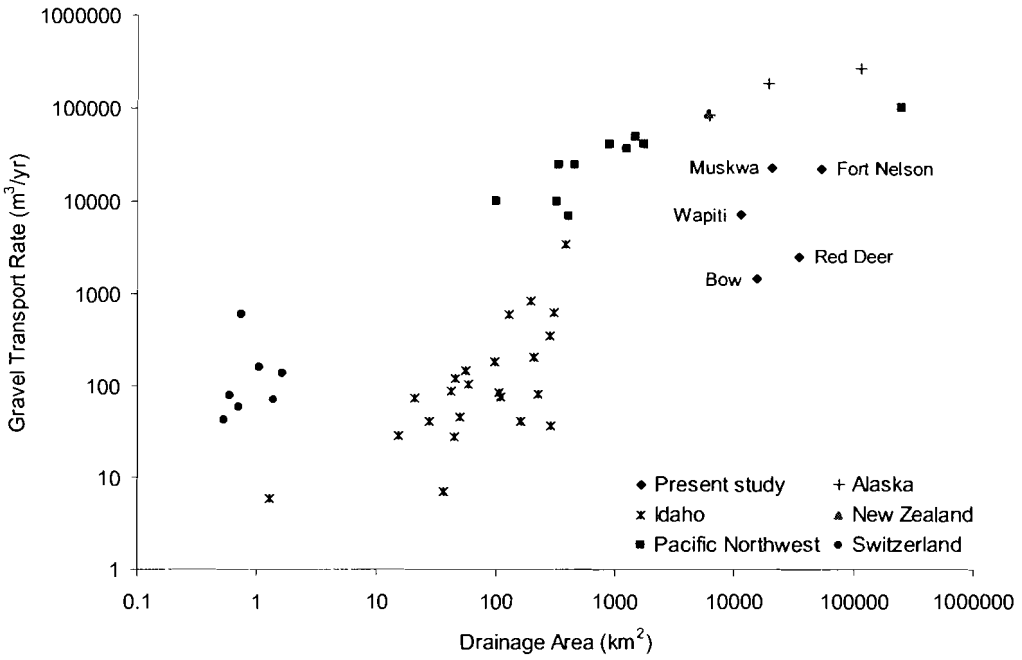

The five rivers examined in this study fall within the range of drainage area of the available published data, and the calculated bedload-transport rates appear to be consistent with the general trend. However, the rates are lower when compared to the published rates for similar-sized drainage areas. This is particularly true of the Bow, Red Deer and Wapiti River sites which have bedload-transport rates an order of magnitude lower than would be expected from the trend apparent in the published data with larger drainage areas (Figure 4.17). The rates for the five sites appear to be more consistent with the trend outlined by the Idaho data, which also generally plot lower than the remaining published data. The Idaho sites are steeply-sloping headwater streams with small drainage areas, vastly different characteristics from the lowland rivers within this study. Consequently, obvious parallels cannot be drawn to provide a common explanation for the lower bedload-transport rates observed

in both groups. Low rates within the Idaho stream sites were attributed to a limited sediment supply (Whiting et. al, 1999); however, limited sediment supply would not be a factor in the calculation of the bedload-transport rates of the five sites using the methodology of this study.

There are several reasons why the rates calculated for this study may be low relative to other rivers of similar scale. First, all of the confined rivers within this study have very low slopes and consequently the stream power available to move sediment will be less than in a similarly-sized river with a higher slope. With regards to the Red Deer River, this site recorded the smallest thickness of the gravel layer of the five sites, even though it is the second largest in terms of drainage area. This relatively small amount of gravel produces a lower transport rate for a river with a comparably large drainage area. Finally, the rates calculated within this study represent a lower bound of the true rate. The morphologic method of calculating bedload-transport rate assumes that all material eroded from one bend is deposited on the next downstream. If material passes through the reach without altering the channel morphology it remains undetected using these methods. The method also fails to account for compensating scour and fill within the reach that occurs between the time period of photography. Unfortunately, there is no way to assess the magnitude of the potential loss to these mechanisms.

4.8.1 Comparison with Bedload Transport Formula Estimates

Bedload-transport formulae have been used to provide estimates of transport rates in a variety of settings, yet field data to critically test these

equations is still lacking. The present data provide an opportunity to assess the utility of bedload transport formulae. The use of formulae to predict transport rate has thus far proven to be unsatisfactory, providing results that can be quite inaccurate (Ashmore and Church, 1998). However, due to the difficulty in measuring bedload transport in the field, the development of bedload formulae with the ability to accurately predict transport rates would be highly useful.

Attempts to reliably predict transport rates have led to the development of several bedload-transport formulae. One which has been proven to be relatively robust is the Meyer-Peter and Müller (MPM) equation (Martin and Ham, 2005). This equation predicts bedload transport based on excess shear stress. The basic expression of the formula is:

$$g_b = K(\tau_0 - \tau_{cr})^{3/2} \qquad \text{(Richards, 1982)}$$

where g_b is the specific bedload transport rate, τ_0 is the mean bed shear stress, τ_{cr} is the critical bed shear stress, and K is an empirical constant commonly taken to be 0.253. Mean bed shear stress (τ_0) is defined by:

$$\tau_0 = \rho_w g d S$$

where ρ_w is the density of water, g is gravitational acceleration, d is mean depth and S is water-surface slope. Critical bed shear-stress (τ_{cr}) is defined using Shields criterion for gravel to be:

$$\tau_{cr} = 0.06(\rho_s - \rho_w)gD \approx 970D$$

where ρ_s is the density of the sediment and D is a representative grain size (m), usually taken to be D_{50}. For the calculations in this study the density of quartz (2650 $kg \cdot m^{-3}$) was chosen as representative of the density of sediment.

The MPM formula calculates a mass rate of transport; for comparison purposes this needs to be converted to a volumetric rate, requiring the bulk density of the sediment. As measurements of bulk density were not undertaken at the five study sites this value has to be estimated. Bulk density at the five sites was assigned based on tables estimating bulk density for sediments of various grain sizes that have been deposited for one year or less (Table 2.5; Vanoni, 2006). A bulk density of 1650 $kg \cdot m^{-3}$, representing bulk density for sediments with a D_{90} of 4 mm, was chosen as representative for the five sites in this study. This estimate seems reasonable when compared with values measured in British Columbia of 1450 $kg \cdot m^{-3}$ on the Squamish River (Hickin, 1989) and values ranging from 1580 to 1790 $kg \cdot m^{-3}$ for the delta on Fitzsimmons Creek in the Coast Mountains (Pelpola and Hickin, 2004).

At-a-station hydraulic geometry was calculated for the five sites based on a representative cross-section within the reach. These hydraulic geometry equations were used to provide values for width and depth for the daily discharges obtained through gauging records. The Muskwa River site had daily discharge records available for all years of the photo period (Table 4.7); for other sites the transport calculations were performed for the available discharge records and the calculated annual average assumed to be representative of transport during the entire photo period.

Table 4.7: Extent of daily discharge records

River	Years of Photo Record	Years with Complete Daily Discharge Records
Bow	48	44
Fort Nelson	30	18
Muskwa	31	31
Red Deer	51	41
Wapiti	51	40

The data in Figure 4.17 are shown with the estimates calculated using the MPM formula for the Bow, Fort Nelson and Wapiti River sites (Figure 4.18). The MPM formula predicted zero bedload transport for the both the Red Deer and Muskwa River sites; for that reason these locations are not graphed.

Figure 4.18: Comparison of transport rates with results from MPM formula

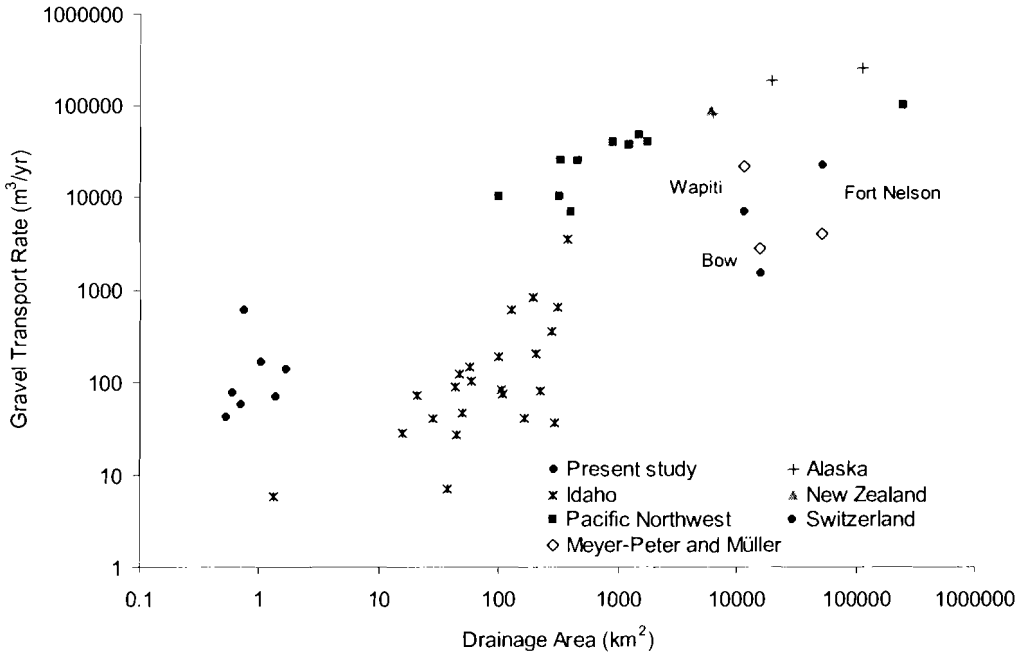

The transport rates calculated for the Bow and Wapiti River sites using the MPM formula are comparable to the rates provided by the morphologic method, although the Wapiti River MPM transport rate is higher by an order of magnitude than the measured morphologic rate. The MPM result for Fort Nelson River is low, and the calculations for Muskwa and Red Deer River sites yield mean bed shear stresses less than critical shear stress, even for the largest discharges. The low estimates on these rivers are most likely due to the inaccuracy of the D_{50} used in the calculations. These three rivers all have a high percentage of sand-sized material which is not captured in the pebble-count method used to provide a median grain-size in this study, a critical value in the MPM formula. The pebble-count method provides a median grain-size for the gravel component of these rivers but a more extensive method of sampling is required to provide a representative D_{50} for the bed material as a whole. The use of the high estimate for D_{50}, combined with the very low slopes on these rivers causes the MPM formula to predict zero transport on the Muskwa and Red Deer Rivers, and is likely responsible for the low transport rate calculated for the Fort Nelson River.

The estimates for the Bow and Wapiti River using the MPM formula were, respectively, 46% and 66% greater than the calculated morphologic rate. Unlike the other three sites, the D_{50} estimates for these rivers may not be the primary reason that the results of the MPM formula varied from the bedload-transport rates calculated using morphologic methods. Although the empirical constant, K, in the MPM formula is commonly taken to be 0.253, this formula may be better applied with calibration of the numerical constant, K. Changing this constant to

0.136 and 0.0852 for the Bow and Wapiti Rivers would equate the rate estimates obtained through both the morphologic methods and the MPM formula.

4.9 Summary

The bedload-transport rates calculated for the five rivers within this study fall within the general trend outlined by previously published data. However, when compared only to published rates for similar-sized drainage areas the bedload-transport rates appear to be low for all five sites. This may be due to the comparatively low stream powers found on these rivers or may be a factor of the failure of morphologic methods to account for all sediment moving through the reach as bedload. It is highly likely some component of sediment throughput and compensating scour and fill is occurring on these reaches although the magnitude of this component cannot be resolved within this study. To that end, the bedload transport estimates provided using the morphologic method will be lower-bound estimates.

Table 4.8 presents a summary of bedload-transport rates calculated for the five rivers using both the MPM formula and the morphologic methods.

Table 4.8: Summary of calculated bedload transport rates

River	Morphologic Bedload Transport Rate (m^3/y)	MPM Bedload Transport Rate (m^3/y)
Bow	1500	2800
Fort Nelson	22 300	3900
Muskwa	23 300	No Transport
Red Deer	2600	No Transport
Wapiti	7200	21 300

Although the Meyer-Peter and Müller formula performed reasonably well for the Bow and Wapiti River sites, for the remaining three sites the results of the formula were inconsistent with the transport rates calculated using morphologic methods. The Fort Nelson, Muskwa, and Red Deer sites illustrate the dependence of the MPM formula on input variables, specifically the D_{50}. The performance of the MPM formula for the Bow and Wapiti River sites could be improved through calibration of the empirical constant, K. A small amount of initial work is required to provide the calibration; however, the results obtained through the formula can be greatly improved. Overall, this study demonstrates that the Meyer-Peter and Müller transport formulae should be used with caution, particularly when lacking detailed information on flow and sediment conditions at study sites.

CHAPTER 5: SUMMARY AND CONCLUSIONS

The general question posed by this study is "Does the morphometry and dynamics of confined-meandering rivers vary significantly from their more common freely-meandering counterparts?" To this end, the planform geometry and kinematics of confined-meandering rivers is described for 24 sites located on the Canadian prairies. To address the general question this study seeks answers to four specific questions as outlined in Chapter 1. The following sections reiterate these questions and summarize the conclusions that are drawn for each.

What is the statistical nature of confined-meander planform geometry? Are there orderly relationships amongst the variables of planform geometry?

Although their meander pattern is distinctive, this study indicates that the planform geometry and dynamics of confined-meandering rivers generally are consistent with the characteristics exhibited by freely-meandering rivers. Various relationships among channel wavelength, bankfull width, discharge and radius of curvature, well-established for free meanders, appear to describe confined meanders as well. However, the unique meander pattern of confined meanders

is reflected in small differences within the overall relationships. Wavelength is commonly reported as 8–12 times the bankfull width in freely-meandering rivers whereas on these confined meanders channel wavelength is generally around 15 times the bankfull width. The median Rc/w of 4.1 calculated in this study is also slightly higher than the median Rc/w=2-3 typical of freely-meandering rivers. These higher values reflect the unique meander pattern of these confined bends with their relatively long segments of open convex-downvalley arc. Furthermore, distinct migration characteristics of confined-meanders will also affect the specific form of the relationships. In general, these rivers do not develop cut-offs and meander bends appear to migrate downstream as a coherent waveform.

What is the rate of migration of confined meanders? How do the migration rates compare to those previously reported for freely meandering rivers?

Average migration rates over the time period of observation for the confined meanders varied greatly, from highly stable reaches such as the Clearwater River migrating at rates of just 0.01 m per year, to decidedly active reaches such as the Wapiti River which migrates downstream at 5.8 m per year. Overall, the migration rates calculated within this study are consistent with values reported for similar-sized rivers worldwide.

How does migration rate vary with planform geometry as well as other factors? Are the relationships observed for freely meandering rivers applicable to confined meanders?

Attempts to predict migration rate based on channel flow and morphometry data are modestly successful. Stream power offers the best statistical predictor of migration rate, accounting for 39% of variance in migration

rate and up to 52% if the dam-impacted reach of the North Saskatchewan River is removed from the data set. Bankfull width and mean annual flood provide nearly the same level of prediction, with respectively 32% and 30% of migration-rate variance explained by each factor alone. Although the level of prediction yielded by these factors is clearly limited, they are nevertheless shown to be significant controlling factors. The levels of explanation of variance in migration rate provided in this study are quite comparable to those achieved by others for freely-meandering rivers.

What is the average rate of bedload moving through the study reaches?

Bedload transport rates are determined by morphologic methods for five sites within the study and are consistent with the general trend of bedload-transport rates published elsewhere. Volumetric estimates of bedload transport rate ranged between a high of 23 280 m^3/yr for the Muskwa River to a low of 1486 m^3/yr for the Bow River. Estimates obtained through the use of morphologic methods represent lower-bound transport estimates and the rates calculated for the five sites within this study are low when compared to rates for similar-sized drainage areas. Whether this difference is due to the failure to account for sediment throughput or due to the low stream powers on these rivers, cannot be resolved within this study.

Although this study provides a general statistical description of confined-meanders, there remain important missing elements whose inclusion would likely strengthen the statistical model of migration rate developed here. Principal

among these is quantitative data on boundary-material strength. Though multiple regression techniques did not improve the level of explanation provided using the variables measured in this study, the addition of detailed data on boundary-material strength may improve this outcome. Inclusion of detailed data on bed material and bank height would also likely improve the accuracy of the estimation of bedload transport rates by the morphologic methods used here. While this study provides a valuable dataset for confined-meandering rivers in western Canada, further work is required to determine if the findings of this study are applicable to confined-meandering rivers in other regions of the world.

Overall, the findings of this study indicate that confined-meandering rivers are best seen as part of a continuum of meandering river pattern rather than as something completely different. The unique meander-pattern of confined rivers does have an effect on their meander morphometry and kinematics but they also have much in common with their freely-meandering counterparts. The predictive capabilities of basic relationships identified within this study between controlling factors and migration rate are limited. Further research is required to strengthen these relationships and to thereby develop a more complete model to allow accurate prediction of channel migration on confined-meandering rivers.

REFERENCES

Alberta Environment. 2006. Water Allocations compared to Natural Flows. In *State of the Environment – Water.* http://www3.gov.ab.ca/env/soe/water_indicators/27_historical_sub.html

Andrle R. 1996. Measuring channel planform of meandering rivers. *Physical Geography* 17 (3): 270 – 281.

Ashmore P.E. and Church M. 1998. Sediment transport and river morphology: a paradigm for study. In *Gravel-bed Rivers in the Environment.* Edited by Klingeman P.C., Beschta R.L., Komar P.D., and Bradley J.B. Water Resources Publications: Highlands Ranch, Colorado pp. 115 - 148.

Bagnold R.A. 1960. Some aspects of river meanders. *U.S. Geological Survey Professional Paper 282E.*

Beeson, C.E. and Doyle, P.F. 1995. Comparison of bank erosion at vegetated and non-vegetated channel bends. *Water Resources Bulletin* 31 (6): 983 – 990.

Brice J.C. 1973. Meandering pattern of the White River in Indiana – An analysis. In *Fluvial Geomorphology.* Edited by Morisawa M. Binghampton State University: New York pp. 178 – 200.

Brice J.C. 1982. *Stream Channel Stability Assessment, January 1982, Final Report.* U.S. Department of Transportation, Federal Highway Administration, Washington, D.C.

Brice J.C. 1984. Planform properties of meandering rivers. In *River Meandering, Proceedings Conference on Rivers '83.* Edited by Elliott, C.M. ASCE: New York pp. 1 – 15.

Burckhardt J.D. and Todd B.L. 1998. Riparian Forest Effect on Lateral Stream Channel Migration in the Glacial Till Plains. *Journal American Water Resources Association* 34: 179 - 184.

Burge, L.M. and Smith, D.G. 1999. Confined meandering river eddy accretions: sedimentology, channel geometry and depositional processes. *Special Publications of the International Association on Sediment* 28: 113 – 130.

Carson, M.A. and Griffiths, G.A. 1989. Gravel transport in the braided Waimakariri River: Mechanisms, measurements and predictions. *Journal of Hydrology* 109: 201 – 220.

Carson, M.A. and LaPointe M.F. 1983. The inherent asymmetry of river meander planform. *Journal of Geology* 91: 41 – 55.

Chen G. and Shen H.W. 1984. River curvature-width ratio effect on shear stress. In *River Meandering, Proceedings Conference on Rivers '83.* Edited by Elliott, C.M. ASCE: New York pp. 687 - 699.

Collins, B. and Dunne, T. 1990. Fluvial geomorphology and river-gravel mining: a guide for planners, case studies included. California Department of Conservation, Division of Mines and Geology, Special Publication 98.

Daniel, J.F. 1971. Channel movement of meandering Indiana streams. *U.S. Geological Survey Professional Paper 732-A.*

De Boer, D.H., Hassan, M.A., MacVicar, B., and Stone, M. 2005. Recent (1999–2003) Canadian research on contemporary processes of river erosion and sedimentation, and river mechanics. *Hydrological Processes* 19: 265 – 283.

Dury, G.H., 1964, Principles of underfit streams: *U.S. Geological Survey Professional Paper 452-A.*

Eaton, B., Church, M. and Ham, D. 2002. Scaling and regionalization of flood flows in British Columbia, Canada. *Hydrological Processes* 16: 3245 – 3263.

Ferguson, R.I. 1984. Kinematic model of meander migration. In *River Meandering, Proceedings Conference on Rivers '83.* Edited by Elliott, C.M. ASCE: New York pp. 942 - 951

Freidkin, J.G. 1945. *A laboratory study of the meandering of alluvial rivers. Waterways experiment station*. US Army Corps of Engineers: Vicksburg.

Fuller, I.C., Large, A., Charlton, M., Heritage, G. and Milan, D. 2003. Reach-scale sediment transfers: An evaluation of two morphological budgeting approaches. *Earth Surface Processes and Landforms* 28: 889 – 903.

Furbish, D.J. 1991. Spatial autoregressive structure in meander evolution. *Bulletin of the Geological Society of America* 103: 1576 – 1589.

Gaeuman, D.A., Schmidt, J.C. and Wilcock, P.R. 2003. Evaluation of in-channel gravel storage with morphology-based gravel budgets developed from planimetric data. *Journal of Geophysical Research* 108(F1): 2-1 – 2-16.

Gilvear, D., Winterbottom, S. and Sinchingabula, H. 2000. Character of channel planform change and meander development: Luangwa River, Zambia. *Earth Surface Processes and Landforms* 25: 421 – 436.

Gurnell, A. 1997. Channel change on the River Dee meanders, 1946-1992, from the analysis of air photographs. *Regulated Rivers: Research & Management* 13: 13 – 26.

Gurnell, A., Downward, S.R., and Jones, R. 1994. Channel planform change on the River Dee meanders, 1876–1992. *Regulated Rivers: Research and Management* 9: 187–204.

Ham, D.G. and Church, M. 2000. Bed-material transport estimated from channel morphodynamics: Chilliwack River, British Columbia. *Earth Surface Processes and Landforms* 25: 1123 – 1142.

Harrelson, C.C., Rawlins, C.L. and Potyondy, J.P. 1994. *Stream channel reference sites: an illustrated guide to field technique.* General Technical Report RM-245, USDA Forest Service: Fort Collins.

Hey, R.D. 1976. Geometry of river meanders. *Nature* 262: 482 – 484.

Hickin, E. J. 1974. The development of meanders in natural river channels. *American Journal of Science* 274: 414 - 442.

Hickin, E. J. 1977. Hydraulic factors controlling channel migration. In *Research into Fluvial Systems.* Edited by Davidson-Arnott, R.E. and Nickling, W. GeoAbstracts: Norwich pp. 59 - 66.

Hickin, E.J. 1986. Concave-bank benches in the floodplains of Muskwa and Fort Nelson Rivers, British Columbia. *The Canadian Geographer* 30 (2): 111 – 122.

Hickin, E. J., 1988. Lateral migration rates of river bends: In *Handbook of Civil Engineering Volume 2: Hydraulics/Mechanics.* Edited by Cheremisinoff, P.N., and Cheng S.L. Technomic Publishing: Lancaster, Pennsylvania pp. 419 – 445.

Hickin, E.J. 1989. Contemporary Squamish River sediment flux to Howe Sound, British Columbia. *Canadian Journal of Earth Sciences* 26: 1953 – 1963.

Hickin, E.J. and Nanson, G.C. 1975. The character of channel migration on the Beatton River, Northeast British Columbia, Canada. *Geological Society of America Bulletin* 86: 487 – 494.

Hickin, E.J. and Nanson, G.C. 1984. Lateral migration rates of river bends. *Journal of Hydraulic Engineering-ASCE*: 110: 1557 - 1567.

Hooke, J.M. 1977. The distribution and nature of changes in river channel patterns: the example of Devon. In *River Channel Changes*. Edited by Gregory, K.J. Wiley: Chichester pp. 206 – 220.

Hooke J.M. 1980. Magnitude and distribution of rates of river bank erosion. *Earth Surface Processes and Landforms* 5: 143 – 157.

Hooke, J.M. 1984. Changes in river meanders: a review of techniques and results of analyses. *Progress in Physical Geography* 8 (4): 473 – 508.

Hooke J.M. 2007. Complexity, self-organization and variation in behaviour in meandering rivers. *Geomorphology* 91: 236 – 258.

Hooke, J.M. and Harvey, A.M. 1983. Meander changes in relation to bend morphology and secondary flows. In *Modern and Ancient Fluvial Systems.* Edited by Collinson, J. and Lewin, J. International Association on Sediment Special Publication 6 pp. 121 – 132.

Hooke, R. Le B. 1975. Distribution of sediment transport and shear stress in a meander bend. *Journal of Geology* 83: 543 – 566.

Hughes, M.L., McDowell, P. and Marcus, W.A. 2006. Accuracy assessment of georectified aerial photographs: Implications for measuring lateral channel movement in a GIS. *Geomorphology* 74: 1 – 16.

Kellerhals, R., Neill, C.R. and Bray, D. I. 1972. Hydraulic and geomorphic characteristics of rivers in Alberta. *Alberta Research Council, River Engineering and Surface Hydrology Report* 72-1.

Knighton, D. 1998. *Fluvial Forms and Processes: A New Perspective*. Oxford University Press Inc.: New York.

Langbein, W.B. and Leopold, L.B. 1966. River meanders – theory of minimum variance. *U.S. Geological Survey Professional Paper 422-H.*

Leopold, L.B. and Wolman, M.G. 1960. River Meanders. *Bulletin of the Geological Society of America* 71: 769 – 794.

Leopold, L.B., Wolman, M.G., and Miller, J.P. 1964. *Fluvial Processes in Geomorphology*. W.H. Freeman: San Francisco.

Lewin J., Brindle B.J. 1977. Confined meanders. In *River Channel Changes.* Edited by Gregory, K.J. John Wiley and Sons: Chichester pp. 221–233.

Lewin, J. 1983. Changes of Channel Patterns and Floodplains. In *Background to Paleohydrology*. Edited by Gregory, K.J. John Wiley and Sons: Chichester pp. 303 - 319.

Lindsay, J.B. and Ashmore, P.E. 2002. The effects of survey frequency on estimates of scour and fill in a braided river model. *Earth Surface Processes and Landforms* 27: 27 – 43.

Martin, Y. and Ham, D. 2005. Testing bedload transport formulae using morphologic transport estimates and field data: lower Fraser River, British Columbia. *Earth Surface Processes and Landforms* 30: 1265 – 1282.

Mathews, W. 1980. Retreat of the last ice sheets in Northeastern British Columbia and adjacent Alberta. *Geological Survey of Canada Bulletin* 331.

Meyer-Peter, R. and Müller, R. 1948. Formulas for bedload transport. In *Proceedings 2nd meeting International Association of Hydraulic Research*. Stockholm: 39 – 64.

Mount, N. and Louis, J. 2005. Estimation and propagation of error in measurements of river channel movement from aerial imagery. *Earth Surface Processes and Landforms* 30: 635 – 643.

Mount, N., Louis, J., Teeuw, R., Zukowskyj, P. and Stott, T. 2003. Estimation of error in bankfull width comparisons from temporally sequenced raw and corrected aerial photographs. *Geomorphology* 56: 65 – 77.

Nanson, G.C. 1977. Channel migration, floodplain formation, and vegetation succession on a meandering-river floodplain in N.E. British Columbia, Canada. PhD. Thesis: Simon Fraser University.

Nanson, G.C. and Hickin, E.J. 1983. Channel migration and incision on the Beatton River. *Journal of Hydraulic Engineering* 109: 327 - 337.

Nanson, G.C. and Hickin, E.J. 1986. Statistical analysis of bank erosion and channel migration in western Canada. *Geological Society of America Bulletin*. 97: 497 – 504.

Neill CR. 1971. River bed transport related to meander migration rates. *Journal of the Waterways, Harbours and Coastal Engineering Division*: Proceedings of the American Society of Civil Engineers 97: 783 - 786.

Neill CR. 1987. Sediment balance considerations linking long-term transport and channel processes. In *Sediment Transport in Gravel-bed Rivers*. Edited by Thorne, C.R., Bathurst, J.C., and Hey R.D. John Wiley & Sons: Chichester pp. 225 - 240.

Page, K. and Nanson, G. 1982. Concave-bank benches and associated floodplain formation. *Earth Surface Processes and Landforms* 7: 529 – 543.

Pelpola, C. and Hickin, E.J. 2004. Long-term bed load transport rate based on aerial-photo and ground penetrating radar surveys of fan-delta growth, Coast Mountains, British Columbia. *Geomorphology* 57: 169 – 181.

Petts, G.E., 1989. Historical analysis of fluvial hydrosystems. In *Historical Change of Large Alluvial Rivers: Western Europe*. Edited by Petts, G.E., Muller, H., and Roux, A.L. Wiley: Chichester pp. 1– 18.

Popov, I.V. 1962. Application of morphological analysis to the evaluation of the general channel deformations of the River Ob. *Soviet Hydrology* 3: 267 - 324.

Pyrce, R.S. and Ashmore, P. 2003. Particle path length distributions in meandering gravel-bed streams: Results from physical models. *Earth Surface Processes and Landforms* 28: 951 – 966.

Richard G.A., Julien, P.Y. and Baird, D.C. 2005. Statistical analysis of lateral migration of the Rio Grande, New Mexico. *Geomorphology* 71: 139 – 155.

Richards, K. 1982. *Rivers: Form and Process in Alluvial Channels*. Methuen & Co.: New York.

Rickenmann, D. 1997. Sediment transport in Swiss torrents. *Earth Surface Processes and Landforms* (22): 937 – 951.

Rohrer W.L. 1984. Effects of flow and bank material on meander migration in alluvial rivers. In *River Meandering, Proceedings Conference on Rivers' 83.* Edited by Elliott, C.M. ASCE: New York pp. 770 - 782.

Schattner, I., 1962. The Lower Jordan Valley. PhD. Thesis: Hebrew University, Jerusalem.

Simon, A. and Castro, J. 2003. Measurement and Analysis of Alluvial Channel Form. In *Tools in Fluvial Geomorphology.* Edited by Kondolf, G.M. and Piégay, H. John Wiley & Sons: Chichester pp. 291 - 322.

Thorne, C.R. 1982. Processes and Mechanisms of River Bank Erosion. In *Gravel-bed Rivers.* Edited by Hey R.D., Bathurst J.C., and Thorne C.R. John Wiley and Sons: New York pp. 227 - 271.

TRB (Transportation Research Board of the National Academies of the US). 2004. *Methodology for predicting channel migration.* NCHRP Web-Only Document 67 (Project 24-16). http://onlinepubs.trb.org/onlinepubs/nchrp/nchrp_w67.pdf.

Van De Wiel, M.J. 2003. Numerical modeling of channel adjustment in alluvial meandering rivers with riparian vegetation. PhD. Thesis: University of Southampton (United Kingdom).

Vanoni, V. 2006. *Sedimentation Engineering.* ASCE Publications: Reston.

Wellmeyer, J., Slattery, M. and Phillips, J. 2005. Quantifying downstream impacts of impoundment on flow regime and channel planform, lower Trinity River, Texas. *Geomorphology* 69: 1 – 13.

Whiting, P., Stamm, J., Moog, D. and Orndorff, R. 1999. Sediment-transporting flows in headwater streams. *Geological Society of America Bulletin* 111 (3): 450 – 466.

Williams, G.P. 1986. River meanders and channel size. *Journal of Hydrology* 88: 147 – 164.

Winterbottom, S. 2000. Medium and short-term channel planform changes of the Rivers Tay and Tummel, Scotland. *Geomorphology* 34: 195 – 208.

Winterbottom, S., Gilvear, D., 2000. A GIS-based approach to mapping probabilities of river bank erosion: regulated River Tummel, Scotland. *Regulated Rivers: Research and Management* 16: 127– 140.

Yarnykh, N.A. 1978. Channel and bank deformations in an acute meander. *Soviet Hydrology Selected Papers* 17: 278 – 281.

APPENDIX A: DETAILS ON AIR PHOTOS AND GEORECTIFICATION ERROR

Table A.1 Information on aerial photography and georectification error

River	Year of Photography	Approximate Scale 1:	Project # (Alberta Sites)	Roll #	Average RMSE
Baptiste River	1997	20000	97-011	4767	4.09
	1975	21120	75-145	1413	5.07
	1951	15840	51-83B	526	3.23
Battle River	2002	20000	02-038	5225	5.34
	1975	31680	75-132	1418	5.98
	1949	40000	49-73E	142	5.24
Beaver River	2000	30000	00-093	5127	6.24
	1988	20000	88-030	3700	5.51
	1969	31680	69-175	1010	6.01
	1952	15840	51-73L	435	4.29
Bow River	1998	20000	98-100	4991	2.51
	1982	15000	82-129	2570	7.30
	1950	40000	49-82I	170	7.75
Clear River	1997	30000	97-159	4891	3.33
	1978	15000	78-052 84D	1813	4.30
	1952	15840	51-84D	261	4.63
Clearwater River	1997	15000	97-205	4885	3.22
	1985	15000	85-001	3186	4.00
	1972	21120	72-133	1200	5.01
	1951	15840	51-74D	212	4.10
Doig River	1997	40000		15BCB97014	4.77
	1975	20000		BC7785	2.31
	1956	30000		BC2175	4.37
Fontas River	1997	40000		15BCB97101	5.55
	1979	16000		30BC79156	5.21
	1967	32000		15BC5253	5.78
Fort Nelson River (downstream)	1997	40000		15BCB97016	5.63
	1967	32000		15BC5235, 15BC5244	4.78

River	Year of Photography	Approximate Scale 1:	Project # (Alberta Sites)	Roll #	Average RMSE
Fort Nelson River (upstream)	1997	40000		15BCB97033, 15BCB97043	3.99
	1979	16000		30BC79170, 30BC79131	5.73
	1966	32000		15BC5180	5.72
Hay River (downstream)	1994	20000	94-099	4530	3.95
	1976	15000	76-076	1495	3.39
	1953	15840	53-1	552	4.31
Hay River (upstream)	1993	40000	93-136	4407	4.68
	1979	15000	79-033 84L	2035	4.07
	1954	40000	49-84L	65	3.94
Klua River	1991	15000		15BCB97103	4.51
	1967	15840		30BC7046	2.08
Kootenay River	2004	30000		15BCC04014	6.47
	1991	20000		30BCB91124, 25, 27	3.35
	1975	20000		30BC7800	2.83
	1952	32000		BC1483	3.95
Milk River	1995	20000	E95-025	4644	10.97
	1983	20000	83-001	2811	3.54
	1962	31680	62-72E	849	1.83
	1951	40000	49-72E	185	3.63
Muskwa River	1997	40000		15BCB97032	5.54
	1975	31680		15BC5672	5.30
	1966	32000		15BC5181	7.85
	1953	18000		BC1767	6.20
North Saskatchewan River	1995	20000	95-135	465D	8.87
	1976	21120	76-072	1487	3.27
	1951	15840	51-83B	528	4.77
Oldman River	1998	30000	98-094 South	4943	2.58
	1975	31680	75-165	1437	4.26
	1961	31680	61-82H	811	3.07
	1951	40000	49-82H	179	4.40

River	Year of Photography	Approximate Scale 1:	Project # (Alberta Sites)	Roll #	Average RMSE
Petitot River	1997	40000		15BCB97029	5.51
	1966	32000		15BC5184	2.45
Pinto River	2001	10000	01-080	5204B	6.14
	1980	15000	80-101	2077	6.16
	1951	15840	51-83F	467	6.80
Prophet River	1997	40000		15BCB97032	4.78
	1979	20000		15BC79130	7.82
	1966	32000		15BC5181	5.48
Red Deer River	2001	30000	01-317	5173B	4.54
	1985	25000	S85-038	3165	4.09
	1962	31680	62-72L, 62-72M	832, 831	4.03
	1950	40000	49-72L, 49-72M	169, 168	4.27
Wapiti River	2001	30000	01-312	5196	5.63
	1989	30000	89-120	3921	3.82
	1972	31680	72-027	1212	6.29
	1950	40000	49-83M	111	6.10
Wildhay River	2001	15000	01-081	5192A	4.08
	1980	15000	80-101	2076	3.27
	1963	31680	63-83F	857	3.93
	1952	15840	51-83F	471	4.40

APPENDIX B: AVERAGE MIGRATION RATES FOR EACH TIME INTERVAL

Table B.1 Average migration rate for each time interval of aerial photography

River	Photo Time Interval	Average Migration Rate (m/year)
Baptiste	1951 - 1975	0.70
	1975 - 1997	0.84
Battle	1949 - 1975	0.80
	1975 - 2002	0.71
Beaver	1952 - 1969	1.51
	1969 - 1988	1.35
	1988 - 2000	1.82
Bow	1950 - 1982	2.17
	1982 - 1998	1.18
Clear	1952 - 1978	2.62
	1978 - 1997	4.60
Clearwater	1951 - 1972	0.00
	1972 - 1985	0.63
	1985 - 1997	0.18
Doig	1956 - 1975	0.63
	1975 - 1997	0.00
Fontas	1967 - 1979	1.90
	1979 - 1997	0.55
Fort Nelson (upstream)	1966 - 1979	5.93
	1979 - 1997	3.68
Hay (downstream)	1953 - 1976	0.63
	1976 - 1994	1.41
Hay (upstream)	1954 - 1979	0.39
	1979 - 1993	0.72
Kootenay	1952 - 1975	0.75
	1975 - 1991	0.88
	1991 - 2004	1.09
Milk	1951 - 1962	1.16
	1962 - 1983	2.42
	1983 - 1995	0.83

River	Photo Time Interval	Average Migration Rate (m/year)
Muskwa	1953 - 1966	5.38
	1966 - 1975	9.26
	1975 - 1997	7.88
North Saskatchewan	1951 - 1976	0.16
	1976 - 1995	0.48
Oldman	1951 - 1961	2.60
	1961 - 1975	4.65
	1975 - 1998	0.92
Pinto	1951 - 1980	1.57
	1980 - 2001	0.42
Prophet	1966 - 1979	6.20
	1979 - 1997	1.04
Red Deer	1950 - 1962	2.94
	1962 - 1985	2.59
	1985 - 2001	2.94
Wapiti	1950 - 1972	7.65
	1972 - 1989	4.37
	1989 - 2001	14.18
Wildhay	1952 - 1963	1.77
	1963 - 1980	0.94
	1980 - 2001	2.11

Figure B.1 Migration rates for individual bends at all time intervals of study

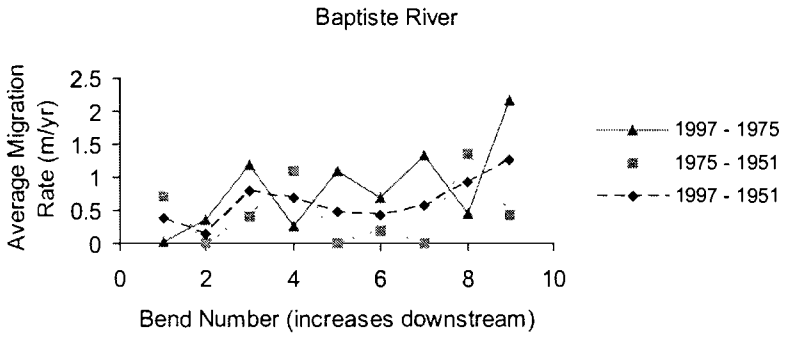
Baptiste River
Average Migration Rate (m/yr)
2.5
2
1.5
1
0.5
0
0
2
4
6
8
10
Bend Number (increases downstream)
1997 - 1975
1975 - 1951
1997 - 1951

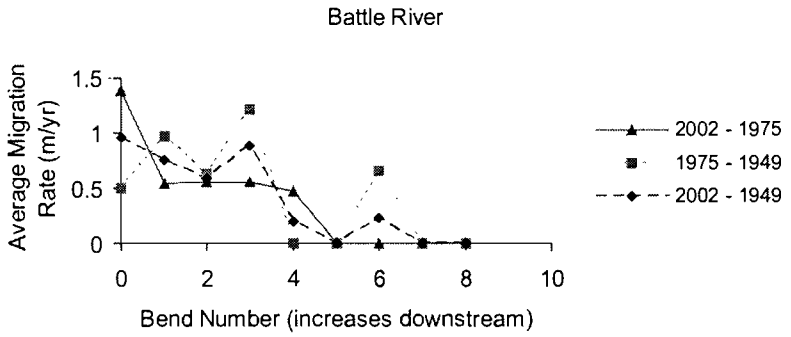
Battle River
Average Migration Rate (m/yr)
1.5
1
0.5
0
0
2
4
6
8
10
Bend Number (increases downstream)
2002 - 1975
1975 - 1949
2002 - 1949

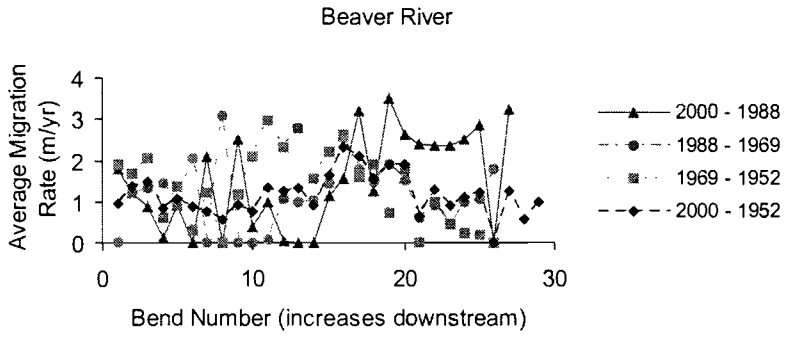
Beaver River
Average Migration Rate (m/yr)
4
3
2
1
0
0
10
20
30
Bend Number (increases downstream)
2000 - 1988
1988 - 1969
1969 - 1952
2000 - 1952

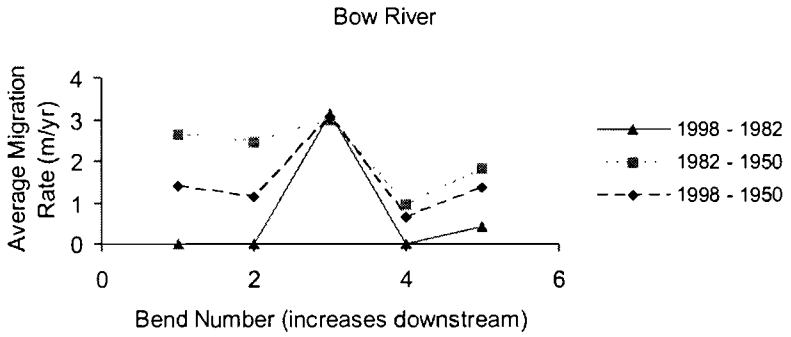
Bow River
Average Migration Rate (m/yr)
4
3
2
1
0
0
2
4
6
Bend Number (increases downstream)
1998 - 1982
1982 - 1950
1998 - 1950

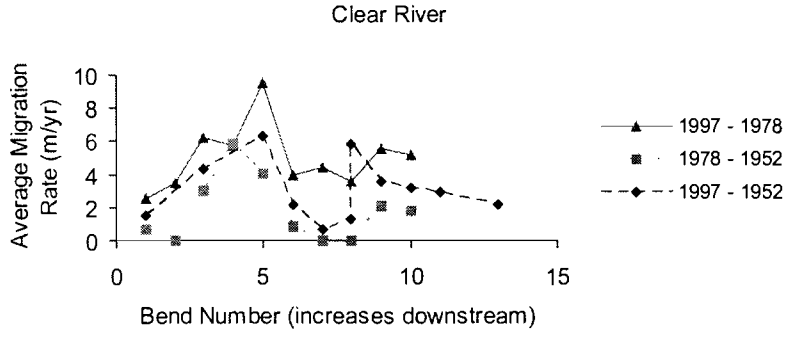
Clear River
Average Migration Rate (m/yr)
10
8
6
4
2
0
0
5
10
15
Bend Number (increases downstream)
1997 - 1978
1978 - 1952
1997 - 1952

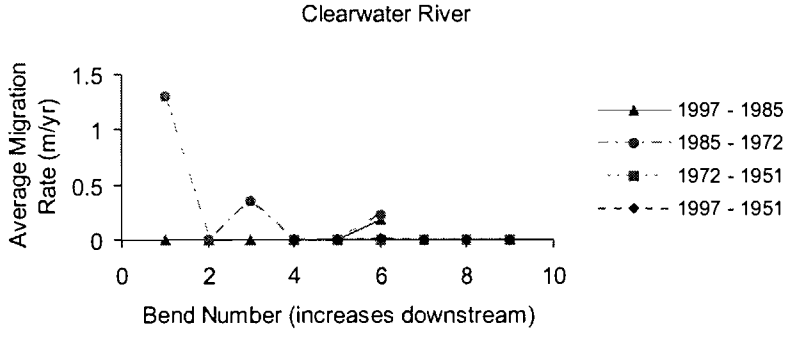
Clearwater River
Average Migration Rate (m/yr)
1.5
1
0.5
0
0
2
4
6
8
10
Bend Number (increases downstream)
1997 - 1985
1985 - 1972
1972 - 1951
1997 - 1951

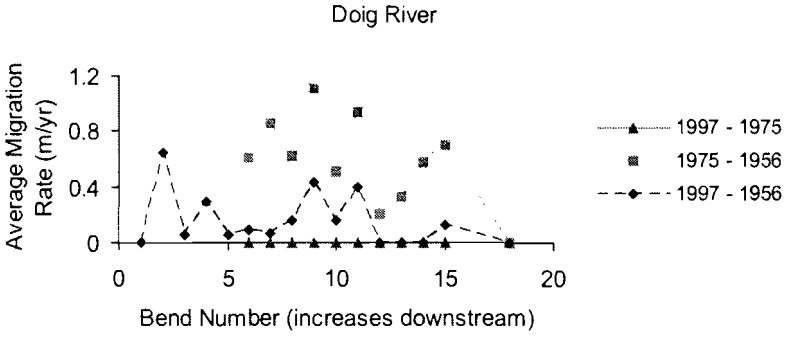
Doig River
Average Migration Rate (m/yr)
1.2
0.8
0.4
0
0
5
10
15
20
Bend Number (increases downstream)
1997 - 1975
1975 - 1956
1997 - 1956

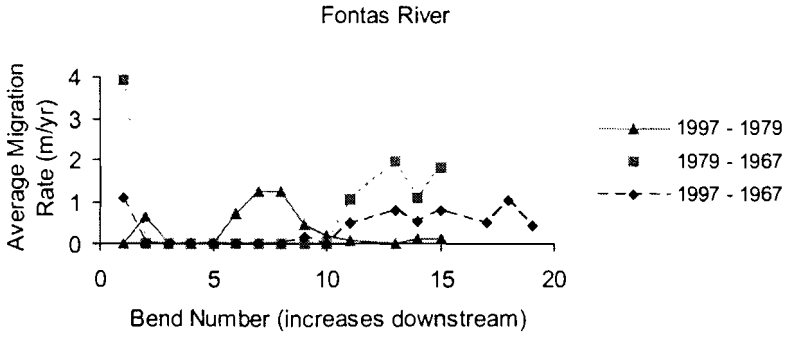
Fontas River
Average Migration Rate (m/yr)
4
3
2
1
0
0
5
10
15
20
Bend Number (increases downstream)
1997 - 1979
1979 - 1967
1997 - 1967

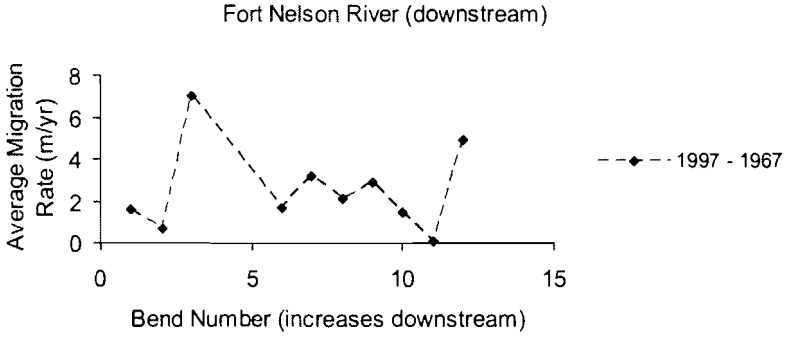
Fort Nelson River (downstream)
Average Migration Rate (m/yr)
8
6
4
2
0
0
5
10
15
Bend Number (increases downstream)
1997 - 1967

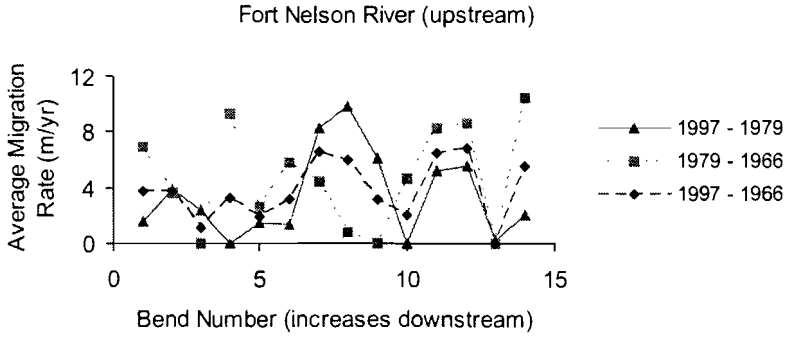
Fort Nelson River (upstream)
Average Migration Rate (m/yr)
12
8
4
0
0
5
10
15
Bend Number (increases downstream)
1997 - 1979
1979 - 1966
1997 - 1966

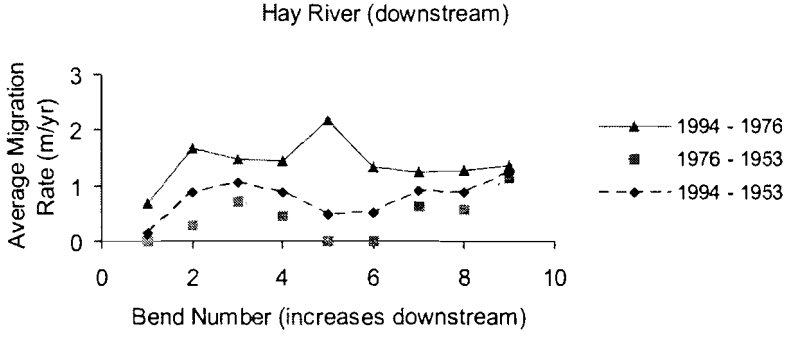
Hay River (downstream)
Average Migration Rate (m/yr)
3
2
1
0
0
2
4
6
8
10
Bend Number (increases downstream)
1994 - 1976
1976 - 1953
1994 - 1953

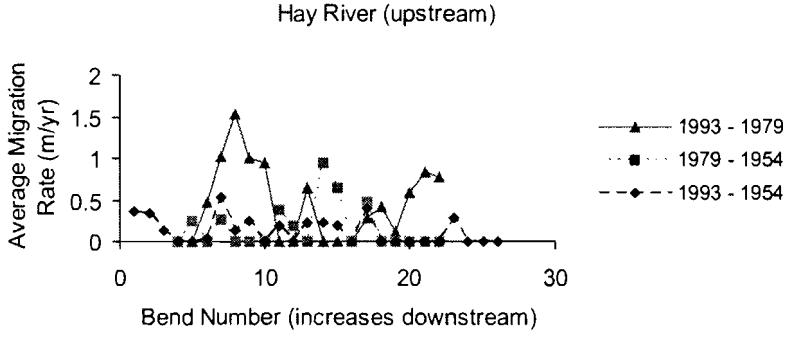
Hay River (upstream)
Average Migration Rate (m/yr)
2
1.5
1
0.5
0
0
10
20
30
Bend Number (increases downstream)
1993 - 1979
1979 - 1954
1993 - 1954

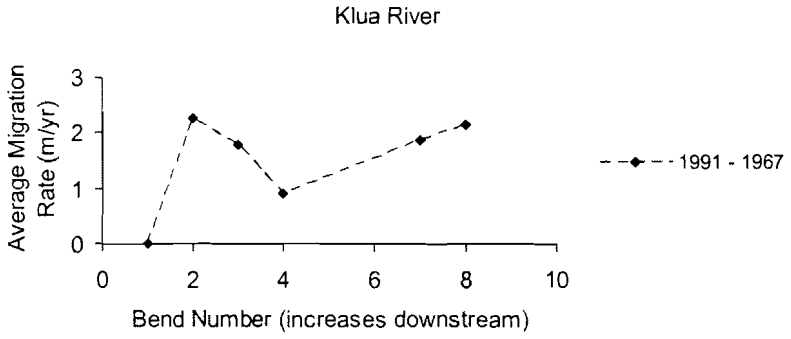
Klua River
Average Migration Rate (m/yr)
Bend Number (increases downstream)
1991 - 1967

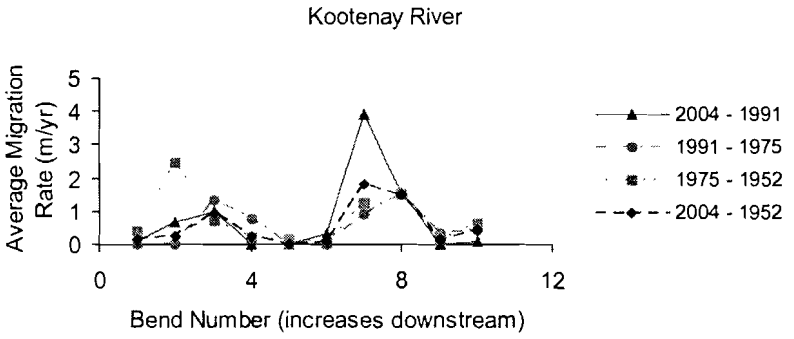
Kootenay River
Average Migration Rate (m/yr)
Bend Number (increases downstream)
2004 - 1991
1991 - 1975
1975 - 1952
2004 - 1952

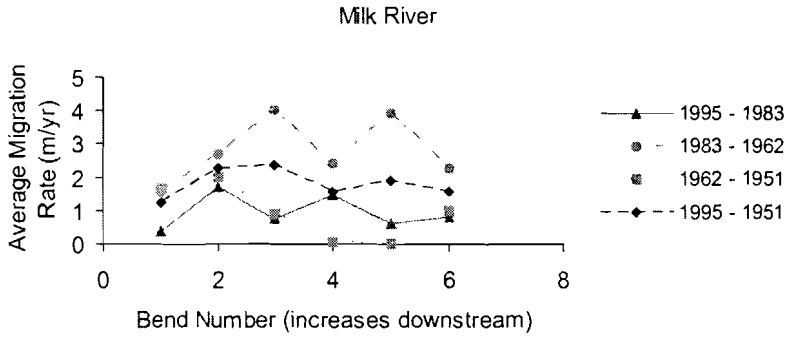
Milk River
Average Migration Rate (m/yr)
Bend Number (increases downstream)
1995 - 1983
1983 - 1962
1962 - 1951
1995 - 1951

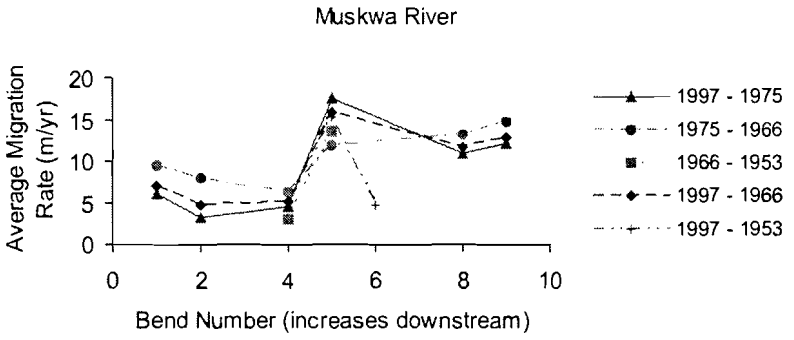
Muskwa River
Average Migration Rate (m/yr)
Bend Number (increases downstream)
1997 - 1975
1975 - 1966
1966 - 1953
1997 - 1966
1997 - 1953

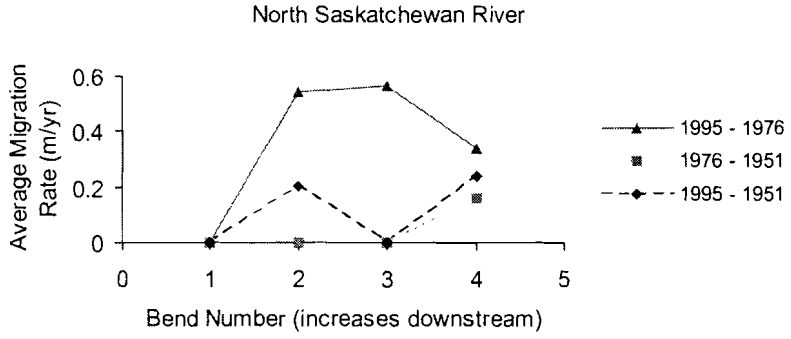
North Saskatchewan River
Average Migration Rate (m/yr)
Bend Number (increases downstream)
1995 - 1976
1976 - 1951
1995 - 1951

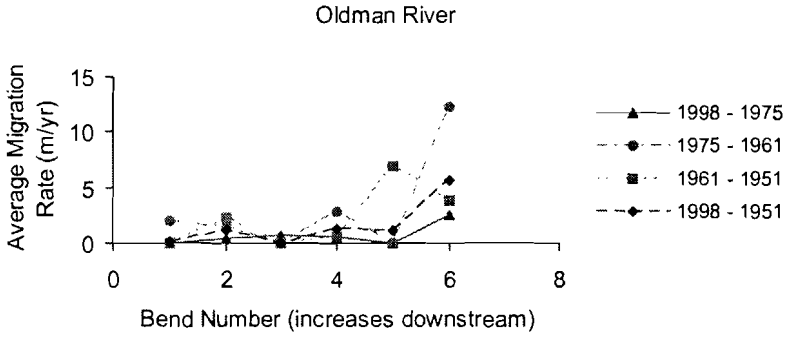
Oldman River
Average Migration Rate (m/yr)
Bend Number (increases downstream)
1998 - 1975
1975 - 1961
1961 - 1951
1998 - 1951

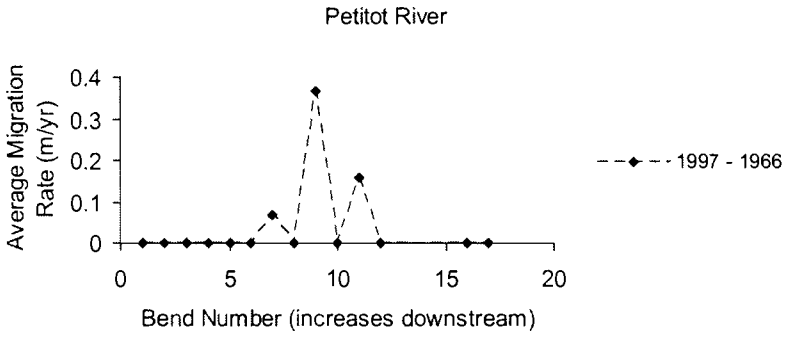
Petitot River
Average Migration Rate (m/yr)
0.4
0.3
0.2
0.1
0
0
5
10
15
20
Bend Number (increases downstream)
1997 - 1966

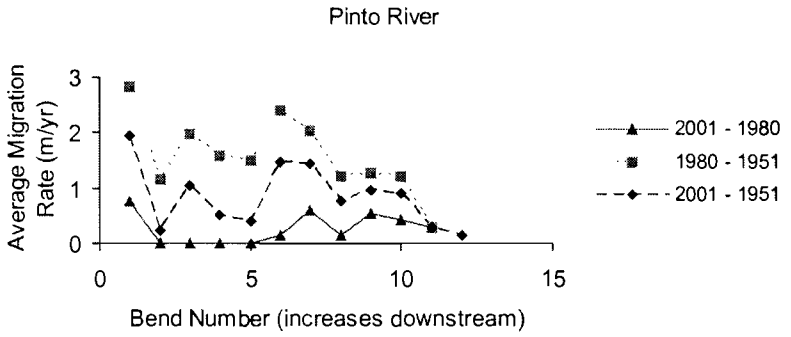
Pinto River
Average Migration Rate (m/yr)
3
2
1
0
0
5
10
15
Bend Number (increases downstream)
2001 - 1980
1980 - 1951
2001 - 1951

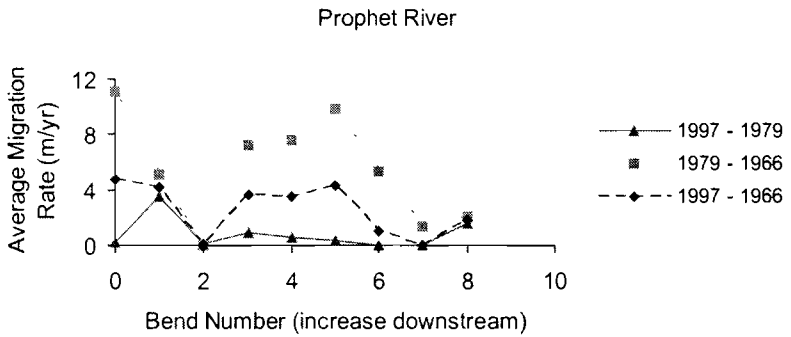
Prophet River
Average Migration Rate (m/yr)
12
8
4
0
0
2
4
6
8
10
Bend Number (increase downstream)
1997 - 1979
1979 - 1966
1997 - 1966

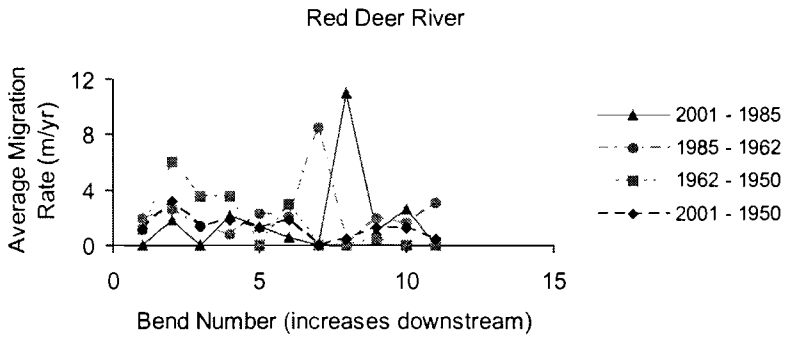
Red Deer River
Average Migration Rate (m/yr)
12
8
4
0
0
5
10
15
Bend Number (increases downstream)
2001 - 1985
1985 - 1962
1962 - 1950
2001 - 1950

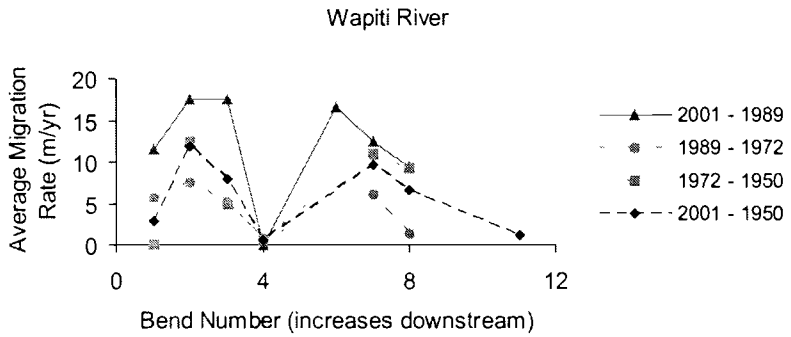
Wapiti River
Average Migration Rate (m/yr)
20
15
10
5
0
0
4
8
12
Bend Number (increases downstream)
2001 - 1989
1989 - 1972
1972 - 1950
2001 - 1950

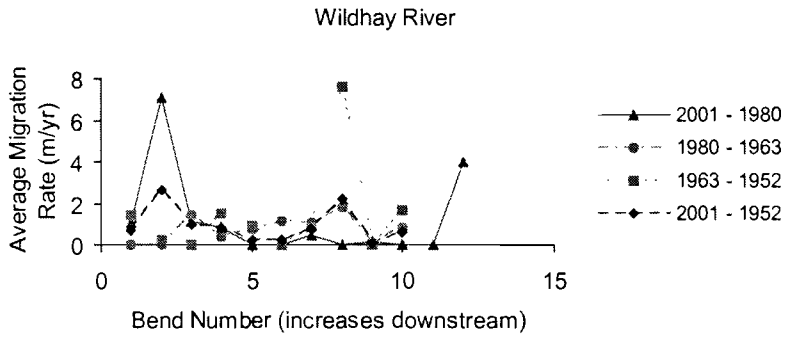
Wildhay River
Average Migration Rate (m/yr)
8
6
4
2
0
0
5
10
15
Bend Number (increases downstream)
2001 - 1980
1980 - 1963
1963 - 1952
2001 - 1952